

DESIGN AND PERFORMANCE ANALYSIS  
OF  
A PUMP-TURBINE SYSTEM USING COMPUTATIONAL FLUID DYNAMICS

A THESIS SUBMITTED TO  
THE GRADUATE SCHOOL OF NATURAL AND APPLIED SCIENCES  
OF  
MIDDLE EAST TECHNICAL UNIVERSITY

BY

MEHMET YILDIZ

IN PARTIAL FULFILLMENT OF THE REQUIREMENTS  
FOR  
THE DEGREE OF MASTER OF SCIENCE  
IN  
MECHANICAL ENGINEERING

SEPTEMBER 2011

Approval of the thesis:  
**DESIGN AND PERFORMANCE ANALYSIS OF A PUMP-TURBINE  
SYSTEM USING COMPUTATIONAL FLUID DYNAMICS**

submitted by **MEHMET YILDIZ** in partial fulfillment of requirements for the degree of **Master of Science in Mechanical Engineering Department, Middle East Technical University** by,

Prof. Dr. Canan ÖZGEN  
Dean, Graduate School of **Natural and Applied Sciences** \_\_\_\_\_

Prof. Dr. Süha ORAL  
Head of Department, **Mechanical Engineering** \_\_\_\_\_

Prof. Dr. Kahraman ALBAYRAK  
Supervisor, **Mechanical Engineering Dept., METU** \_\_\_\_\_

Dr. Kutay ÇELEBİOĞLU  
Co-Supervisor, **Civil Engineer, General Manager, SU-ENER** \_\_\_\_\_

**Examining Committee Members:**

Prof. Dr. Haluk AKSEL  
Mechanical Engineering Dept., METU \_\_\_\_\_

Prof. Dr. Kahraman ALBAYRAK  
Mechanical Engineering Dept., METU \_\_\_\_\_

Assoc. Prof. Dr. Cemil YAMALI  
Mechanical Engineering Dept., METU \_\_\_\_\_

Assist. Prof. Dr. Cüneyt SERT  
Mechanical Engineering Dept., METU \_\_\_\_\_

Dr. Kutay ÇELEBİOĞLU  
Civil Engineer, General Manager, SU-ENER \_\_\_\_\_

**Date:** \_\_\_\_\_ 13.09.2011

**I hereby declare that all information in this document has been obtained and presented in accordance with academic rules and ethical conduct. I also declare that, as required by these rules and conduct, I have fully cited and referenced all material and results that are not original to this work.**

Name, Last name : Mehmet YILDIZ

Signature :

## ***ABSTRACT***

### **DESIGN AND PERFORMANCE ANALYSIS OF A PUMP-TURBINE SYSTEM USING COMPUTATIONAL FLUID DYNAMICS**

YILDIZ, Mehmet

M. Sc., Department of Mechanical Engineering

Supervisor: Prof. Dr. Kahraman ALBAYRAK

Co-Supervisor: Dr. Kutay ÇELEBİOĞLU

September 2011, 130 pages

In this thesis, a parametric methodology is investigated to design a Pump-Turbine system using Computational Fluid Dynamics ( CFD ). The parts of Pump-Turbine are created parametrically according to the experience curves and theoretical design methods. Then, these parts are modified to obtain 500 kW turbine working as a pump with 28.15 meters head. The final design of Pump-Turbine parts are obtained by adjusting parameters according to the results of the CFD simulations. The designed parts of the Pump-Turbine are spiral case, stay vanes, guide vanes, runner and draft tube. These parts are designed to obtain not only turbine mode properties but also pump mode properties.

**Keywords:** Hydro Turbine, Computational Fluid Dynamics (CFD), Pump-Turbine, Hydropower, Pump

## **ÖZ**

### **POMPA TÜRBİN SİSTEMİNİN HESAPLAMALI AKIŞKANLAR DİNAMİĞİ İLE TASARIMI VE PERFORMANS ANALİZLERİNİN YAPILMASI**

YILDIZ, Mehmet

Yüksek Lisans, Makina Mühendisliği Bölümü

Tez Yöneticisi: Prof. Dr. Kahraman ALBAYRAK

Ortak Tez Yöneticisi : Dr. Kutay ÇELEBİOĞLU

Eylül 2011, 130 sayfa

Bu araştırmada Pompa-Türbin sisteminin Hesaplamalı Akışkanlar Dinamiği (HAD) metodları kullanımı ile tasarımı parametrik bir metodoloji olarak araştırılmıştır. Pompa-Türbin parçaları deneyim eğrileri ve teorik tasarım metodlarına göre parametrik olarak oluşturulmuştur. Oluşturulan bu parçalar daha sonra 28 metrelik düşüde pompa olarak çalışabilen 500 kW türbin elde etmek için değiştirilmiştir. Pompa-Türbin parçalarının son tasarımları HAD simulasyon sonuçlarına göre parametreler değiştirilerek elde edilmiştir. Tasarımı yapılan Pompa-Türbin parçaları salyangoz, sabit kanatlar, ayar kanatları, çark ve emme borusudur. Bu parçalar sadece türbin modu özellikleri için değil aynı zamanda pompa modu özellikleri için de tasarımı yapılmıştır.

**Anahtar Kelimeler:** Su Türbini, Hesaplamalı Akışkanlar Dinamiği (HAD), Pompa-Türbin , Hidroelektrik, Pompa

To my beautiful family

## ***ACKNOWLEDGMENTS***

I express my sincere appreciation to my supervisors Prof. Dr. Kahraman ALBAYRAK and Dr. Kutay ÇELEBİOĞLU for their guidance, understanding and advice.

I would like thank the thesis committee members for their advice and comments.

Finally, I would like to thank my family for their love and endless support.

## ***TABLE OF CONTENTS***

ABSTRACT.....	iv
ÖZ.....	v
ACKNOWLEDGMENTS.....	vii
TABLE OF CONTENTS.....	viii
LIST OF FIGURES.....	xii
LIST OF TABLES.....	xvii
CHAPTERS	
1.INTRODUCTION.....	1
1.1. Introductory Remarks on hydropower as a Renewable Energy.....	1
1.2. Scope and Objective of the Work.....	1
1.3. Literature Survey about Hydraulic Machines and CFD Tool Applications...2	
1.3.1. Turbine.....	2
1.3.2. Pump.....	5
1.3.3. Pump-Turbine.....	6
1.3.4. CFD Tools for Turbo Machinery Applications.....	6
1.4. Description of the Thesis.....	7
2.PUMPED-HYDRO STORAGE SYSTEM.....	9
2.1. History of Pumped-Storage Hydroelectricity .....	9
2.2. Pumped-Hydropower Storage System Types.....	11
2.2.1. Four-Machine Scheme .....	11
2.2.2. Three-Machine Scheme .....	12
2.2.3. Two-Machine Scheme .....	13
3.REVERSIBLE HYDRAULIC MACHINE DESIGN METHODOLOGY.....	17
3.1. Overview of a Pump-Turbine Design Methodology.....	17
3.2. Main Input Parameters of a Pump-Turbine.....	20
3.2.1. Head.....	20
3.2.2. Power.....	22



3.3. Main Design Parameters of a Pump-Turbine.....	22
3.3.1. Efficiency.....	23
3.3.2. Design Discharge .....	24
3.3.3. Design Rotational Speed.....	25
3.3.4. Specific Speed.....	27
3.3.5. Turbine Runner Type According to Specific Speed.....	28
3.3.6. Meridional Profile of a Runner Blade.....	28
3.3.7. Preliminary Dimensions of a Pump-Turbine Runner.....	29
3.3.8. Guide Vane Properties.....	33
3.3.9. Velocity Triangle Adjustments of a Runner Blade.....	36
3.3.10. Blade Angles.....	40
3.3.11. Turbine Working Process.....	41
3.3.12. Euler Equation for Turbine.....	46
3.3.13. Euler Equation for Pump.....	48
4. NUMERICAL SIMULATION AND CFD METHODS .....	52
4.1. CFD Tool Application .....	52
4.1.1. Turbulence Models.....	53
4.1.2. Advection Schemes.....	53
4.1.3. Discretization Scheme.....	53
4.1.4. Topology Definition.....	54
4.1.5. Generating Mesh.....	55
4.1.6. Mesh Connection.....	56
4.1.7. Boundary Conditions.....	57
4.2. Runner Blade Simulation Details.....	59
4.3. Guide Vane Simulation Details.....	61
4.4. Stay Vane Simulation Details.....	62
4.5. Spiral Case Simulation Details.....	62
4.6. Draft Tube Simulation Details.....	62
5. TURBINE MODE RESULTS.....	64
5.1. Final Design Mesh Characteristics.....	64
5.2. Runner Simulations in Turbine mode.....	64
5.2.1. Meridional Profile Design in Turbine Mode.....	65

5.2.2. Leading Edge Design in Turbine Mode.....	66
5.2.3. Outlet Swirl Elimination in Turbine Mode.....	69
5.2.4. Design without Cavitation in Turbine Mode.....	70
5.2.5. Mesh Independency in Turbine Mode.....	72
5.2.6. Roughness Effect for the Runner in Turbine Mode.....	73
5.2.7. Runner Blade in Turbine Mode.....	73
5.3. Spiral Case Results in Turbine Mode.....	77
5.4. Stay Vane Results in Turbine Mode.....	79
5.5. Guide Vane Results in Turbine Mode.....	82
5.6. Draft Tube Results in Turbine Mode.....	86
5.7. Final Model CFD Results and Hydraulic Losses in Turbine Mode.....	89
5.8. Discussion of Turbine Mode Results.....	90
6. PUMP MODE RESULTS.....	93
6.1. Final Design Mesh Characteristics.....	93
6.2. Runner Simulation in Pump Mode.....	93
6.2.1. Meridional Profile Design in Pump Mode.....	93
6.2.2. Leading Edge Design in Pump Mode.....	94
6.2.3. No Swirl Inlet Condition in Pump Mode.....	96
6.2.4. Design without Cavitation in Pump Mode.....	97
6.2.5. Mesh Independency in Pump Mode.....	99
6.2.6. Roughness Effect for the Runner in Pump Mode.....	100
6.2.7. Runner Blade Final Version in Pump Mode.....	100
6.3. Spiral Case Results in Pump Mode.....	103
6.4. Stay Vane Results in Pump Mode.....	104
6.5. Guide Vane Results in Pump Mode.....	107
6.6. Draft Tube Results in Pump Mode.....	111
6.7. Final Model CFD Results and Hydraulic Losses in Pump Mode.....	113
6.8. Discussion of Pump Mode Results.....	114
7. CHARACTERISTICS OF THE PUMP-TURBINE.....	116
7.1. Pump-Turbine Working Conditions.....	116
7.2. Four Quadrant Characteristics of the Pump-Turbine .....	117
7.2.1. 1st Quadrant Normal Pump Mode.....	119

7.2.2. 2nd Quadrant Reverse Turbine Mode.....	120
7.2.3. 3rd Quadrant Normal Turbine Mode.....	121
7.2.4. 4th Quadrant Reverse Pump Mode.....	122
8. CONCLUSION.....	123
8.1. Summary of the Developed Work.....	123
8.2. Contributions of the Developed Work.....	124
8.3. Conclusion.....	125
8.4. Future Works.....	126
REFERENCES.....	127

## ***LIST OF FIGURES***

### **FIGURES**

Figure 1. Schematic Drawing of a Pelton Turbine.....	3
Figure 2. Schematic Drawing of a Kaplan Turbine.....	3
Figure 3. Turbine selection chart (VA TECH ) [5].....	4
Figure 4. Four-machine scheme: separate pump and turbine units.....	12
Figure 5. Three-machine scheme: separate pump and turbine units that are connected to one motor-generator.....	12
Figure 6. Pump-Turbine cross-section [5].....	13
Figure 7. General layout of a Pump-Turbine in a hydropower project [19].....	14
Figure 8. Flow inside a Pump-Turbine in the meridional representation.....	15
Figure 9. Pump-Turbine components .....	16
Figure 10. Pump-Turbine design methodology chart.....	19
Figure 11. Energy change from the upper reservoir to lower reservoir.....	21
Figure 12. Turbine runner types for specific speed value [23].....	28
Figure 13. Meridional profile of the runner a) in turbine mode b) in pump mode. .	29
Figure 14. Runner dimensions.....	30
Figure 15. Guide vane regulation center and runner.....	33
Figure 16. Adjustment of turbine flow rate by guide vanes.....	34
Figure 17. Guide vane properties.....	34
Figure 18. Guide vane throat area a) isometric b) top view.....	35
Figure 19. Inlet and outlet velocities at leading and trailing edges of the runner blade.....	36
Figure 20. Fluid velocity at the runner inlet and outlet in turbine mode.....	37
Figure 21. Meridional flow direction in a) turbine mode b) pump mode.....	39
Figure 22. Flow created by guide vanes.....	42
Figure 23. Velocities at leading and trailing edges of impeller pump.....	49
Figure 24. Draft tube mesh (290224 elements and 23392 nodes).....	54

Figure 25. Final runner blade grid topology.....	54
Figure 26. $y^+$ distribution on the runner blade surface.....	55
Figure 27. Generated mesh data for final Pump-Turbine runner (238560 elements and 255200 nodes for one runner blade passage).....	56
Figure 28. The runner blade meridional section.....	60
Figure 29. The runner blade thickness profile.....	60
Figure 30. Area distributions of the runner blade passage.....	61
Figure 31. Runner blade meridional shapes: a) preliminary b) final.....	66
Figure 32. Blade Loading at closer shroud span on non-final blade design.....	67
Figure 33. Blade Loading at closer shroud span on final blade design.....	67
Figure 34. Velocity vectors at closer to the hub meridional section for non-final runner blade .....	68
Figure 35. Velocity vectors at closer to the hub meridional section for final runner blade .....	69
Figure 36. Streamwise Plot of Alpha and Beta in turbine mode.....	70
Figure 37. Pressure distribution on the runner blade in turbine mode.....	71
Figure 38. Pressure on the blade meridional section at section closer to the shroud .....	71
Figure 39. Runner efficiency and head difference versus mesh size in turbine mode .....	72
Figure 40. The velocity vectors on meridional section in turbine mode.....	74
Figure 41. Total pressure distribution on meridional section in turbine mode.....	74
Figure 42. Velocity vectors at meridional mid-section in turbine mode.....	75
Figure 43. Velocity vectors at closer to the hub meridional section in turbine mode .....	75
Figure 44: Velocity vectors at closer to the shroud meridional section in turbine mode.....	76
Figure 45. Velocity streamlines in runner blade passage in turbine mode.....	76
Figure 46. Radial and peripheral velocity distributions at the spiral case outlet.....	77
Figure 47. Total pressure distribution on the spiral case mid-plane in turbine mode .....	78
Figure 48. Velocity vectors on the spiral case mid-plane in turbine mode.....	78

Figure 49. Velocity vectors on the spiral case mid-plane in turbine mode.....	79
Figure 50. Blade loading on stay vane at mid-meridional section in turbine mode	80
Figure 51. Streamwise Plot of Total pressure and Pressure through the stay vane passage in turbine mode.....	80
Figure 52. The Static Pressure Distributions in stay vane passage in turbine mode .....	81
Figure 53. Velocity streamlines in stay vane passage in turbine mode.....	81
Figure 54. Total pressure distribution and velocity streamlines on the mid-plane of spiral case and stay vanes in turbine mode.....	82
Figure 55. Blade loading on guide vane at mid-section in turbine mode.....	83
Figure 56. Streamwise Plot of Total pressure and Pressure through the guide vane passage in turbine mode.....	84
Figure 57. The Static Pressure Distributions in guide vane passage.....	85
Figure 58. Velocity streamlines in guide vane passage in turbine mode.....	85
Figure 59. Velocity streamlines in guide vane and runner passage in turbine mode .....	86
Figure 60: Parametric Draft Tube flow geometry.....	86
Figure 61. Total pressure change through the draft tube in turbine mode.....	87
Figure 62. Pressure change through the draft tube in turbine mode.....	88
Figure 63. Velocity vectors and contours on the draft tube mid-section in turbine mode.....	88
Figure 64. Draft tube velocity contours and streamlines in turbine mode.....	89
Figure 65. Blade Loading at closer to the shroud meridional section on non-final blade design in pump mode.....	94
Figure 66. Blade Loading at closer to the shroud meridional section on final blade design.....	95
Figure 67. Velocity vectors at mid-meridional section for preliminary runner blade in pump mode.....	95
Figure 68. Velocity vectors at mid-meridional section for final runner blade in pump mode.....	96
Figure 69. Streamwise Plot of Alpha and Beta in pump mode.....	97
Figure 70. Pressure distribution on the runner blade in pump mode .....	98

Figure 71. Pressure on the blade meridional section with minimum pressure zone	98
Figure 72. Runner efficiency and head difference versus mesh size in pump mode	99
Figure 73. The velocity vectors on meridional section in pump mode	100
Figure 74. Total pressure distribution on meridional section in pump mode	101
Figure 75. Velocity vectors at meridional mid-section in pump mode	101
Figure 76. Velocity vectors at closer to the hub meridional section in pump mode	102
Figure 77: Velocity vectors at closer to the shroud meridional section in pump mode	102
Figure 78. Velocity streamlines in pump mode	103
Figure 79. Pressure distribution on the spiral case mid-plane with stay vanes in pump mode	103
Figure 80. Velocity distribution on the spiral case mid-plane with stay vanes in pump mode	104
Figure 81. Blade loading on stay vane at mid-span	105
Figure 82. Stream wise Plot of Total pressure and Pressure through the stay vane passage in pump mode	105
Figure 83. The Static Pressure Distributions in stay vane passage in pump mode	106
Figure 84. Velocity streamlines in stay vane passage	106
Figure 85. Pressure distribution and velocity streamlines on the mid-plane of spiral case and stay vanes	107
Figure 86. Blade loading on guide vane at mid-span	108
Figure 87. Stream wise Plot of Total pressure and Pressure through the guide vane passage	109
Figure 88. The Static Pressure Distributions in guide vane passage	109
Figure 89. Velocity streamlines in guide vane passage in pump mode	110
Figure 90. Velocity streamlines in guide vane and runner passage in pump mode	110
Figure 91. Total pressure change through the draft tube in pump mode	111

Figure 92. Pressure change through the draft tube in pump mode.....	112
Figure 93. Velocity vectors and contours on the draft tube mid-section in pump mode.....	112
Figure 94. Draft tube velocity contours and streamlines in pump mode.....	113
Figure 95. Four-quadrant Characteristics of the Pump-Turbine.....	117



## ***LIST OF TABLES***

### **TABLES**

Table 1. Turbine types for specific speed and maximum head [4].....	4
Table 2. Pumped Storage projects in TURKEY prepared by EIEI [1].....	18
Table 3. Generator synchronization speeds .....	26
Table 4. Preliminary runner dimensions.....	30
Table 5. Mesh connection types between mesh of the Pump-Turbine parts.....	57
Table 6. Pump-Turbine runner boundary conditions.....	57
Table 7. Mesh characteristics of each turbine component for final design.....	64
Table 8. Draft Tube Simulation Results in Turbine Mode.....	87
Table 9. Efficiencies of the Pump-Turbine parts and hydraulic losses.....	89
Table 10. Efficiencies of the Pump-Turbine parts and hydraulic losses.....	113
Table 11. The Simulation Conditions of the Pump-Turbine.....	118

## ***CHAPTER 1***

### ***INTRODUCTION***

#### **1.1. Introductory Remarks on hydropower as a Renewable Energy**

Energy demand increases with every passing day. Renewable energy is a good solution for the increasing energy demand due to climate change, fossil amounts and carbon credit. Renewable energy sources are solar, wind, water, wave, biomass, geothermal, etc. The use of these sources should be increased. In this research, water energy that is available in Turkey will be discussed. Water energy is not only used for generating electricity but also used for storing the energy. In this respect, Hydropower Storage Plants ( HPSP ) can be used to store huge amount of energy. There are some areas that is suitable to construct HPSP in Turkey [1].

In Turkey, there is no HPSP and no design know-how to design Pump-Turbine which is the most convenient type of HPSP. The types of HPSP and their working principles are detailed in the section 2.2.

#### **1.2. Scope and Objective of the Work**

The objective of this thesis is to design a Pump-Turbine with CFD methods. In the world, there are many academic researches about Pump-Turbine design, and the CFD results are validated by the model test results [2, 3].

In this thesis, a parametric methodology is created to design a Pump-Turbine using

CFD methods. In the design methodology, Computational Fluid Dynamics methods are used to improve the Pump-Turbine parts created with the theoretical design methods and experience curves.

The design methodology starts with preliminary design obtained from empirical formulas and theoretical hydraulic machinery principles. It continues with modification of the geometry by considering the result of the CFD analysis. In this design methodology head and discharge are the main inputs.

### **1.3. Literature Survey about Hydraulic Machines and CFD Tool Applications**

Hydraulic machines are used for two main aims. One of them is transferring energy from operating member (runner for pump-turbine) to the liquid passing through the machine in pump mode condition. Other is the energy transferring from the liquid passing through the machine to the operating member in turbine mode condition. In this respect, hydraulic machines are classified into three groups:

1. Turbine
2. Pump
3. Pump-Turbine

#### ***1.3.1. Turbine***

Shaft power and torque are obtained with absorbing the momentum of the water passing through turbines. Turbines are used with the generators in a hydropower plant. The working principle of the turbine is to generate electricity with converting water potential energy to mechanical energy. The runner of the turbine is rotated by the water inside turbine and rotor of the generator rotates inside its stator. Then, the generator generates electricity from the rotor and stator interaction of generator. Turbines are machines that develop torque and shaft power as a result of momentum changes in the fluid that flows through them. Turbines are classified in two groups.

**Impulse type:** In the impulse turbines, the velocity of the fluid increases in the stator and pressure decreases at this location. After passing through the stator, fluid pressure remains almost constant in rotor. Only the velocity of the fluid decreases in rotor. So, the water coming from the nozzles hits the runner blades locally and the runner rotates as illustrated in Fig. 1. Pelton turbine is an example of impulse type turbine group.

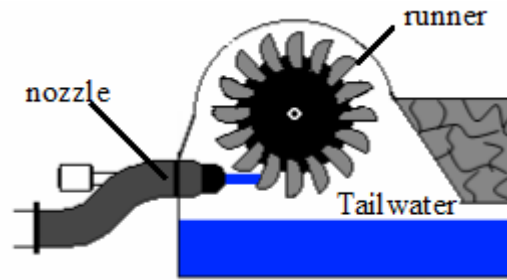


Figure 1. Schematic Drawing of a Pelton Turbine

**Reaction type:** In the reaction turbines, the velocity of the fluid increases in rotor and pressure decreases at this location. After passing through the stator with an almost constant pressure, the pressure decreases in rotor and velocity increases. So, the pressurized water hits the runner peripherally and water pressure decreases. Francis and Kaplan are the examples of reaction type turbine group. Kaplan turbine schematic drawing is shown in Fig. 2.

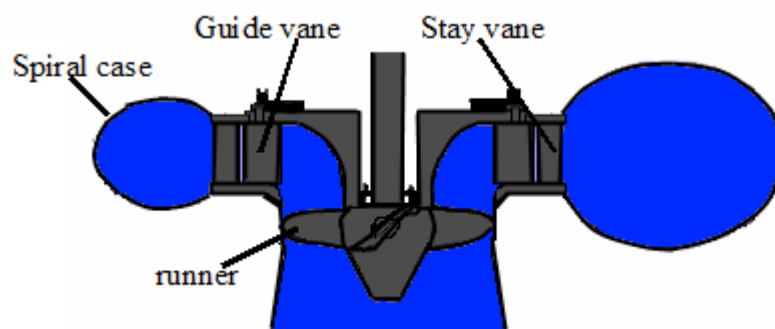


Figure 2. Schematic Drawing of a Kaplan Turbine

Turbine types are characterized to obtain some standard conditions. Geometrically similar turbines can work at different conditions. One of the standard criteria of the turbines is the specific speed  $n_s$ . Turbine types according to the specific speed  $n_s$

are tabulated in Table 1. The specific speed is determined according to head, discharge and rotational speed. The maximum head is also advised for turbine type in Table 1.

Table 1. Turbine types for specific speed and maximum head [4]

Turbine type					
	Impulse	Reaction			
	Pelton	Francis			Kaplan
		Slow	Medium	Fast	
$n_s$ [rpm]	7 – 26	51 - 107	107 -190	190 - 250	250 - 300
Max. H [m]	1800 - 350	700 - 410	410 - 150	150 - 64	50 – 6

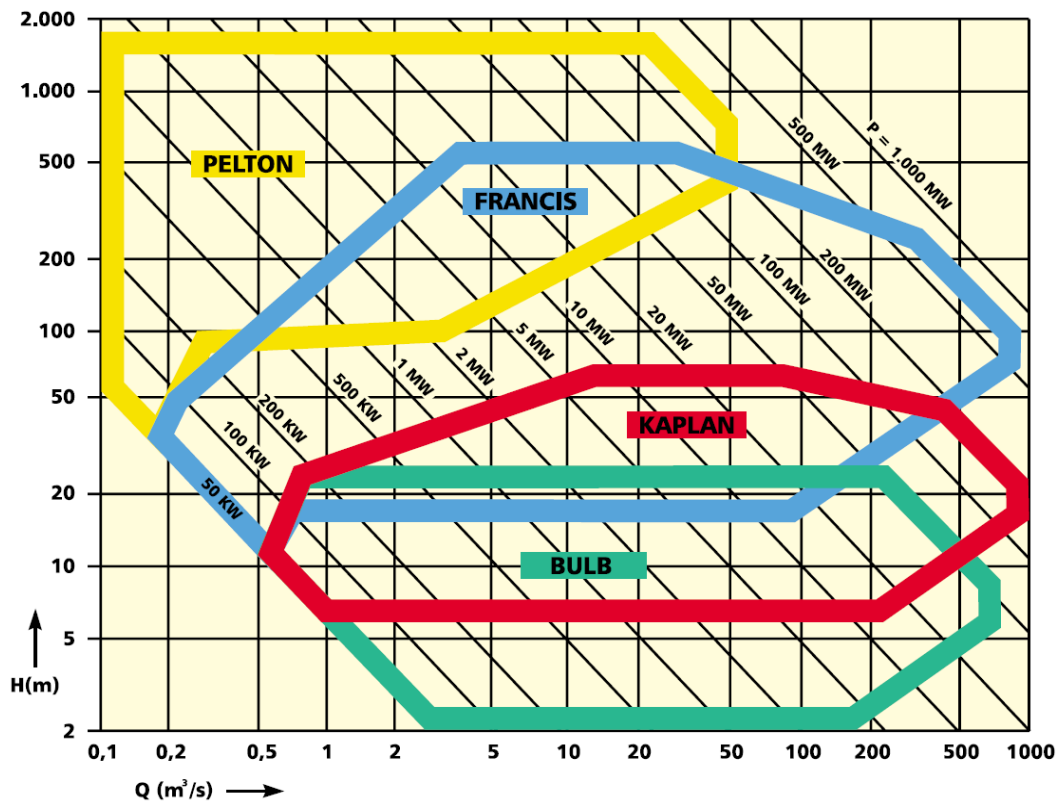


Figure 3. Turbine selection chart (VA TECH ) [5]

The turbine type is chosen with respect to the specific speed. However in order to choose the type of the turbine, the companies provides turbine selection charts according to their experiences. The advised turbine selection chart from VA TECH

Hydro is given in Fig. 3 for head and discharge values of the turbine. Pelton is an impulse turbine. Francis and Kaplan are reaction turbines. The bulb given in Fig. 3 is a reaction type turbine and designed for low head values.

### **1.3.2. Pump**

Pump is a hydraulic machine in which energy is transferred from impeller to the passing liquid inside. So, the energy of the liquid increases from inlet to outlet in pumps.

In pumping stations, pumps are used to increase water pressure. The energy is taken from the network with motors. However, some of mobile units are used with the internal combustion engines.

There are two water level for the hydraulic machines. One of them is the lower reservoir which is known as 'Tailwater' for the turbines. Other is the upper basin (or upper reservoir) which is known as 'Headwater' for the turbines. Pumps are used to draw the water from the lower reservoir to the upper reservoir.

There are two main characteristic parameters for the pumps. One of them is head which is the difference between the elevation of the reservoirs. The other is the discharge, which is the amount of the liquid transferred from lower to upper reservoir. Pumps are used for different reasons in many areas. For this reason, they are designed in wide range. The head changes from 5-10 m to 600-800 m. The delivery amount changes 0.001-0.005 m<sup>3</sup>/s to 3-40 m<sup>3</sup>/s and more. So, there are many types of pumps. They can be classified as [6]:

1. Positive displacement pumps
2. Plunger pump
3. Double-acting piston pump
4. Diaphragm-type pump
5. Gear pump
6. Screw pump

7. Rotor dynamic pumps
8. Centrifugal pump
9. Axial flow pump
10. Peripheral pump
11. Jet pump

In this thesis centrifugal pump (8) in a Pump-Turbine arrangement is studied. Centrifugal pump is designed like a Pump-Turbine in pump mode.

### ***1.3.3. Pump-Turbine***

Pump-Turbine is a reversible hydraulic machine that has two cycles. One of them is pumping cycle when water is transferred from lower reservoir to upper reservoir in night hours. Other is the generator mode (or turbine mode) when the high elevation water is used to generate electricity to cover peaks of the power grid load curve in day hours.

Pump-Turbine is used with the generator-motor in the Hydro Storage Power Plants. This hydraulic machine is reversible and it not only works on turbine mode but also works on pump mode with same hydraulic equipment i.e. Francis type turbine and centrifugal pump. Pump-Turbine will be briefly discussed in Chapter 2.

Pump mode of the Pump-Turbine is designed for the generator-motor to pump up water to upper levels. The runner (or impeller) of the Pump-Turbine is rotated with electricity taken from the network. Then the kinetic energy and static pressure of the water passing through the Pump-Turbine are increased by rotating runner.

### ***1.3.4. CFD Tools for Turbo Machinery Applications***

They have been used over a century. The Pump-Turbine history also started in 1929 with the Niederwartha station with significant amount of capacity. The need of the electricity increases gradually. So, the machines should be design more efficiently to reach the requirements. The CFD tools makes it possible to design more efficient hydraulic machines. Highly developed computers, computer codes

and programs are used together with the CFD tools. So, the efficiency of the Pump-Turbine can be increased by using CFD tools with an optimization process of the Pump-Turbine. For this reason, the manufacturers of pumps, turbines and Pump-Turbines have used modern design tools such as CFD implementations for a long time. In the literature, there are many papers and researches about design of a Pump-Turbine with CFD tools [7, 8, 9, 10].

The Pump-Turbine is a unique technology for storage of huge amount of energy. In this technology, the energy is stored by pumping up water. The turbine mode efficiency is important to gain power with water pumped up with pump mode efficiency. So, the design of the HPSP should make possible good efficiency of the hydraulic machines.

In the analysis the parametric geometries are created to obtain the Pump-Turbine parts. When making CFD simulations with parametric modeling, various geometry combinations can be made in a short time interval [11]. If these results are compared with the test results, the method can be made better with the related modifications.

Now, the flow inside the hydraulic machines can be simulated closer to the real behavior with developed technology, computer codes and CFD tools. In this respect, the design of the Pump-Turbine can be made with CFD tools.

#### **1.4. Description of the Thesis**

In this thesis, preliminary design of Pump-Turbine parts are made using theoretical methods and empirical formulas. Then designed parts are investigated with CFD methods. The design of a Pump-Turbine system is investigated as a parametric methodology.

There are eight chapters in this thesis. In Chapter 1, hydropower is explained as a renewable energy. The hydraulic machines and working principles are detailed.



The CFD tool applications are discussed. History of the pumped-storage system is explained. Types of the pumped-hydropower Storage System are detailed in Chapter 2 and two-machine scheme is chosen for design methodology. In Chapter 3, reversible hydraulic machine design is explained as a methodology. Design parameters of a Pump-Turbine are explained and Euler equations are obtained for both turbine and pump mode to understand the relationship between each mode. Numerical simulations and CFD methods that are used in methodology is explained in Chapter 4. The results of the optimum points of turbine and pump mode are discussed in Chapters 5 and 6 respectively. After reaching the design requirements, the performance analysis are made for different flow conditions to understand the Pump-Turbine behavior for all working conditions in Chapter 7. Finally, summary and contributions of the developed work is written in Chapter 8.

## ***CHAPTER 2***

### ***PUMPED-HYDRO STORAGE SYSTEM***

#### **2.1. History of Pumped-Storage Hydroelectricity**

Storing energy with pumping water up to higher reservoirs has been used for a long time. Back from 1882 this system was used with a reciprocating pump in Zurich, Switzerland [12]. A few years later, 50 kW centrifugal pump was used to drive a spinning mill in Luino, Italy [12]. This centrifugal pump had a head of about 70 meters. In the water supply industry, running pump as a turbine is an idea to generate electricity. For this process the pump is used in reverse rotation mode. In the literature there have been some researches about running pumps as turbines [13, 14]. In Schlaffhausen, Switzerland the first pumped storage plant was built in 1909 . The capacity of this plant was 1500 kW. The first significant size pumped storage plant called Niederwartha with 120 MW power was built in Germany in 1928 [12].

After World War II there have been some development about pumped storage system's technology. Power more than 100 MW was built as Cruachan station in Scotland in 1961. After this station, power more than 200 MW was built as Vianden station in Luxemburg in 1970. Then, a multi-stage pumped storage system was built to increase head range like Chiotas station in Italy in 1974 [15].

To store huge quantities of energy a Pumped-Storage system is one of the most efficient way. In this system losses are created from electrical and hydraulic reasons. Hydraulic losses are generated when liquid goes through inside hydraulic

machine parts. Electrical losses are generated by transformer and generator-motor.

Pumped Storage system is used to stabilize power usage in daily period. It does not increase energy supply power at normal conditions. However, if there is a natural inflow into the upper reservoir, this amount of water is used to generate an extra power.

Pumped-Storage system has two cycle. One of these cycle is pumping mode. In this mode, system transfers water with an amount related to upper and lower reservoir difference. In this mode to pump water up, motor ( for reversible pump-turbine there is only one generator-motor ) takes energy from network. This energy depends on head (  $H$  ) and discharge (  $Q$  ) which are the properties of flow from lower reservoir to upper reservoir. But, when head is increased, delivery amount (  $Q$  ) decreases so the power taken from outside of the system is taken as constant. For huge pump-turbines, this power is too great, so network connection should be well designed. Other cycle is turbine mode. In this mode, system generates power with passing water inside a pump-turbine. Generated power depends on head (  $H$  ) and discharge (  $Q$  ). For each head (  $H$  ), system optimum point is used to generate more power.

Pumped-Storage system can be used as complementary for unconventional sources namely solar, wind etc. [16], since a pumped-storage system can start to generate power quickly [15]. So, if there is a necessity of power when the power generating mechanism is unconventional, it can be used to store and use power at a later time. Also this system is free of emissions.

There are some extensive research about pumped storage technology. For instance design features of The Helms Pumped storage Project are described. Mechanical features, electrical features, generator/motors, pump mode operation, transformers, control, protection, station service, powerhouse cranes, startup experiences, rotor dynamics, field pole buckling, thrust bearing, cold loading and project performance were explained. It has been in operation since 1984. Also, cycle efficiency was

given as 72% in 1989 [17]. Cycle efficiency is the ratio of pump power over generated power in turbine mode. It means that 4 kilowatts of input returns about 3 kilowatts.

To utilize river water makes some restrictions about a pumped-storage. For this reason, there are some researches like using seawater. The first pumped-storage using seawater is Okinawa Yanbaru Seawater Pumped Storage Power Station. In this design procedure, main shaft sealing box, wicket gate seal packing, main shaft, wicket gate, runner, spiral case, stay ring, head cover, discharge ring, draft tube are designed by considering the corrosion environment conditions [18].

## **2.2. Pumped-Hydropower Storage System Types**

Hydro Storage Power Plants can be classified into three groups by considering hydraulic equipment forms. These groups are:

1. Four-machine scheme
2. Three-machine scheme
3. Two-machine scheme

### ***2.2.1. Four-Machine Scheme***

In this scheme, pump and turbine systems are used separately. Hydraulic machines (pump and turbine), motor and generator are installed separately. So, design of each components are developed for only one general working condition. Overall efficiency of a system is higher but cost of the installation is too much. This system was used earlier times, since a design of this system is more simple than other schemes. Layout of four-machine scheme Hydro Storage Power Plant is given in Fig. 4.

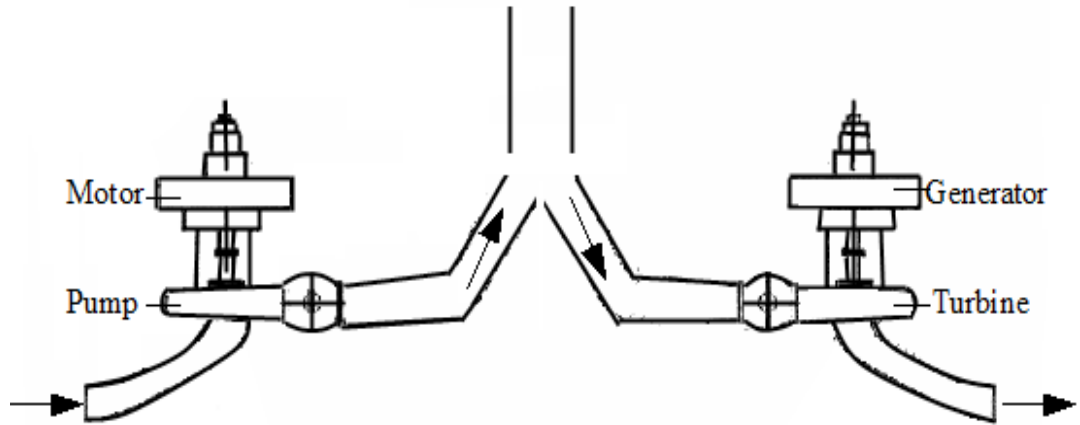


Figure 4. Four-machine scheme: separate pump and turbine units

### 2.2.2. Three-Machine Scheme

In this scheme, pump and turbine systems are used together with connecting one shaft. So, there is only one generator-motor. This scheme is more compact than four-machine scheme. So, an installation cost is less than cost of four-machine scheme. Design of a system as simple as four-machine scheme. However, there is one shaft connected to each machine and generator-motor. Length of this shaft is sometimes too long and it makes some problem on the system. Layout of three-machine scheme Hydro Storage Power Plant is given in Fig. 5.

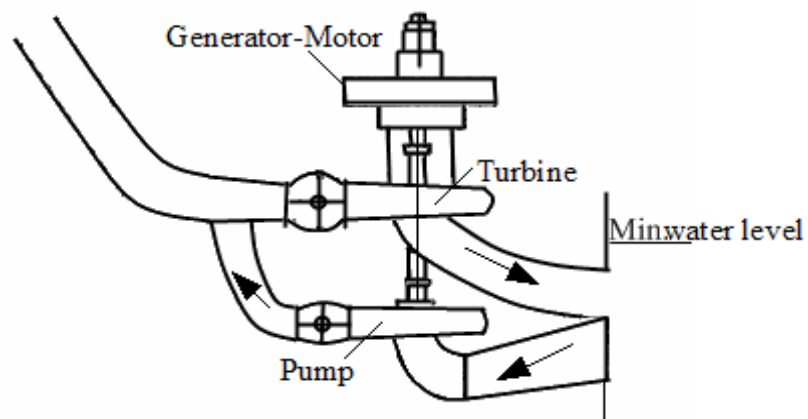


Figure 5. Three-machine scheme: separate pump and turbine units that are connected to one motor-generator

### 2.2.3. Two-Machine Scheme

In this scheme, there is one reversible hydraulic machine which is a Pump-Turbine and one generator-motor. A Pump-Turbine is a hydraulic machine that can work in two modes. It generates power in turbine mode. In pump mode, it transfers water from lower reservoir to upper reservoir. This scheme is most compact case. So, an installation cost is minimum with comparing the other schemes. However, design of a system is the most complicated for this scheme. But with the help of the CFD methods, highly developed computers and programs, a system can be simulated closer to the real behavior. So, design of a pump-turbine can be achieved.

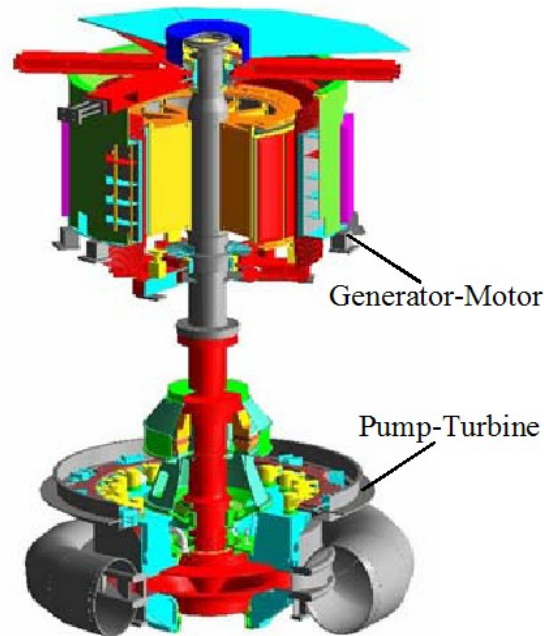


Figure 6. Pump-Turbine cross-section [5]

A Pump-Turbine has two working principles. One of them is converting water potential energy to kinetic energy at the entrance of turbine. A Pump-Turbine runner is rotated with the help of this kinetic energy. This rotation is transferred to a generator-motor by shaft. A generator-motor generates an electrical energy. Other principle is converting an network electrical energy to water potential energy by rotating runner connected to shaft. Same hydraulic machine and generator-motor are used for each working conditions. They are illustrated as in Fig. 6.

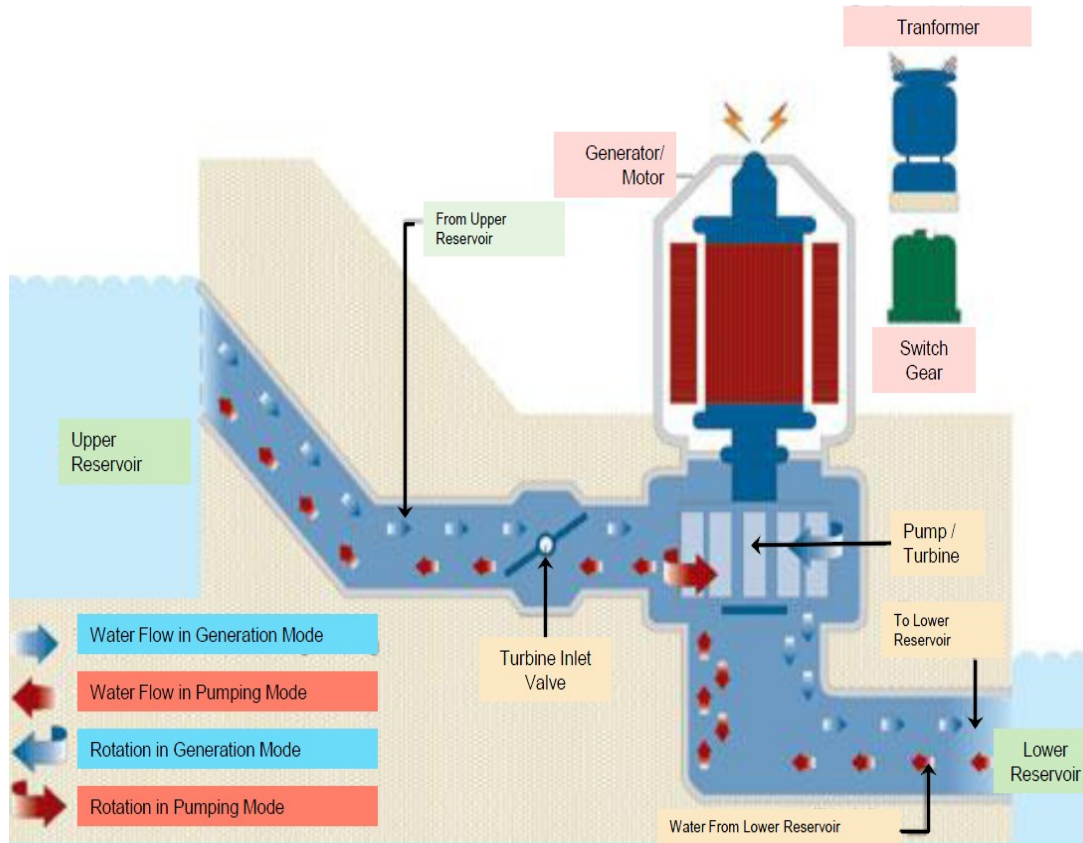


Figure 7. General layout of a Pump-Turbine in a hydropower project [19]

Pump-Turbine parts are illustrated in Fig. 6. A generator-motor generates an electricity by rotating shaft power. This power is generated by transferring water from upper reservoir to lower reservoir in turbine mode. Also, it transfers water by rotating a Pump-Turbine runner. In pump mode, a system takes an energy from network to transfer water from lower reservoir to upper reservoir as shown in Fig 7.

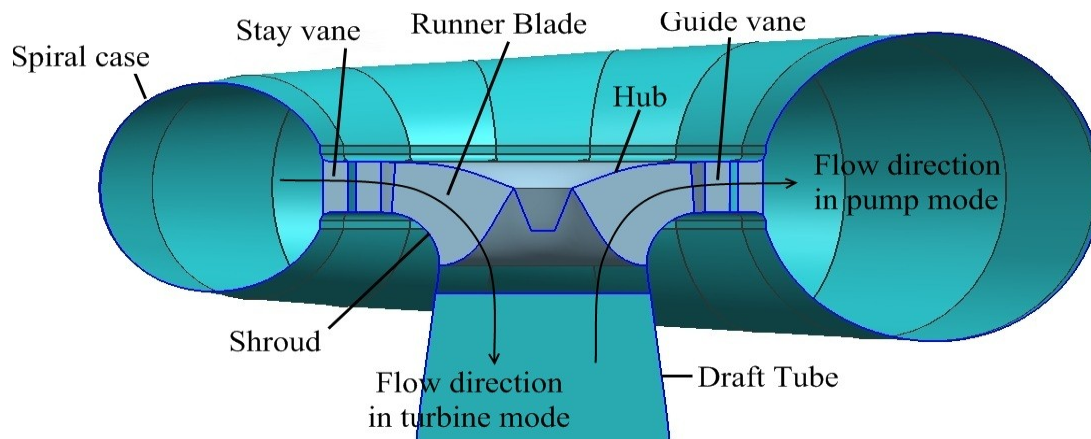


Figure 8. Flow inside a Pump-Turbine in the meridional representation

These type of hydraulic machines are called as radial-axial turbine due to radial inlet and axial outlet conditions. In turbine mode, pressurized water passes through a spiral case. Flow is distributed by a spiral case around runner. Flow passes through stay and guide vanes. Guide vanes determine runner inlet flow angle. After passing vanes, water hits a runner and exits runner axially. Then, it goes through a draft tube as given in Fig. 8.

In pump mode, water is sucked by rotating runner from a draft tube. Then water total energy increases as it passes through runner. After passing water through other components of a machine, it is pumped up to upper reservoir as given in Fig. 8.



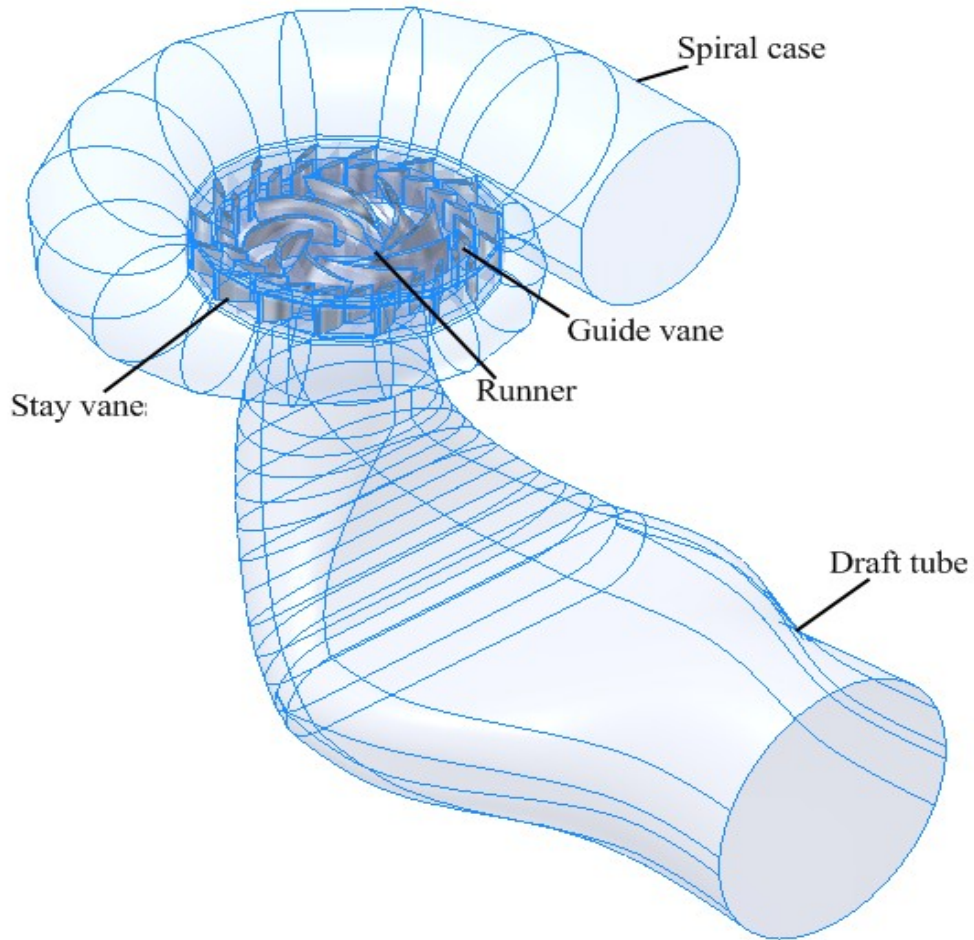


Figure 9. Pump-Turbine components

In this thesis, hydraulic components of a Pump-Turbine are modeled parametrically as shown in Fig. 9. These components are spiral case, stay vanes, guide vanes, runner and draft tube in stream wise direction of turbine mode. In pump mode, water flows in reverse direction. The purpose of a Pump-Turbine parts in turbine mode can be described as:

- ***Spiral Case:*** to distribute flow around stay vanes uniformly
- ***Stay vane:*** to carry the load between the upper and lower head cover as structurally and also to change flow direction before guide vanes
- ***Guide vane:*** to correct the flow angle for runner inlet condition and to control discharge by adjusting guide vane throat area
- ***Runner:*** to rotate a generator shaft by taking the circulated flow energy
- ***Draft tube:*** to increase the static pressure by decreasing the flow velocity

## ***CHAPTER 3***

### ***REVERSIBLE HYDRAULIC MACHINE DESIGN METHODOLOGY***

#### **3.1. Overview of a Pump-Turbine Design Methodology**

Hydro Storage Power Plants are developed according to power and reservoir locations. There are many projects which are available in Turkey as given in Table 2. These projects show that huge amount of power is available for the pumped storage in Turkey. The table shows an available power and difference of two reservoirs. Design head is known for each project. However, design discharge is determined with the number of units. Therefore, there are two main input parameters at the beginning of a Pump-Turbine design. These are design heads and determined design discharges for each unit. Head  $H_t$  and discharge  $Q_t$  of turbine mode are related to head  $H_p$  and discharge  $Q_p$  of pump mode. So, head and discharge values should be chosen properly.

Table 2. Pumped Storage projects in TURKEY prepared by EIEI [1]

	<b>Generated Power (Planned)</b>	<b>Lower Reservoir (Planned)</b>	<b>Upper Reservoir (Planned)</b>	<b>Location</b>
<b>Sarıyar Pumped Storage HES</b>	1000 MW	Sarıyar Dam	435 m above artificial basin	Ankara
<b>Bayramhacılı Pumped Storage HES</b>	1000 MW	Bayramhacılı Dam	161 m above artificial basin	Kayseri
<b>Hasan Uğurlu Pumped Storage HES</b>	1000 MW	Hasan Uğurlu Dam	570 m above artificial basin	Samsun
<b>Adıgüzel Pumped Storage HES</b>	1000 MW	Adıgüzel Dam	242 m above artificial basin	Denizli
<b>Kargı Pumped Storage HES</b>	1000 MW	Kargı Dam	513 m above artificial basin	Ankara
<b>Yalova Pumped Storage HES</b>	500 MW	Yalova Dam	400 m above artificial basin	Yalova
<b>Yamula Pumped Storage HES</b>	500 MW	Yamula Dam	260 m above artificial basin	Kayseri
<b>Oymapınar Pumped Storage HES</b>	500 MW	Oymapınar Dam	372 m above artificial basin	Antalya
<b>Aslantaş Pumped Storage HES</b>	500 MW	Aslantaş Dam	154 m above artificial basin	Osmaniye
<b>Demirköprü Pumped Storage HES</b>	300 MW	Demirköprü Dam	215 m above artificial basin	Manisa

There are many parameters in design of a Pump-Turbine. Also, each turbine can be used for different working conditions. Therefore, a design methodology is developed to design a Pump-Turbine. This methodology is shown in Fig. 10.

After choosing head and discharge values, Pump-Turbine parts are designed with preliminary values calculated by the experience curves and theoretical design methods. After obtaining a preliminary design, it is improved in turbine mode according to the CFD results. Improved parts in turbine mode are simulated with pump mode properties. If they are not work properly in pump mode, they are designed according to pump mode CFD results. Then, they are redesigned in turbine mode by considering pump mode results. After improvement in turbine mode, they are simulated with pump mode properties. This loop continues to obtain final models that are working in each mode properly. This methodology is illustrated in Fig. 10.

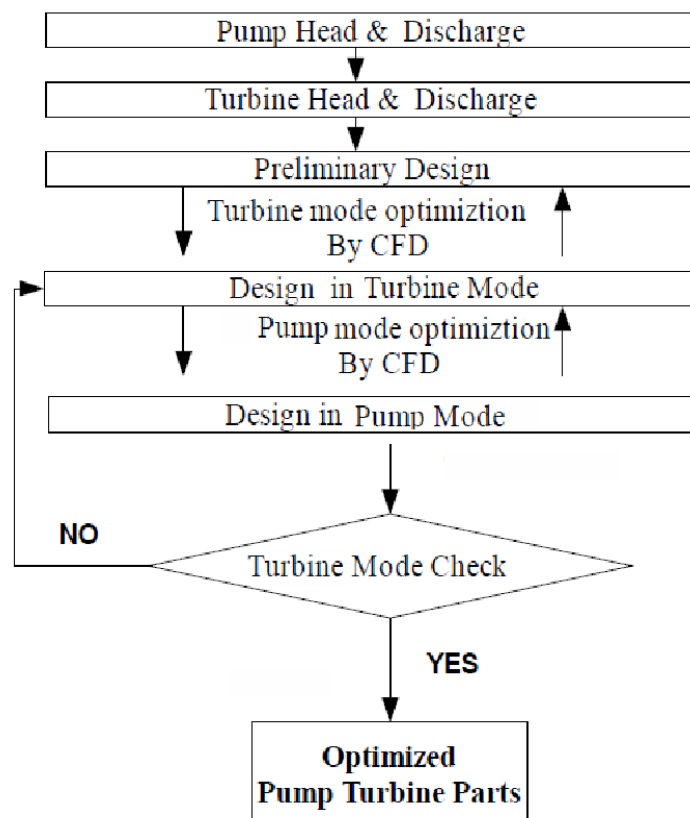


Figure 10. Pump-Turbine design methodology chart

Preliminary parts are simulated for each mode together. These parts can be designed for one mode and they can be checked for other mode. A design procedure can start from each mode. In this thesis, a turbine design is chosen to start due to the experience of a turbine design [11, 20, 21, 22]. Then, pump mode is checked. Designs of Pumped-Turbine parts are changed by considering the CFD simulations results in pump mode. Then, they are designed again in turbine mode and checked for pump mode. This cycle continuous until design requirements in each mode are fulfilled.

A Pump-Turbine design requirements can be described as:

- meridional profile for high performance runner
- shock free entrance at leading edge of each mode
- no swirl at outlet of the runner in turbine mode
- cavitation free runner in each mode
- mesh independence solution

## **3.2. Main Input Parameters of a Pump-Turbine**

### ***3.2.1. Head***

Hydro Storage Power Plants are designed with two reservoirs. Generally one of the reservoirs is chosen as a dam. Properties of other reservoir ( area , location, etc.) are determined by considering the ground. Then, the turbine mode design head  $H_t$  is determined for a plant according to the operating head range. In a Pump-Turbine design, head determination is important.

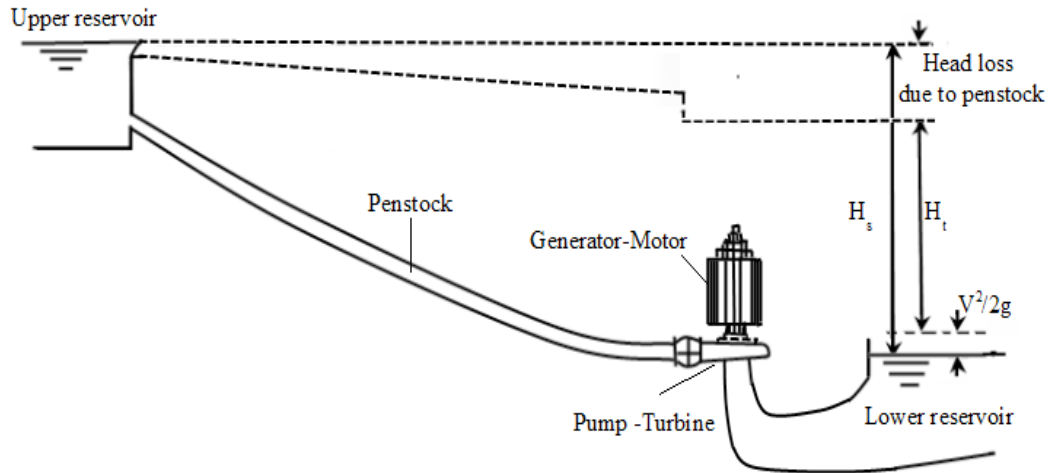


Figure 11. Energy change from the upper reservoir to lower reservoir

The gross static head available is determined with reservoir elevations. However, this head value cannot be used in design of a turbine. Head loss should be considered to transferring water from upper reservoir to lower reservoir. Therefore, design head of a turbine is illustrated in Fig. 11 and it can be determined from the following equation:

$$H_t = H_s - h_L \quad (1)$$

where

$H_s$  : the gross static head available for the turbine

$h_L$  : the head loss term including hydraulic losses

However, a Pump-Turbine should be designed according to both turbine and pumping mode conditions. Head values of pump and turbine are related to each other as in the following equation [6]:

$$\frac{H_p}{H_t} = \eta_t \eta_p \quad (2)$$

where

$H_p$  : pump mode design head [ m ]

$H_t$  : turbine mode design head [ m ]

$\eta_t$  : the Pump-Turbine hydraulic efficiency in turbine mode

$\eta_p$  : the Pump-Turbine hydraulic efficiency in pump mode

The equation (2) can be obtained with Euler equations (60) and (70) for each mode. Therefore, design of a Pump-Turbine can start with turbine mode or pump mode. Efficiency terms in equation (2) will be detailed in the following sections.

### **3.2.2. Power**

Power of Hydro Storage Power Plants is determined firstly for each location like in Table 2. After determination of the number of units, turbine design discharge  $Q_t$  is obtained for power of each unit according to feasible head.

The available power for decided turbine design discharge  $Q_t$  can be given as:

$$P = \rho g Q_t H_t \quad (3)$$

where

$g$  : the gravitational acceleration [ m/s<sup>2</sup> ]

$Q_t$  : the turbine design discharge for one turbine [ m<sup>3</sup>/s ]

$H_t$  : the design head of the turbine [ m ].

### **3.3. Main Design Parameters of a Pump-Turbine**

Main design parameters are used to design a Pump-Turbine for required working conditions. These can be arrange in order as:

1. Efficiency
2. Design discharge
3. Rotational speed
4. Specific speed

5. Turbine Runner Type According to Specific Speed
6. Preliminary Dimensions of the Runner Blade
7. Meridional Profile of the Runner Blade
8. Guide Vane Properties
9. Velocity Triangle Adjustments of Runner Blade
10. Turbine Working Process
11. Euler Equation in Turbine mode
12. Euler Equation in Pump mode

### ***3.3.1. Efficiency***

In a Pump-Turbine, there are two main components: a generator-motor and Pump-Turbine reversible hydraulic machine. So, Overall efficiency contains some terms. First one is an electrical losses from a generator-motor and transformer. Second is hydraulic losses. In this thesis, losses due to a generator-motor, transformer and transmission is not included. Only hydraulic efficiency  $\eta_h = \eta$  is considered. Also, volumetric efficiency which is the ratio of the quantity that passes through inside a Pump-Turbine runner to an actual capacity of it is not included. Turbine efficiency  $\eta_t$  and pump efficiency  $\eta_p$  are the most commonly used efficiency terms for a Pump-Turbine.

In turbine mode, potential energy of water in upper reservoir is used to rotate a generator-motor. But all of this energy is not used. The ratio of the energy obtained from upper reservoir to potential energy of water in upper reservoir gives turbine efficiency (  $\eta_t$  ) of a Pump-Turbine.

In pump mode, an electrical energy is used to rotate a generator-motor. A generator-motor is connected to a Pump-Turbine runner. Then, static pressure and dynamic pressure of water in the lower reservoir are increased. And, water is pumped up from lower reservoir to upper reservoir. The ratio of total pressure increment to an electric energy used gives pump efficiency (  $\eta_p$  ) of a



Pump-Turbine.

By considering efficiency terms mentioned, some of available power can be used due to losses. If power terms, in equation (3), is multiplied by efficiency, the amount of the power that can be generated (design power  $P_d$  in turbine mode) is determined. Therefore, design power can be calculated as in the following equation:

$$P_t = \rho g Q_t H_t \eta_t \quad (4)$$

where

- $P_t$  : the turbine design power [ Watts ].
- $g$  : the gravitational acceleration [  $\text{m/s}^2$  ]
- $Q_t$  : the design discharge for one turbine [  $\text{m}^3/\text{s}$  ]
- $H_t$  : the design head of the turbine [ m ]
- $\eta_t$  : hydraulic efficiency of the turbine mode

Also, power in "metric horsepower" can be calculated as in the following equation:

$$P_{hp} = \frac{P_t}{0.7355} \quad (5)$$

### 3.3.2. Design Discharge

Turbine design power,  $P_t$ , for chosen efficiency value is determined in equation (4). Turbine design head  $H_t$  is also known from the equation (1) and Fig. 11. Therefore, turbine design discharge  $Q_t$  can be calculated with rearranging the equation (4):

$$Q_t = \frac{P_t}{\rho g H_t \eta_t} \quad (6)$$

where

$g$  : the gravitational acceleration [ m/s<sup>2</sup> ]

$Q_t$  : the design discharge for one turbine [ m<sup>3</sup>/s ]

$H_t$  : the design head of the turbine [ m ].

### 3.3.3. Design Rotational Speed

Rotational speed  $n$  of a turbine runner is calculated according to design head  $H_t$  and design power  $P_t$  as in the following equation:

$$n = n_q \frac{H_t^{1.25}}{P_t^{0.5}} \quad (7)$$

where

$n$  : the rotational speed of the runner [ rpm ]

$n_q$  : the specific speed of the runner [ metric hp ]

$H_t$  : the design head of the turbine [ m ].

$P_t$  : the power generated by the hydraulic turbine [ Watts ].

The specific speed of the runner in metric hp  $n_q$  is calculated according to design head as in the following equations:

$$n_q = \frac{c_{nq}}{H_t^{0.535}} \quad (8)$$

$$c_{nq} = \min(2600; 2600 - (200000 - P_t)/365) \quad (9)$$

Number of poles for frequency values are shown in Table 3. Number of poles is chosen from Table 3 below. In a design procedure, design frequency value is chosen as 50 Hz.

Table 3. Generator synchronization speeds

Number of poles	Frequency ( 50 Hz )
2	3000
4	1500
6	1000
8	750
10	600
12	500
14	428
16	375
18	333
20	300
22	272
24	250
26	231
28	214

Rotational speed  $n$ , which is calculated with equation (7), sometimes does not have a value exactly the same value in Table 3. This table values are also used for design of a generator-motor. So, value of a rotational speed of a Pump-Turbine runner should have the value in Table 3. These values are called as synchronous speeds. Synchronous speed  $n_{sync}$  of a turbine can be calculated as in the following formula:

$$n_{sync} = \frac{120 f}{2 (\text{number of poles})} \quad (10)$$

where

$n_{sync}$  : the synchronous rotational speed [ *rpm* ]

$f$  : the frequency [ *Hertz* ]

### 3.3.4. Specific Speed

Specific speed is used to classify hydraulic machines. Same value shows geometrically similar machines. Specific speed definition is different for turbine and pump. It is speed of rotation to ensure 75 l/s delivery at 1 m head for pumps. Also, it is speed of rotation to generate 1 hp power with 1 m head. In this design procedure calculation of specific speed of a turbine is given in the following equation:

$$n_q = n \frac{Q_t^{1/2}}{H_t^{3/4}} \quad (11)$$

where

$Q_t$  : the design discharge for one turbine [ m<sup>3</sup>/s ]

$H_t$  : the turbine design head [ m ]

$n$  : runner speed of rotation [ rpm ]

Specific speed also can be calculated with synchronous speed as in the following equation:

$$n_s = n_{sync} \frac{P_t^{0.5}}{H_t^{1.25}} \quad (12)$$

where

$n_{sync}$  : the synchronous rotational speed of the turbine runner [ rpm ]

$P_t$  : the turbine power [ metric hp ]

$H_t$  : the turbine design head [ m ]

$n_s$  : the specific speed [ metric hp ]

Both specific speed definitions can be used for designing turbines, since each of them shows same machine with different calculated values. In design methodology

of a Pump-Turbine specific speed  $n_s$  is used.

### 3.3.5. Turbine Runner Type According to Specific Speed

Turbine runner can be designed with considering Fig. 3. However, meridional profile is main issue for design of a runner. Meridional profile is adjusted for chosen specific speed. A Pump-Turbine runner should be designed for pump meridional shape. An example of determination general pump meridional profile according to specific speed is illustrated in Fig. 12.

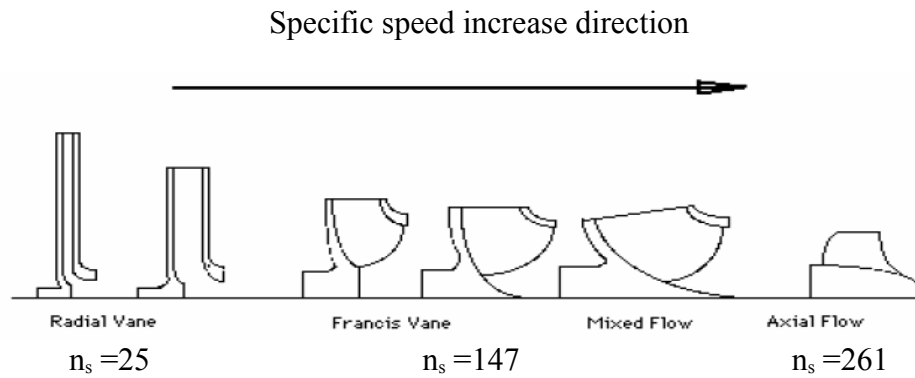


Figure 12. Turbine runner types for specific speed value [23]

Meridional profile of a runner is determined for each specific speed value. Therefore, after designing meridional profile for one specific value, a turbine runner can be designed easily by scaling. After determining runner dimensions, meridional profile of a runner likes the shape above for related specific speed.

### 3.3.6. Meridional Profile of a Runner Blade

Meridional profile of a runner is designed by considering the calculation of the specific speed. Also, runner type gives an information about a runner blade meridional profile shape given in Fig. 12. Preliminary dimensions of a runner is used to illustrate a Pump-Turbine runner meridional section. Blade inlet and outlet locations are defined by meridional profile. Meridional profile is defined by the

cross-section of the revolution of a runner blade on the rotation axis.

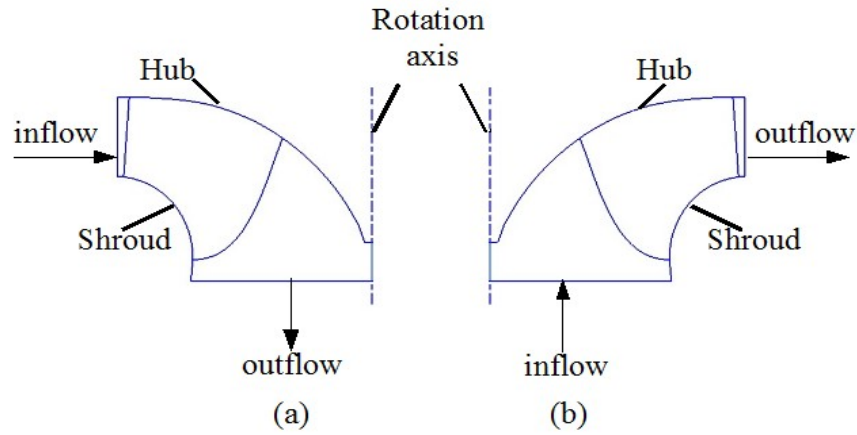


Figure 13. Meridional profile of the runner a) in turbine mode b) in pump mode

Meridional profile of a runner is illustrated in Fig. 13. Turbine mode inflow and outflow directions are given in Fig. 13 (a). Turbine mode inlet angle of a runner blade is designed closer to inflow region in turbine mode in Fig. 13 (a). Pump mode inflow and outflow directions are also given in Fig. 13 (b). Pump mode inlet angle of a runner blade is designed closer to inflow region in pump mode Fig. 13 (b). After adjusting inlet and outlet blade angles, hub and shroud profiles are also adjusted. Hub and shroud profiles also effect performance of a runner. Velocity vectors on meridional section should follow hub and shroud profiles to increase performance of a runner as illustrated in Fig. 40 and Fig. 73.

### 3.3.7. Preliminary Dimensions of a Pump-Turbine Runner

A Pump-Turbine runner diameter is determined according to each mode with the equation (2). Turbine design is detailed in this section.

Once specific speed of a Pump-Turbine is known preliminary dimensions of a Pump-Turbine runner is calculated by empirical curves, where discharge, head, rotational speed and specific speed are main inputs. So, preliminary dimensions of a Pump-Turbine runner are calculated. Preliminary dimensions of a Pump-Turbine

runner are given in Fig. 14.

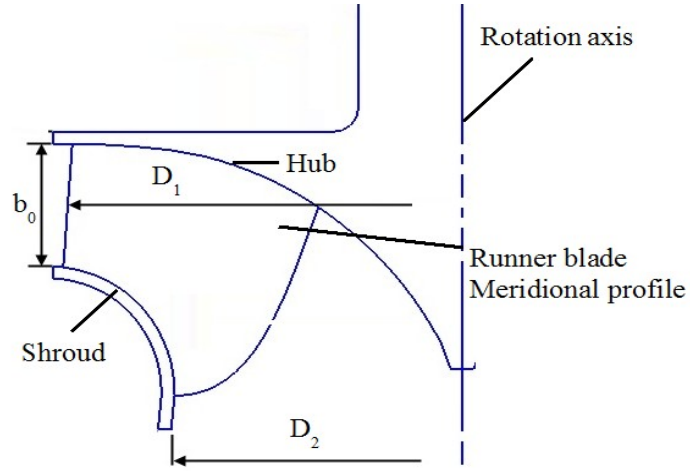


Figure 14. Runner dimensions

Where preliminary dimensions of a runner are:

- $D_1$  : inlet diameter of a Pump-Turbine runner in turbine mode
- $D_2$  : outlet diameter of a Pump-Turbine runner in turbine mode
- $b_0$  : height of a guide vane

Table 4. Preliminary runner dimensions

$D_1$ ( calculated in equation (19) )	1.09 [ m ]
$D_2$ ( calculated in equation (32) )	0.48 [ m ]
$b_0$ ( calculated in equation (34) )	0.05 [ m ]

Inlet diameter of a Pump-Turbine runner in turbine mode  $D_1$  is calculated according to head, discharge, rotational speed and specific speed. Sample calculation of a discharge value is given for head  $H_t=35\text{m}$  and power  $N_{u.t.}=750\text{kW}$  as in the following equation:

$$Q_t = \frac{N_{u.t.}}{g H_t \eta_t} = 2.44 \frac{\text{m}^3}{\text{s}} \quad (13)$$

where

- $H_t$  : the design head of a turbine [ m ]  
 $N_{u.t.}$  : the design power of a turbine [ kW ]  
 $\eta_t$  : the turbine mode efficiency (assumed as 0.9)  
 $Q_t$  : the design discharge of a turbine [  $\frac{m^3}{s}$  ]

After calculating turbine discharge, specific speed  $n_{st}$  is calculated for turbine mode as in the following equations:

$$n_{st} = n \frac{\sqrt{N_{u.t.hp}}}{H_t^{1.25}} = 187.55 \quad (14)$$

where

- $n$  : the runner rotational speed [ rpm ] (chosen as 500)  
 $N_{u.t.hp}$  : the design power of a turbine [ metric hp ]  
 $n_{st}$  : the turbine mode specific speed

$$n_{sp} = (0.85 - 0.95)n_{st} = 169.37 \quad (15)$$

where

- $n_{sp}$  : the pump mode specific speed

After calculating specific speeds, reduced speed of rotation  $n'_{lp}$  is calculated as in the following equation :

$$n'_{lp} = \frac{84.8}{\sqrt{\Psi}} = 91.7 \quad (16)$$

$$\Psi = 1.2 e^{\left(\frac{-n_{sp}}{500}\right)} \quad (17)$$

where

- $\Psi$  : the head coefficient



Reduced discharge in turbine mode  $Q'_{lt}$  is calculated as in the following equation:

$$Q'_{lt} = \frac{\left( \frac{n_{st}}{3.65 n'_{lp}} \right)^2}{\eta_t} = 0.35 \frac{\text{m}^3}{\text{s}} \quad (18)$$

Runner inlet diameter is calculated with reduced discharge in turbine mode, head and discharge as in the following equation:

$$D_1 = \sqrt{\frac{Q_t}{Q'_{lt} \sqrt{H_t}}} = 1.09 \text{ m} \quad (19)$$

The delivery in pump mode  $Q'_{lp}$  is calculated as in the following equation:

$$Q'_{lp} = \left( \frac{n_{sp}}{3.65 n'_{lp}} \right)^2 = 0.26 \frac{\text{m}^3}{\text{s}} \quad (20)$$

Head of pump mode is determined by modifying the equation (2) as in the following equation:

$$H_p = H_t \eta_t \eta_p = 28 \text{ m} \quad (21)$$

where

$\eta_t \eta_p$  : efficiency multiplication of each mode (assumed as 0.8)

Pump delivery is determined by using a delivery in pump mode and equation (21) as in the following equation:

$$Q_p = Q'_{lp} \frac{D_1^2}{\sqrt{H_p}} = 1.6 \frac{\text{m}^3}{\text{s}} \quad (22)$$

### 3.3.8. Guide Vane Properties

Guide vanes not only control the turbine load but also adjust a delivery of pump mode. Pump-Turbines have been designed with and without guide vanes. However, a Pump-Turbine efficiency with guide vanes is higher than others in pump mode [24], since delivery of a pump is adjusted with a guide vane throat area.

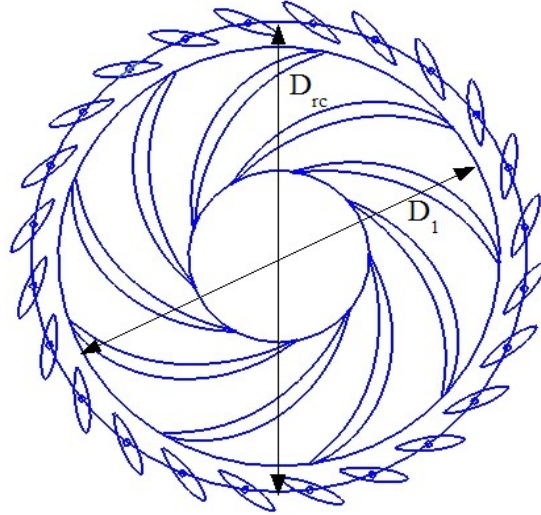


Figure 15. Guide vane regulation center and runner

where

$D_1$  : inlet diameter of a Pump-Turbine runner in turbine mode

$D_{rc}$  : regulation center diameter of guide vanes

After determining runner inlet diameter of a Pump-Turbine in turbine mode, guide vane location and regulation center are adjusted to obtain correct inflow angle of a runner with allowing to pass design discharge between guide vanes. Also, guide vane position and location are determined. Since, guide vanes should not hit a runner at maximum opening condition. Guide vanes and runner are illustrated in turbine mode working condition in Fig. 15.

A regulation system rotates guide vanes about regulation center. Open and closed positions of guide vanes are given in Fig. 16 (a) and Fig. 16 (b) respectively. When flow passes through a spiral case and stay vanes, it is not distributed uniformly. So, guide vanes make it possible to give uniform inflow for a runner by

distributing flow uniformly.

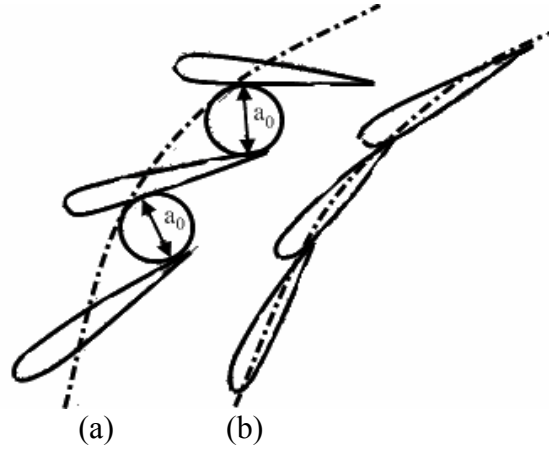


Figure 16. Adjustment of turbine flow rate by guide vanes

Length, profile and number of guide vanes are adjusted to obtain required throat area for design working condition by considering determined guide vane location. Guide vane number is chosen as 12, 16 and 24. In this thesis guide vane number is chosen as 24. Length of guide vanes  $L$  is chosen 10% greater than distance  $t$  between two adjacent guide vane regulation centers to prevent water leakage between guide vanes. So, guide vane length can be designed with equation (23) [6].

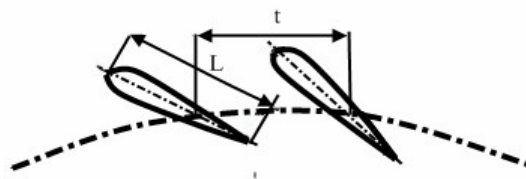


Figure 17. Guide vane properties

$$L/t = 1.1 \quad (23)$$

where

$L$  : the length of a guide vane

$t$  : the distance between two adjacent guide vane regulation centers

So, length of the guide vanes can be determined with the following equation:

$$L = \frac{1}{0.9} \frac{\pi D_{rc}}{n_{gv}} \quad (24)$$

where

$n_{gv}$  : number of guide vanes

Distance between two adjacent guide vane regulation centers also can be determined as in the following equation with assuming arc length as linear.

$$t \approx \frac{D_{rc} \pi}{n_{gv}} \quad (25)$$

Also, throat area of guide vanes can be determined between final guide vanes with the help of CAD programs as given in Fig. 18.

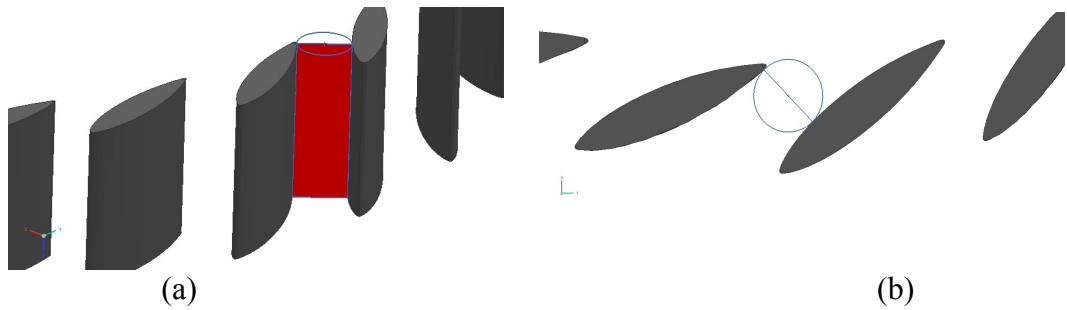


Figure 18. Guide vane throat area a) isometric b) top view

### 3.3.9. Velocity Triangle Adjustments of a Runner Blade

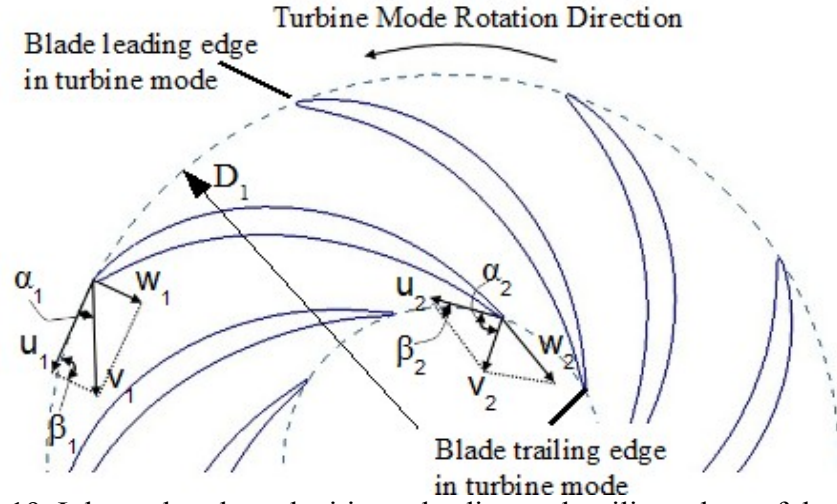


Figure 19. Inlet and outlet velocities at leading and trailing edges of the runner blade

A Pump-Turbine runner works in two mode. So, inlet and outlet locations of a runner changes with related to each mode working condition. The subscript "1" and "2" are chosen as below to prevent a confusion about the inlet and outlet of the runner calculations. A velocity subscript of the velocity "1" shows leading edge of a runner blade in turbine mode and the subscript "2" shows trailing edge of a runner blade in turbine mode. Also subscript "0" represents guide vane outlet location in turbine mode. Fluid velocity  $\mathbf{v}$  in stationary frame at blade leading and trailing edges can be described as vector summation of blade peripheral velocity  $\mathbf{u}$  and relative  $\mathbf{w}$  velocity in cylindrical coordinates as in the following equation:

$$\mathbf{v} = \mathbf{u} + \mathbf{w} \quad (26)$$

where

- $\mathbf{v}$  : the fluid velocity in stationary frame [ m / s ]
- $\mathbf{u}$  : blade peripheral velocity [ m / s ]
- $\mathbf{w}$  : relative fluid velocity [ m / s ]

A blade peripheral velocity can be determined with respect to rotational speed and radial distance from a rotation axis as in the following equation:

$$u = \omega r \quad (27)$$

where

$\omega$  : the angular rotational speed of a Pump-Turbine runner [ 1 / s ]

$r$  : the radial distance from the rotation axis [ m ]

Therefore, relative fluid velocity can be determined as subtraction of blade peripheral velocity from the stationary frame fluid velocity. Then, relative fluid velocity  $\mathbf{w}$  can be obtained. Velocity components can be described as radial  $v_{1r}$  and peripheral  $v_{1u}$  velocity components at leading edge of a runner blade in turbine mode. Moreover, velocity components can be described as radial  $v_{2r}$  and a peripheral  $v_{2u}$  velocity components at trailing edge of a runner blade in turbine mode. These velocities are illustrated in Fig. 20.

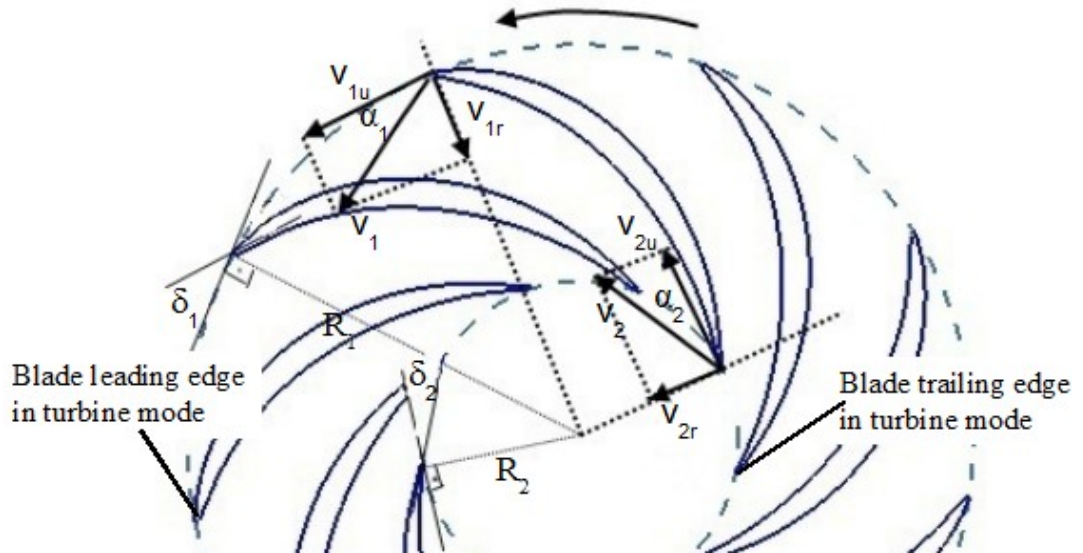


Figure 20. Fluid velocity at the runner inlet and outlet in turbine mode

It is known that flow velocity is sum of radial and peripheral components for cylindrical coordinates. So, fluid velocity at the leading edge of a Pump-Turbine runner in turbine mode:

$$v_1 = v_{1r} + v_{1u} \quad (28)$$

where

- $v_1$  : the flow velocity at runner blade leading edge [ m/s ]
- $v_{1r}$  : the radial velocity component of flow at a runner blade leading edge [ m/s ]
- $v_{1u}$  : the peripheral velocity component of flow at a runner blade leading edge [ m/s ]

Also, the fluid velocity at the trailing edge of a Pump-Turbine runner in turbine mode:

$$v_2 = v_{2r} + v_{2u} \quad (29)$$

where

- $v_2$  : the flow velocity at runner blade trailing edge [ m/s ]
- $v_{2r}$  : the radial velocity component of the flow at the runner blade trailing edge [ m/s ]
- $v_{2u}$  : the peripheral velocity component of the flow at the runner blade trailing edge [ m/s ]

Blade angles are obtained from calculated flow velocities for leading and trailing edges. Then, blade angles are adjusted leading edge to trailing edge in streamwise. Blade leading edge angle  $\delta_1$  and trailing edge angle  $\delta_2$  are illustrated in Fig. 20.

A spiral case, stay vanes and guide vanes are designed with radial and peripheral flow velocity components. However, these radial components in a Pump-Turbine runner are represented as meridional components. So, in turbine mode flow enters radially to a Pump-Turbine runner after passing through guide vanes. Then flow follows meridional path and leaves a Pump-Turbine runner axially in Fig. 21 (a).

Also, in pump mode flow enters axially to a Pump-Turbine runner after passing through draft tube. Then flow follows meridional path and leaves a Pump-Turbine runner radially in Fig. 21 (b). This means that radial component can be described as meridional velocity components in a Pump-Turbine. So, radial velocity components at runner leading edge, trailing edge and outlet of guide vanes can be represented as meridional components.

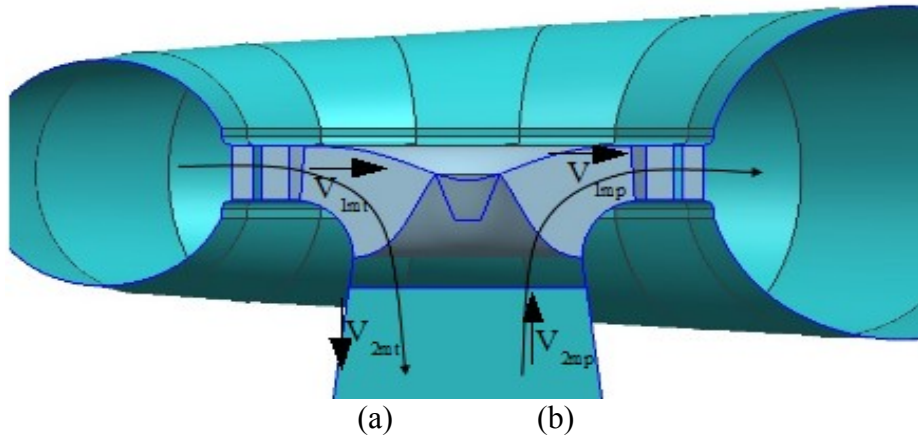


Figure 21. Meridional flow direction in a) turbine mode b) pump mode

Runner outlet condition is designed as axially exit condition in turbine mode. Therefore, there is no peripheral component at trailing edge of a Pump-Turbine runner blade. This condition is described in no swirl condition section.  $v_{2u}$  is chosen in turbine mode calculation as zero and a velocity at the outlet section can be described as only meridional component [6]. So,  $v_2 = v_{2m}$  in turbine mode outlet condition. Also, inlet condition of a runner in pump mode chosen as axially exit condition. So,  $v_2 = v_{2m}$  in pump mode inlet condition.

Outlet diameter of a runner in turbine mode is calculated according to meridional velocity  $v_{2m}$ , since  $v_{2m}$  can be described as in the following equation [25]:

$$v_{2m} = \sqrt{2gH_t \varepsilon} = \sqrt{2 \times 9.81 \times 35 \times 0.268} = 13.57 \frac{\text{m}}{\text{s}} \quad (30)$$



where

$\varepsilon$  : the design variable ( determined as 0.268 for  $n_q=54.3$  [25])

Runner outlet area  $A_2=\pi D_2^2/4$  in turbine mode can be calculated by using design discharge as in the following equation:

$$A_2=\pi \frac{D_2^2}{4}=\frac{Q_t}{v_{2m}} \quad (31)$$

The equation (31) can be rearranged to obtain outlet diameter for turbine mode as in the following equation:

$$D_2=\sqrt{\frac{4 Q_t}{v_{2m} \pi}}=\sqrt{\frac{4 \times 2.44}{13.57 \pi}}=0.478 \text{ m} \quad (32)$$

In the preliminary runner design inlet meridional velocity  $v_{1m}$  is chosen as equal to outlet meridional velocity  $v_{2m}$  [25]. Runner inlet area  $A_1=\pi D_1 b_0$  in turbine mode can be calculated by using design discharge as in the following equation:

$$A_1=\pi D_1 b_0=\frac{Q_t}{v_{1m}} \quad (33)$$

The equation (33) can be rearranged to obtain guide vane height  $b_0$  of a turbine as in the following equation:

$$b_0=\frac{Q_t}{v_{1m} \pi D_1}=\frac{2.44}{13.57 \pi 1.09}=0.053 \text{ m} \quad (34)$$

### 3.3.10. Blade Angles

Blade angles are determined by a blade meridional shape. Stay and guide vane

angles can be determined with considering runner inlet angle in turbine mode. Runner blade metal angle is illustrated as  $\delta$  in Fig. 20. Blade metal angles are determined with calculating flow angle  $\beta$  as illustrated in Fig. 19. Flow angle  $\beta$  is the angle between peripheral and fluid velocity in rotational frame. A Pump-Turbine runner blade leading edge metal angle is determined in each mode separately. When determining metal angles, flow angle  $\beta$  is used. At optimum points, angles  $\beta$  and  $\delta$  are chosen as same values. So, blade metal angles determined with the theoretical methods according to the velocity triangles. Then, they are improved according to the CFD simulation results.

### ***3.3.11. Turbine Working Process***

Design of a Pump-Turbine can be start with each mode. However, the Pump-Turbine design in this thesis is made for turbine design and pump mode working condition is checked due to the experience in turbine design [11, 20, 21, 22]. Therefore, design of the Pump-Turbine is made simultaneously in each mode. Turbine working process can be described in water movement direction. Firstly, potential energy of water is converted to kinetic energy when it passes from upper reservoir to lower reservoir. Some water potential energy can not be used due to losses. Flow created by guide vanes is given in Fig. 22.

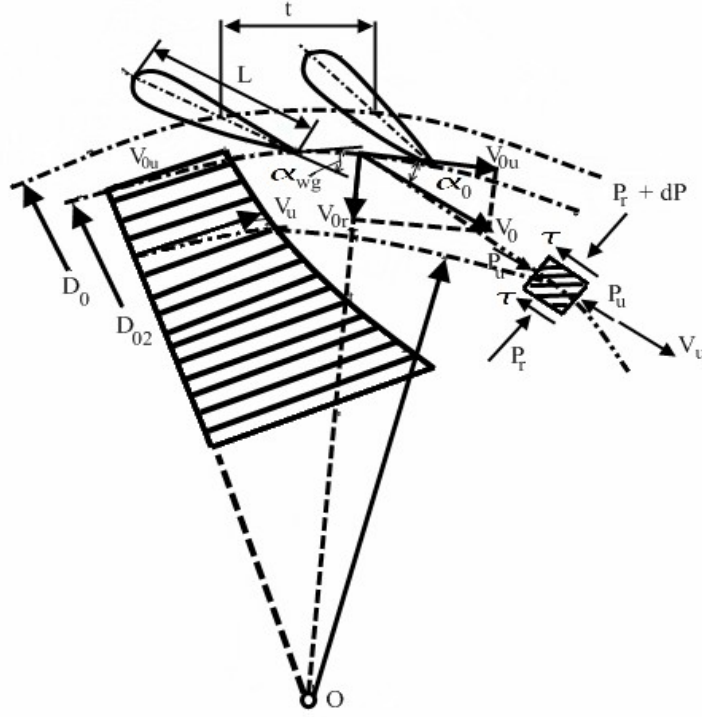


Figure 22. Flow created by guide vanes

Velocity vector components at guide vane trailing edge is used to find the velocity at the inlet condition of a runner in turbine mode.  $D_0$  and  $D_{02}$  in Fig. 22 is chosen as  $D_{rc}$  and  $D_0$  respectively in calculations to prevent confusion. So, the velocity vector components in Fig. 22 can be written as in the following equation:

$$\mathbf{v}_0 = \mathbf{v}_{0u} + \mathbf{v}_{0r} \quad (35)$$

where

$\mathbf{v}_0$  : the guide vane exit velocity [ m/s ]

$\mathbf{v}_{0u}$  : the peripheral guide vane exit velocity component [ m/s ]

$\mathbf{v}_{0r}$  : the radial guide vane exit velocity component [ m/s ]

Water enters a turbine with kinetic energy and turbine parts create circulation around a Pump-Turbine runner. This circulation can be understood with writing water velocity integral around closed curve as in the following equation:

$$\Gamma = \oint_S \mathbf{V} \cdot d\mathbf{S} \quad (36)$$

where

- $\Gamma$  : the circulation in turbine [ m<sup>2</sup>/s ]
- $S$  : the closed contour drawn in the flow in Fig. 22 [ m ]
- $\mathbf{V}$  : the velocity vector of water [ m/s ]
- $d\mathbf{S}$  : the closed contour differential part

Circulation can be rewritten equation (36) by expanding the dot product as:

$$\Gamma = \oint_S V \cos(\widehat{\mathbf{V} d\mathbf{S}}) dS \quad (37)$$

where

- $\widehat{\mathbf{V} d\mathbf{S}}$  : the angle  $\alpha$  between the directions  $\mathbf{V}$  and  $d\mathbf{S}$ .

With considering the equation (37), circulation can be calculated for an average flow downstream of guide vane at outlet diameter  $D_0$  as in the following equation:

$$\Gamma_0 = (\pi D_0) v_0 \cos(\alpha_0) \quad (38)$$

where

- $\Gamma_0$  : the circulation at guide vane outlet diameter [ m<sup>2</sup>/s ]
- $D_0$  : the design condition guide vane exit diameter [ m ]
- $v_0$  : the average flow downstream of the guide vane [ m/s ]
- $\alpha_0$  : the flow angle between the directions  $v_0$  and  $v_{0u}$  in Fig. 22.

Runner inlet circulation can also be calculated with considering Fig. 22. When water flows from guide vane to a runner in turbine mode, it is taken as in free flow [6]. The streamline of fluid particle passing guide vane exit to runner blade leading edge is illustrated as curve in Fig. 22. Elementary mass  $m$  at radius  $r$  is chosen to

streamline properties. It is known that the time derivative of the moment about rotation axis is equal to sum of all external force moments acting upon this elementary mass  $m$  about rotation axis from the law of momentum. So, the momentum law can be defined as in the following equation:

$$\frac{d(mv_u r)_0}{dt} = \sum M_0 \quad (39)$$

where

$m$  : the elementary mass in streamline Fig. 22 [ kg ]

$v_u$  : the peripheral velocity component [ m/s ]

$r$  : the radius about rotation axis of a runner [ m ]

$\sum M_0$ : the sum of all external force moments acting upon this elementary mass  $m$  about rotation axis of a runner [ Nm ]

Sum of the moment can be found by using external forces of the elementary mass  $m$  in Fig. 22.  $P_r$  and  $P_r + dP$  are radial forces and they create no moment about rotation center.  $P_u$  pressure on end faces are equal for an averaged flow and they create no moment about rotation center. Tangential shear forces  $\tau$  are too low and they can be ignored [6]. So, flow between guide vane exit and the runner blade leading edge is obtained as in free flow. The sum of the all external force moments acting upon this elementary mass  $m$  about rotation axis of the runner is assumed zero as in the following equation:

$$\sum M_0 = 0 \quad (40)$$

The equation (39) can be modified by using the equation (40):

$$\frac{d(mv_u r)_0}{dt} = 0 \quad (41)$$

It is obvious that the momentum value is found as constant from the equation (41)

as in the following equation:

$$m v_u r = \text{constant} \quad (42)$$

Elementary mass  $m$  is constant. Therefore, the equation (42) can be modified as:

$$v_u r = \text{constant} \quad (43)$$

The equation (43) shows free liquid flow condition and it is referred to as "*the law of conservation of velocity momentum*". The greater peripheral component of the velocity is obtained at the smaller radius  $r$  according to the equation (43). Therefore, a peripheral velocity component can be written with using guide vane outlet properties as in the following equation:

$$v_u = v_{0u} \frac{D_0}{2r} \quad (44)$$

The circulation at the guide vane exit in equation (38) can be modified as:

$$\Gamma_0 = 2\pi r_0 v_{0u} \quad (45)$$

where

$\Gamma_0$  : the circulation at runner inlet [  $\text{m}^2/\text{s}$  ]

$r_0$  : the radius at runner inlet [  $\text{m}$  ]

The circulation at runner inlet can be written with considering the momentum conservation law according to the equation (45) as:

$$\Gamma_1 = 2\pi r_1 v_{1u} \quad (46)$$

where

$\Gamma_1$  : the circulation at the runner inlet [  $\text{m}^2/\text{s}$  ]

$r_1$  : the radius at the runner inlet [ m ]

From the equations (43), (45) and (46), the circulation is obtained as constant from spiral case outlet to runner inlet as in the following equation:

$$\Gamma = \Gamma_0 = \text{const} \quad (47)$$

As a conclusion, a circulation can be assumed as constant from the guide vane exit to the runner inlet in preliminary design calculations.

### 3.3.12. Euler Equation for Turbine

The momentum law in equation (40) can be applied to flow inside the runner. A runner passage can be chosen as a control volume. So, in turbine mode inflow region, outflow region and walls are chosen as control surfaces of the control volume. Therefore, the net momentum flux is equal to the time rate of change of angular momentum:

$$M_0 = \frac{d(m v_u r)_0}{dt} = \frac{d(m v_u r)}{dt} \quad (48)$$

Where mass  $m$  is constant, so the equation (48) can be modified as in the following equation:

$$M_0 = m \frac{d(v_u r)}{dt} \quad (49)$$

Mass  $m$  is equal to  $\rho Q$ , and the equation (49) can be modified for runner inlet to outlet in turbine mode:

$$M_0 = \rho Q (v_{2u} R_2 - v_{1u} R_1) \quad (50)$$

Design power for a turbine mode can be written in terms of a momentum as in the following equation:

$$P_t = M_0 \omega \quad (51)$$

where

$\omega$  : the angular rotational speed of a Pump-Turbine runner [ 1/s ]

From the equations (50) and (4), the equation (51) can be modified as in the following equation:

$$\rho g Q_t H_t \eta_t = \rho Q_t (v_{2u} R_2 - v_{1u} R_1) \omega \quad (52)$$

The equation (52) can be modified as in the following equation:

$$g H_t \eta_t = (v_{2u} R_2 \omega - v_{1u} R_1 \omega) \quad (53)$$

The peripheral velocity component can be defined as:

$$R \omega = u \quad (54)$$

The equation (53) can be modified with respect to the equation (54) as in the following equation:

$$g H_t \eta_t = (v_{2u} u_2 - v_{1u} u_1) \quad (55)$$

The peripheral velocity components can be expand as:

$$v_u = v \cos \alpha \quad (56)$$

The equation (55) can be modified with respect to the equation (56) as in the following equation:



$$H_t \eta_t = \frac{1}{g} (u_1 v_1 \cos \alpha_1 - u_2 v_2 \cos \alpha_2) \quad (57)$$

The circulation terms can be defined as:

$$\Gamma = 2 \pi R v_u \quad (58)$$

The equation (55) can be modified with respect to the equation (56) and it can be written in terms of circulation as in the following equation:

$$H_t \eta_t = \frac{\omega}{g 2 \pi} (\Gamma_1 - \Gamma_2) \quad (59)$$

The equations (57) and (59) can be written together and the "*Euler equation*" is obtained as in the following equation:

$$H_t \eta_t = \frac{\omega}{g 2 \pi} (\Gamma_1 - \Gamma_2) = \frac{1}{g} (u_1 v_1 \cos \alpha_1 - u_2 v_2 \cos \alpha_2) \quad (60)$$

### **3.3.13. Euler Equation for Pump**

In pump mode, same subscript is used at same location of a runner. Only velocity directions and magnitudes are changed as in Fig. 23. Therefore, the subscript "1" and "2" are chosen as below. Velocity subscript of the velocity "1" shows trailing edge of a runner blade in pump mode and the subscript "2" shows leading edge of a runner blade in pump mode.

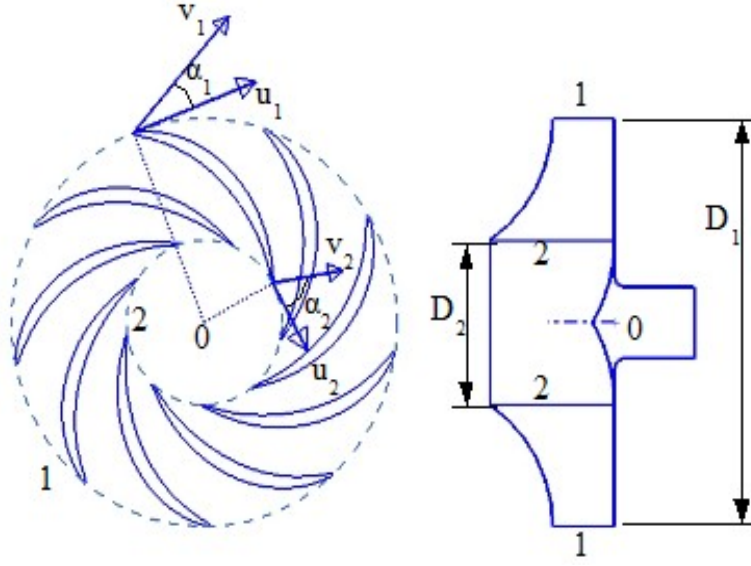


Figure 23. Velocities at leading and trailing edges of impeller pump

The law of momentum can be used to find power of the pump mode as in equation (50). So, the momentum equation can be written for liquid passing through a runner in pump mode shown in Fig. 23 as in the following equation:

$$M_0 = \rho Q_p (v_{1u} R_1 - v_{2u} R_2) \quad (61)$$

where

$Q_p$  : pump delivery amount [ m<sup>3</sup>/s ]

$\rho$  : density of the liquid [ kg/m<sup>3</sup> ]

The average velocity values can be taken for the equation (61) as in the following equations [6]:

$$v_u r = 0.5 D v \cos \alpha \quad (62)$$

Then, torque  $M_0$  can be found with modifying the equation (61) :

$$M_0 = \rho Q_p (0.5 D_1 v_1 \cos \alpha_1 - 0.5 D_2 v_2 \cos \alpha_2) \quad (63)$$

The circulation term in equation (58) can be used to modify the equation (63) as in the following equation:

$$M_0 = \frac{\rho Q_p}{2\pi} (\Gamma_1 - \Gamma_2) \quad (64)$$

The circulation term in a pump is chosen as zero inlet circulation. This condition is also obtained in pump mode results. Then, pump power can be written with using the equation (51) as in the following equation:

$$M_0 \omega = \omega \rho Q_p (0.5 D_1 v_1 \cos \alpha_1 - 0.5 D_2 v_2 \cos \alpha_2) \quad (65)$$

$$M_0 \omega = \rho g Q_p H = \omega \rho Q_p (0.5 D_1 v_1 \cos \alpha_1 - 0.5 D_2 v_2 \cos \alpha_2) \quad (66)$$

where

$H$  : theoretical head of a pump [ m ]

Then, the equation (65) can be modified as in the following equation :

$$g H = \omega (0.5 D_1 v_1 \cos \alpha_1 - 0.5 D_2 v_2 \cos \alpha_2) \quad (67)$$

Head of a pump is not equal to theoretical head of a pump due to hydraulic losses. Head of a pump can be defined with hydraulic losses as in the following equation:

$$\eta_p = \frac{H_p}{H_p + h_{loss}} = \frac{H_p}{H} \quad (68)$$

Then, the equation (67) can be modified with considering equations (54) and (68) as in the following equation :

$$\frac{H_p}{\eta_p} = \frac{1}{g} (u_1 v_1 \cos \alpha_1 - u_2 v_2 \cos \alpha_2) \quad (69)$$

The equation (69) is modified with considering the circulation term in equation (58) to obtain "*Euler equation*" for pump as in the following equation:

$$\frac{H_p}{\eta_p} = \frac{\omega}{g 2\pi} (\Gamma_1 - \Gamma_2) = \frac{1}{g} (u_1 v_1 \cos \alpha_1 - u_2 v_2 \cos \alpha_2) \quad (70)$$

## ***CHAPTER 4***

### ***NUMERICAL SIMULATION AND CFD METHODS***

#### **4.1. CFD Tool Application**

The design of a Pump-Turbine has mainly two requirements. One of them is turbine power and other is pump head. A Pump-Turbine is designed with other design parameters to obtain these requirements mainly. The simulations in this thesis are made with ANSYS v.12 CFX.

In the turbo machinery simulations, there are some difficulties. Meshes should be generated properly for each turbine parts. Furthermore, mesh connections between rotating and stationary part should be chosen properly according to the literature. There are also some researches about rotor-stator interaction in the literature [26, 27, 28, 29]. In this thesis, the interface between rotor and stator is chosen as frozen rotor according to Ansys CFX v.12 user manual [30].

In this thesis, the created parametric parts are modified to reach the requirements in each mode according to the results of the CFD simulations. The parts of the Pump-Turbine are spiral case, stay vanes, guide vanes, runner and draft tube. The spiral case is designed to obtain not only uniform flow distribution at the outlet section of the turbine but also pressure recovery section (volute) of the pump. The stay vane and guide vane are designed to obtain required runner inlet condition. The runner is also designed to obtain smooth pressure distribution from inlet to outlet in each mode simultaneously. Finally draft tube is designed according to the pressure

recovery factor. This design methodology can be supported with the model test results for construction of the HPSP.

#### ***4.1.1. Turbulence Models***

In the simulations, the standard k- $\epsilon$  and Shear Stress Transport (SST) model are used. The standard k- $\epsilon$  model is used in the simulations because it is convenient and one of the simplest model for the hydraulic machinery simulations [31]. SST model is used to catch the flow separations of the runner simulations. Also, the wall functions in the simulations are created automatically according to the mesh quality.

#### ***4.1.2. Advection Schemes***

In the simulations, upwind and high resolution are used as advection schemes. Upwind scheme is used for the preliminary simulations with the course mesh to minimize the simulation requirements. In the preliminary design procedure, wide range is simulated quickly with course mesh, upwind scheme and standard k- $\epsilon$  model. Then, the fine mesh simulations are performed with high resolution advection scheme and standard k- $\epsilon$  model. The runner simulations are also performed with SST model for comparison.

#### ***4.1.3. Discretization Scheme***

In the simulations, finite volume method is used as a discretization scheme. In this scheme, the flow geometry is divided into control volumes. Draft tube mesh is illustrated to visualize the finite volume as in Fig. 24.

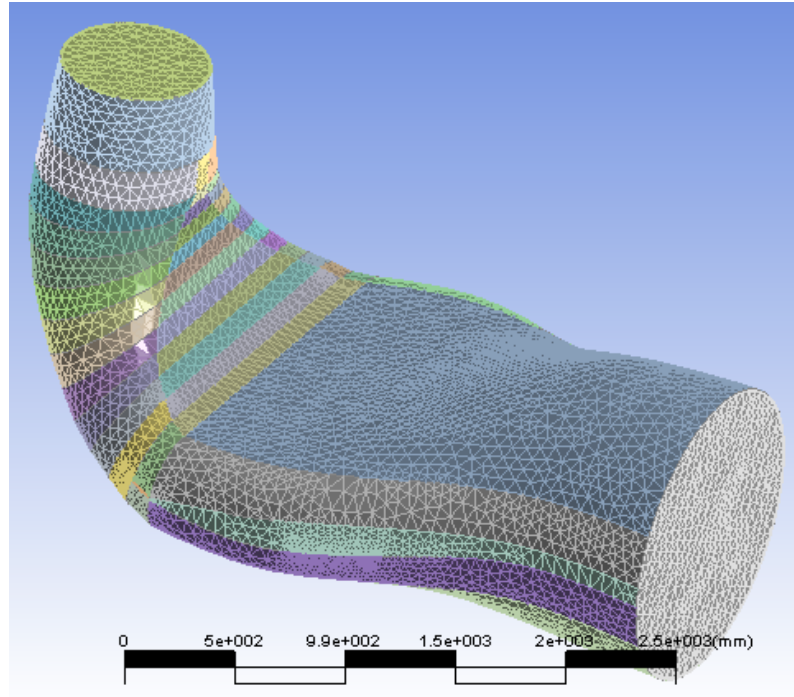


Figure 24. Draft tube mesh (290224 elements and 23392 nodes)

#### 4.1.4. Topology Definition

Topology or the type of grid definitions are important to obtain high quality mesh. TurboGrid in ANSYS v.12 is used to generate the topology of the blades. When creating the topology, mixed topology which includes H/J/L/C-Grid and O-Grid is used together to generate mesh of the runner blades. This type of topology is convenient for the Francis turbine [30].

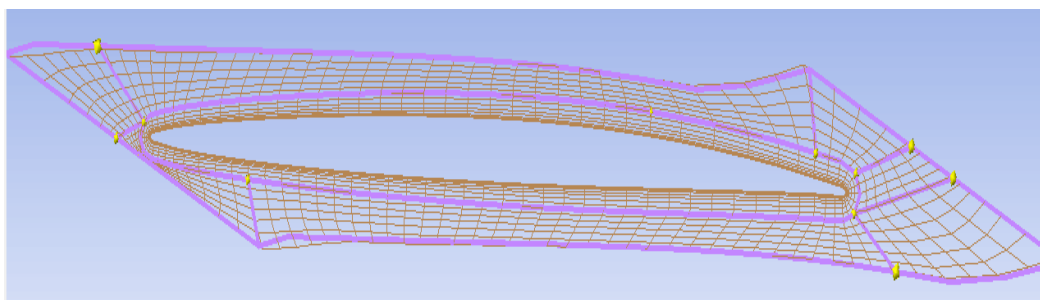


Figure 25. Final runner blade grid topology

Mesh of the guide vanes and stay vanes are also created with mixed topology. O-Grid that creates the loops around the blade is useful to investigate the boundary

layer. The width of the O-Grid is advised as 0.4 as illustrated in Fig. 25, but it can be chosen smaller than this value [30]. The wall and first node difference is defined in the program as:  $y^+$ , normalized or absolute. The normalized option is used in the topology definitions. Also,  $y^+$  on the runner blade surface is investigated and  $y^+$  distribution on the final blade surface is plotted as in Fig. 26. And this tells that runner simulation properties are convenient as a turbine runner.

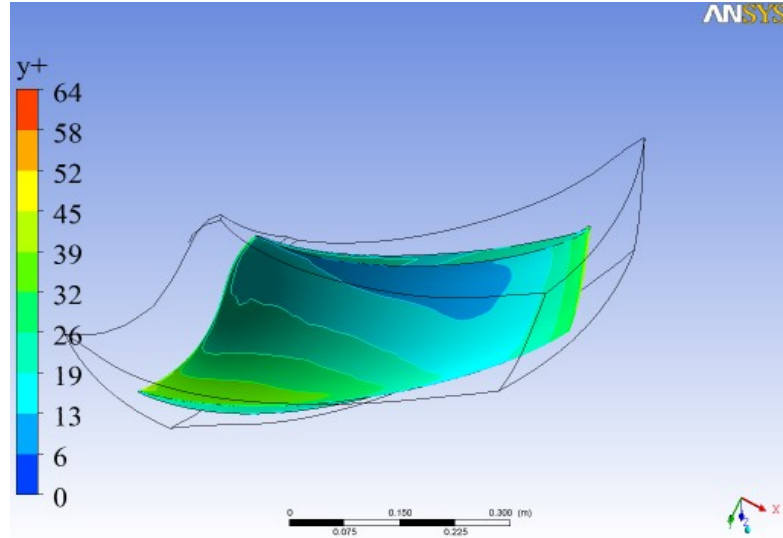


Figure 26.  $y^+$  distribution on the runner blade surface

#### 4.1.5. Generating Mesh

Automatic mesh generation is applied to the blades with TurboGrid according to the decided topology definition. This topology definition makes it possible to generate high quality mesh for the blades with optimizing the face angles. The generated mesh of the runner is illustrated in Fig. 27.



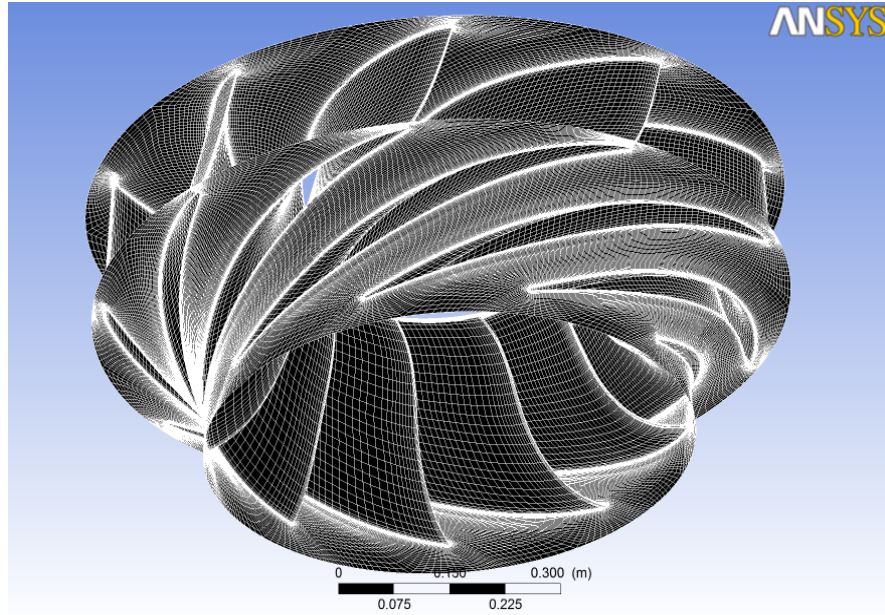


Figure 27. Generated mesh data for final Pump-Turbine runner (238560 elements and 255200 nodes for one runner blade passage)

CFX-Mesh is used for the other parts of the turbine. Draft tube and spiral case geometries are used to generate the CFX-Mesh. When creating the CFX-Mesh, the surface mesh options are used to obtain convenient connection with the blade mesh. In this respect, the inlet of the draft tube and exit of the spiral case are adjusted. Also, the inflation layers ( steady growing mesh thickness ) are generated for the wall of the geometries to give the roughness.

#### ***4.1.6. Mesh Connection***

In the turbine, there are rotating and stationary parts. Stage is used between the stationary mesh connection areas. However, the frozen rotor is used between the stationary and rotating part mesh connection. Also, the mesh connection type and connected mesh options are given as in Table 5.

Table 5. Mesh connection types between mesh of the Pump-Turbine parts

<b>Mesh Connection Location</b>	<b>Mesh Connection Type</b>
Spiral case + Stay vanes	stage
Stay vanes + Guide vanes	stage
Guide vanes + Runner	Frozen rotor
Runner + Draft tube	Frozen rotor

#### **4.1.7. Boundary Conditions**

Table 6. Pump-Turbine runner boundary conditions

	<b>inlet</b>	<b>outlet</b>
<b>Turbine mode</b>	365215 Pa	2 m <sup>3</sup> /s
<b>Pump mode</b>	101325 Pa	1.6 m <sup>3</sup> /s

There are two modes for the Pump-Turbine. The design of the Pump-Turbine starts with the runner design. So, the runner boundary conditions should be chosen carefully. In this respect, the boundary conditions are adjusted for each mode.

In the turbine mode, pressure inlet and mass flow outlet are given as a boundary conditions. These boundary conditions are advised for the turbine simulations [30]. The inlet pressure in turbine mode is chosen by considering the hydraulic efficiency of the spiral case, stay vanes and guide vanes. These hydraulic efficiencies are chosen according to the experiences [11, 20, 21, 22]. Guide vane, stay vane and spiral case are designed after runner design according to the assumed hydraulic efficiencies. After design of the vanes and spiral case, the pressure inlet of the turbine should be controlled. If the results do not match, runner or other parts should be redesigned. In the simulations, the head and discharge values of the turbine are chosen as 28.15 m and 2 m<sup>3</sup>/s to obtain 500 kW power. The runner inlet pressure condition is assumed as 26.9 m and the other parts of the Pump-Turbine are designed according to the runner.

In pump mode, pressure inlet and mass flow outlet are also given as a boundary

conditions. These boundary conditions are advised for the pump simulations [30]. Then, the walls of the runner blade passage mesh chosen as no slip condition. In the pump mode simulations, the inlet pressure and mass flow outlet values of the turbine runner are chosen as 1 atm and 1.6 m<sup>3</sup>/s.

The simulations are performed with the smooth wall assumption. So, the wall roughness are also investigated for the runner simulation to see the effect of the roughness in sections 5.2.6. and 6.2.6. for each mode. Since, the manufacturing methods effect the surface roughness.

Guide vanes are designed after the runner design to obtain required runner inlet condition. The position and profile are also detailed in the following sections. The pressure inlet and mass flow outlet conditions are also given in the guide vane simulations. In pump mode simulations, guide vanes are simulated with the runner.

Stay vanes are designed after the guide vane design to obtain required guide vane inlet condition. The position and profile are also detailed in the following sections. The pressure inlet and mass flow outlet conditions are also given in the stay vane simulations. In pump mode simulations, stay vanes are simulated with the guide vanes.

Spiral case is designed after the design of the vanes. The pressure inlet and mass flow outlet conditions are also given in the spiral case simulations. The cross-sections of the spiral case are adjusted to distribute flow uniformly around the Pump-Turbine runner. In pump mode simulations, spiral case is simulated with the stay vanes.

Draft tube is designed with the runner outlet condition. The pressure inlet according to the runner outlet condition and mass flow outlet conditions are given in the draft tube turbine mode simulations. In pump mode simulations, draft tube is simulated with the pressure inlet and mass flow outlet conditions of pump mode.

## 4.2. Runner Blade Simulation Details

In the runner simulations, the runner mesh is created with predetermined runner dimensions and blade angles. So, the mesh of the runner blade is created including runner blade angles. Runner blade leading and trailing edge angles are calculated theoretically and smooth runner blade angle distribution is obtained from leading edge to trailing edge. The outlet flow angle of the guide vanes are determined by the conservation of circulation. The circulation at the guide vane outlet is calculated with Euler equation by assuming zero swirl at the runner outlet. The circulation is assumed as constant from guide vane outlet to runner inlet. The runner inlet peripheral velocity and radial velocity are calculated from the circulation term. The leading edge angle of runner blade is designed according to relative inlet flow angle. The peripheral velocity component at trailing edge of the runner blade is chosen as zero for swirl free condition. The trailing edge angle of the runner blade is designed according to relative outlet flow angle.

The profile of the runner blade is chosen considering not only turbine mode but also pump mode. After the determination of the angles, meridional profile and blade thickness, the runner blade is created with *BladeGen* that is a blade generator of ANSYS v.12. The simulation of the runner blade is performed according to the boundary conditions of each mode that is discussed in section 4.1.7. Then, the passage is improved according to the CFD results.

The important point of the runner design is determining the meridional section of the runner. The meridional profile of the runner blade is created according to the specific speed that is discussed in section 3.3.4. The meridional profile is designed with adjusting blade angles, hub profile and shroud profile. The final meridional profile of the runner blade is illustrated in Fig. 28.

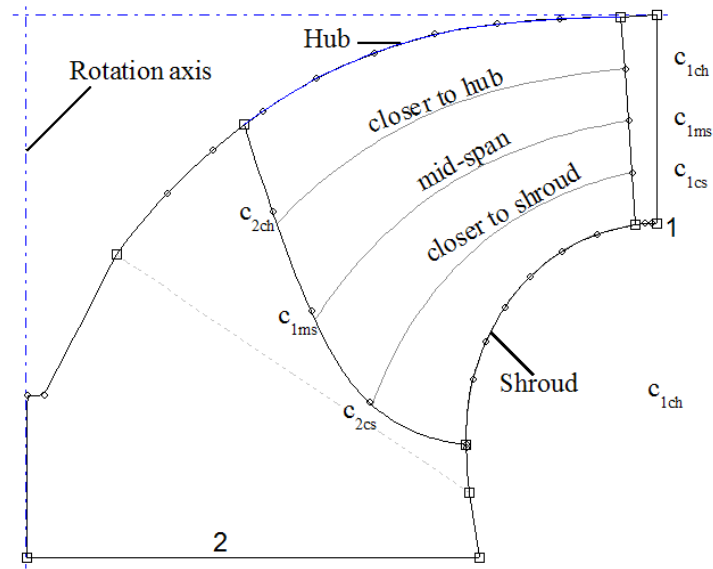


Figure 28. The runner blade meridional section

The blade angles are adjusted for the blade sections: hub, shroud, mid-span, closer to hub and closer to shroud sections. These meridional sections are illustrated in Fig. 28. Turbine mode inlet and outlet sections are described as 1 and 2 respectively. The meridional lines are adjusted with experiences according to the CFD results [11, 20, 21, 22]. When designing the meridional profiles, the blade thickness, blade numbers and blade angles are also adjusted. The number of runner blades is chosen as 9 according to the literature. The blade thickness profile is also chosen as symmetrical NACA 0010-05 with considering not only turbine mode but also pump mode as illustrated in Fig. 29.

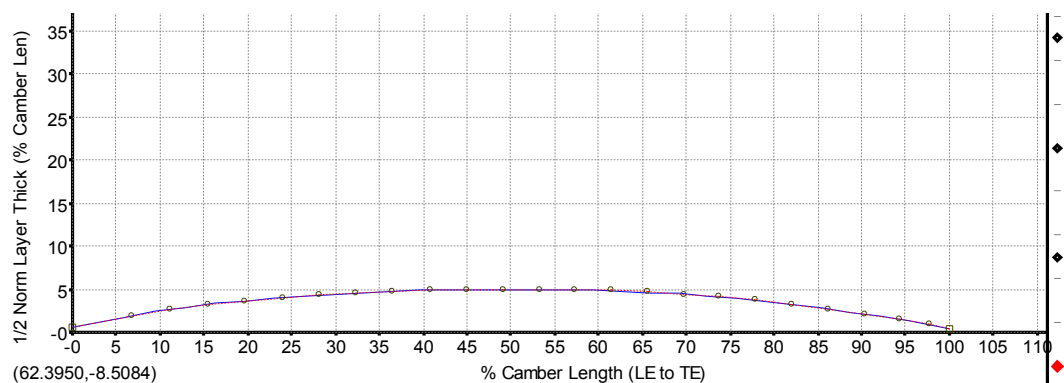


Figure 29. The runner blade thickness profile

The blade angles are calculated according to the theoretical calculations. The runner blade angles are improved with the help of the area distributions taken from *BladeGen* as shown in Fig. 30.

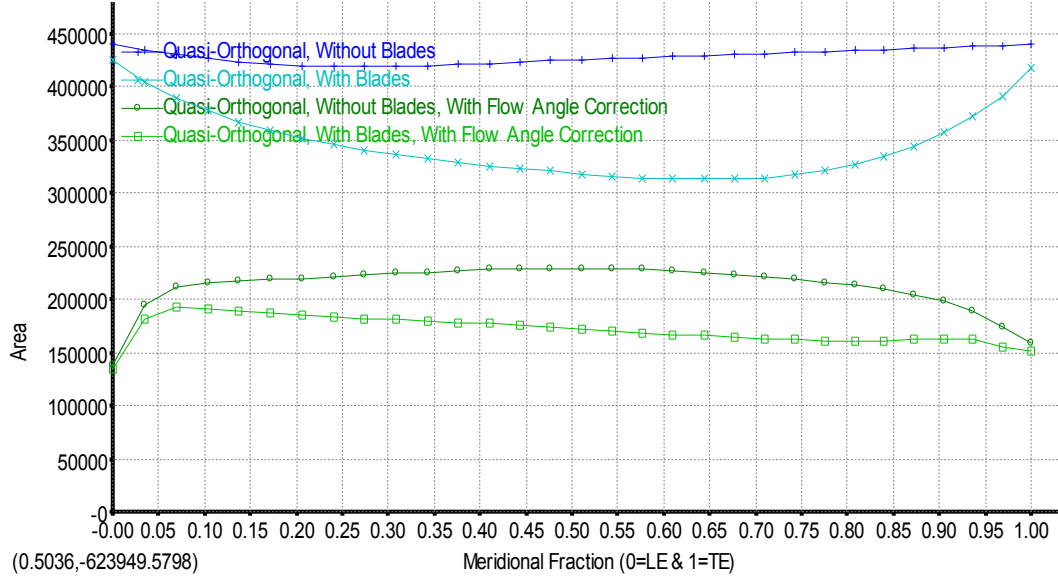


Figure 30. Area distributions of the runner blade passage

The blade angles are calculated considering the area, blade thickness and meridional locations. The point locations in Fig. 28 are used to determine the peripheral speed at that location. The meridional velocity of the flow is calculated with an area obtained from Fig. 30 according to the discharge value. Then, the velocity triangles are calculated for the points on the blade edges in Fig. 28.

#### 4.3. Guide Vane Simulation Details

Guide vanes are designed after the runner design to obtain required runner inlet condition in turbine mode. The calculated inlet flow angle of the guide vane and height of the blades are adjusted to obtain required runner inlet condition. In pump mode, the guide vanes are simulated with the runner. So, the inlet condition of the guide vane is the outlet condition of the runner in pump mode.

#### 4.4. Stay Vane Simulation Details

Stay vanes are designed after the guide vane design to obtain required guide vane inlet condition in turbine mode. The calculated inlet flow angle of the stay vane and height of the blades are adjusted to obtain required guide vane inlet condition. In pump mode, the stay vanes are simulated with the guide vanes. So, the inlet condition of the stay vane is the outlet condition of the guide vane in pump mode.

#### 4.5. Spiral Case Simulation Details

Spiral case is designed after the stay vane design. Since, the outlet section of the spiral case is determined as the stay vane inlet section. The area distribution of the spiral case is determined to distribute flow uniformly around the runner according to the "*law of constance of the velocity moment*" and it is adjusted with the simulation results. The spiral case also simulated with the stay vanes to see their effects to each other.

#### 4.6. Draft Tube Simulation Details

Draft tube flow geometry is determined for the outlet condition of the Pump-Turbine runner. The draft tube flow geometry is created parametrically [11]. Draft tube is designed according to the pressure recovery factor for the turbines as in the following equation:

$$C_p = \frac{P_{\text{out}} - P_{\text{in}}}{\frac{1}{2} \rho \left( \frac{Q_t}{A_{\text{in}}} \right)^2} \quad (71)$$

Where:

- $C_p$  : pressure recovery factor of the draft tube
- $P_{\text{out}}$  : draft tube outlet pressure
- $P_{\text{in}}$  : draft tube inlet pressure

$Q_t$  : turbine design discharge

$A_{in}$  : draft tube inlet cross-sectional area

The pressure recovery factor reaches 0.80-0.85 for good draft tubes [6]. The cross-sections, inlet and outlet angles are designed carefully. Inlet and outlet cone angles are adjusted not to separate flow from the walls of the draft tube. The smooth area distribution is also adjusted from inlet to outlet [11].



## ***CHAPTER 5***

### ***TURBINE MODE RESULTS***

#### **5.1. Final Design Mesh Characteristics**

The mesh data of the final designed Pump-Turbine part is given in Table 7.

Table 7. Mesh characteristics of each turbine component for final design

<b>Component</b>	<b>Mesh type</b>	<b>Number of elements</b>	<b>Number of nodes</b>
Spiral case	Tetrahedral	209602	40152
Stay vane	Hexahedral	240000 (x 12 blades)	256680
Guide vane	Hexahedral	240912 (x 24 blades)	254560
Runner blade	Hexahedral	238560 (x 9 blades)	255200
Draft tube	Tetrahedral	290224	23392

#### **5.2. Runner Simulations in Turbine mode**

The design of the runner is the most difficult part of this thesis. The obtained runner should work not only with turbine mode conditions but also with pump mode conditions.

The runner is designed with not only changing the blade angles but also adjusting the meridional profile. In the design step of the Pump-Turbine runner too many design combinations are tested, because there are many parameters for the runner design. After the preliminary design, each case is simulated to see the results. Then, the final model of the Pump-Turbine runner is obtained. In this section, the

results of the Pump-Turbine runner simulations are illustrated in turbine mode. The calculated preliminary runner dimensions are used in these simulations. The power of the Pump-Turbine in turbine mode with considerable efficiency value is the main target for turbine design condition.

Firstly, the general dimensions of the runner is obtained. In these simulations, the wide range is investigated with the coarser mesh ( approximately  $3 \times 10^4$  elements per 1 blade passage ) and upwind scheme to minimize the computational effort. Finally, the blade angles are adjusted in each mode. In these simulations, the fine mesh ( approximately  $25 \times 10^4$  elements per 1 blade passage ), high resolution and Shear Stress Transform (SST) turbulence model are used to obtain results closer to the real flow behaviors. SST is used to catch flow separations from the walls. Because, the turbulence production term in turbulent kinetic energy equation is modified firstly in SST model and turbulent viscosity is calculated with specific dissipation rate. Therefore, it combines advantages the standard k- $\epsilon$  model and k- $\omega$  model [30].

#### ***5.2.1. Meridional Profile Design in Turbine Mode***

The results of the simulations gives the importance for the meridional profile of the Pump-Turbine runner. In the design procedure, the inlet and outlet locations are decided for the specific speed of the Pump-Turbine. Then the angles are adjusted for the chosen meridional profile.

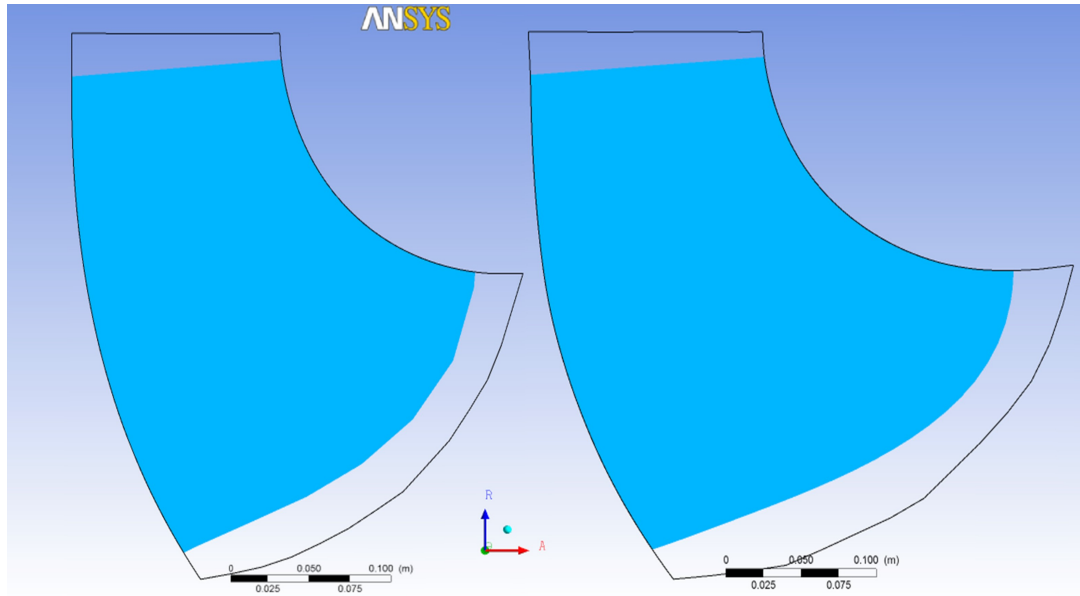


Figure 31. Runner blade meridional shapes: a) preliminary b) final

In this thesis, there is not meridional shape for each specific speed. For this reason, the meridional shape also changed to reach the design requirements with the angles together. The final meridional profile and one of the preliminary designs are illustrated in Fig. 31.

### 5.2.2. Leading Edge Design in Turbine Mode

The angles are calculated according to the rotation speed, runner dimensions, discharge and head. Then, the leading edge of each mode is designed for shock free entrance. After calculating the inlet flow angle, the runner inlet angles are calculated according to the inlet area, flow discharge and rotation speed. However, the angles are not convenient for the real flow behavior due to the estimations. This angle misalignment is defined by pressure distribution around the blades. Furthermore, the velocity vector in the runner blade passage helps to detect the inlet angle misalignment. These velocity vector separations at the leading edge can be used to distinguish inlet angle misalignment. These misalignments are eliminated with the results of the simulations. Then, the velocity vector separations are disappeared.

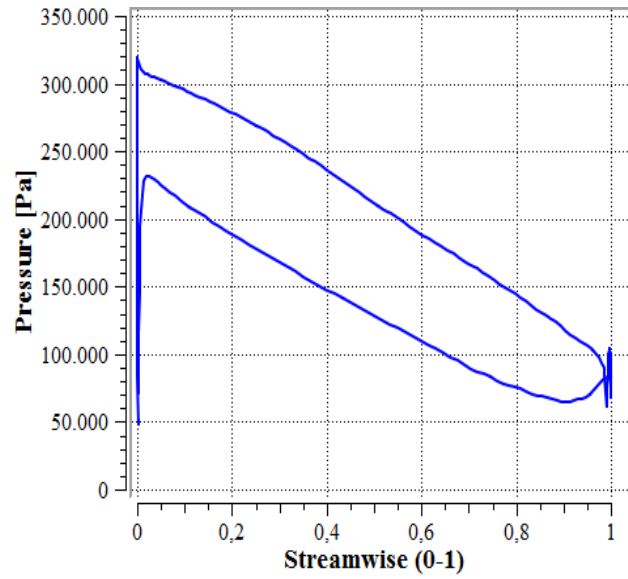


Figure 32. Blade Loading at closer shroud span on non-final blade design

In turbine mode previous simulations, the results show the wrong blade inlet angle due to the peak pressure at the blade leading edge. As an example, one of the previous blade loading of the turbine mode simulation is given in Fig. 32. This peak pressure is eliminated with adjusting the blade leading edge angle of the turbine mode. After adjusting the angles, the blade loading of the runner blade is obtained smoothly. In turbine mode, the blade loading of the final design is given in Fig. 33.

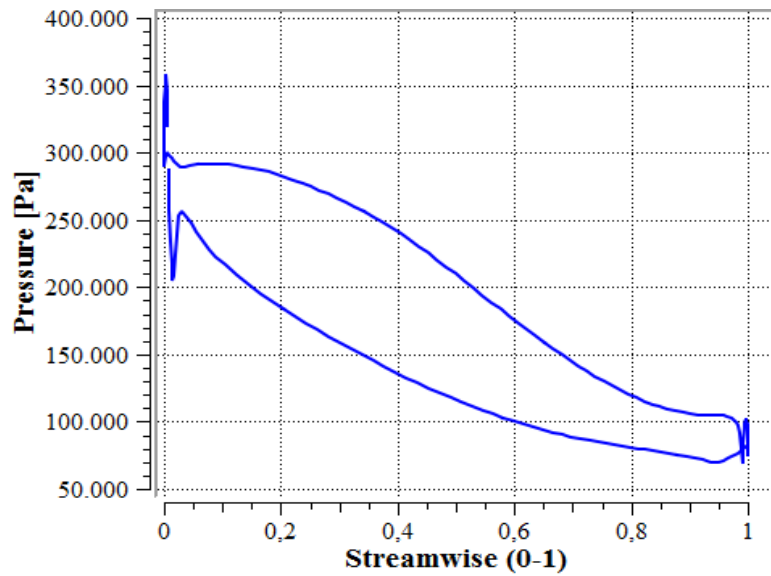


Figure 33. Blade Loading at closer shroud span on final blade design

The inlet and outlet angles of the runner blade are adjusted with not only eliminating the peaks of the blade loadings but also obtaining radially exit flow. Before adjusting the blade angles leading edge to trailing edge, the velocity vectors are plotted to see the blade profile and flow angle inside the runner passage as in Fig. 34.

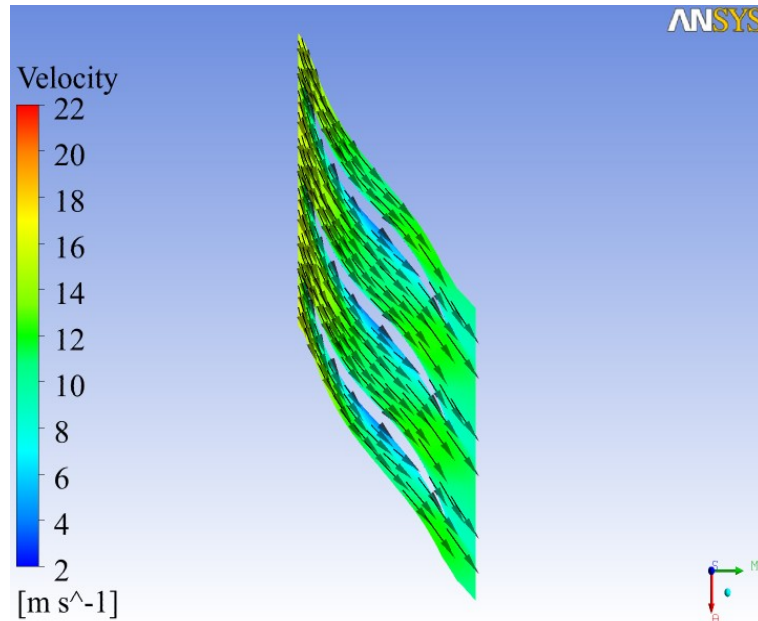


Figure 34. Velocity vectors at closer to the hub meridional section for non-final runner blade

After adjusting the blade inlet and outlet angles, the smooth angle change is made from leading edge to trailing edge of the blade. It is obtained that the profile of the final runner blade is followed by the liquid flow inside the passage. This can be seen from the velocity vector plot of the final runner design in Fig. 35.

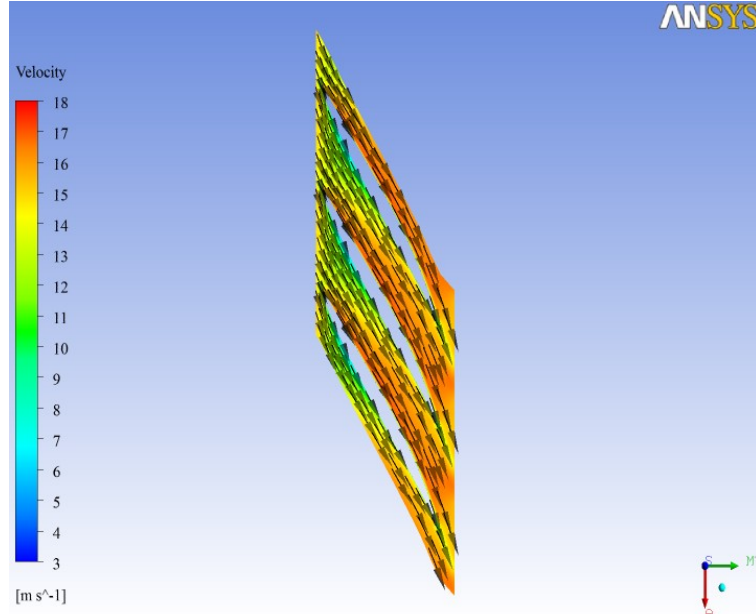


Figure 35. Velocity vectors at closer to the hub meridional section for final runner blade

### 5.2.3. Outlet Swirl Elimination in Turbine Mode

The runner of the Pump-Turbine is designed for no swirl condition. The blade angles are adjusted to obtain no swirl at runner outlet in turbine mode. The swirl at the outlet indicates that the trailing edge blade angles are not convenient for the design condition. The blade angles are adjusted to obtain no swirl condition for the outlet with considering the simulations results. The final blade simulation results are obtained with an outlet angle nearly perpendicular at the trailing edge of the runner blade as given in Fig. 36. Zero alpha degree means the perpendicular outlet condition in turbine mode. Also, the outlet condition of the runner is assumed as no swirl in the design procedure calculations. This results shows the design procedure and results are appropriate each other.

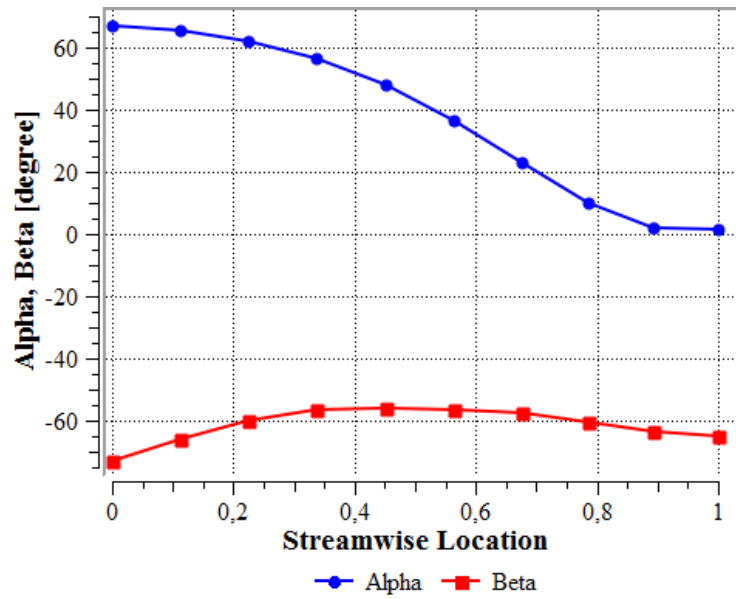


Figure 36. Streamwise Plot of Alpha and Beta in turbine mode

#### 5.2.4. Design without Cavitation in Turbine Mode

The pressure distribution is plotted on blade surfaces to determine and to prevent cavitation on the blade. The pressure on the blade less than water vapor pressure is determined in previous simulations with plotting the pressure contour on the blade surface. In turbine mode, the minimum pressure zone is obtained on suction side. It is closer to the trailing edge of the shroud side.

The pressure contour on the final runner blade for each mode is obtained with minimum pressure greater than the water vapor pressure. The pressure distribution on the runner blade surface in turbine mode is given in Fig.37. Therefore, cavitation on the runner blade is eliminated.

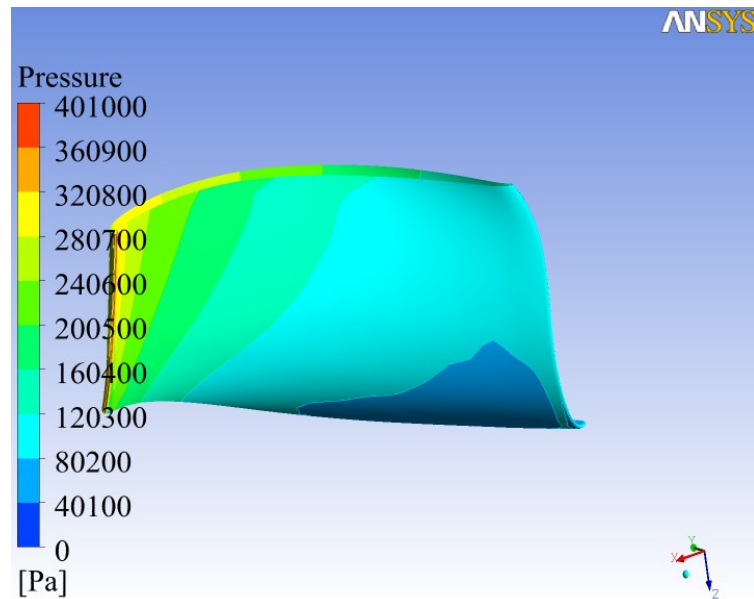


Figure 37. Pressure distribution on the runner blade in turbine mode

The pressure on the blade is also investigated by the stream wise blade loadings. The stream wise blade loadings of the final runner blade at mid-section is plotted in Fig. 38.

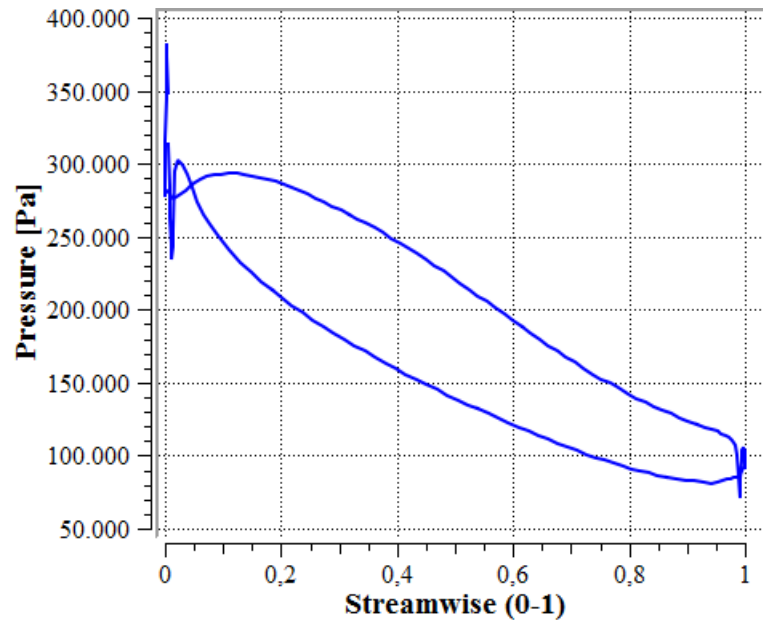


Figure 38. Pressure on the blade meridional section at section closer to the shroud



### 5.2.5. Mesh Independency in Turbine Mode

The aim of the mesh independency is to find the results without change with increasing mesh fineness. The simulation results should converged and they should be independent from mesh fineness.

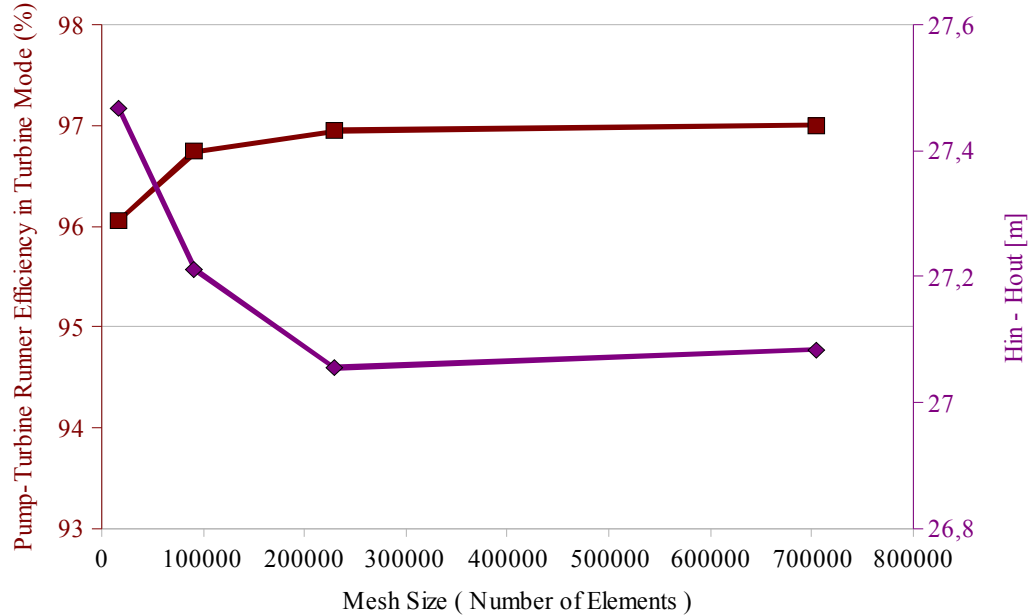


Figure 39. Runner efficiency and head difference versus mesh size in turbine mode

Due to the crucial importance of the design of the Pump-Turbine runner, the results of its simulations are investigated for mesh independency. Consequently, head difference between inlet and outlet of the Pump-Turbine runner and its hydraulic efficiency are plotted in Fig. 37 in turbine mode.

When the number of the mesh element increases, the time and performance needs of the simulation increases. Mesh independency criteria is chosen for nearly constant results to obtain closer results to accurate results. So, the mesh independent solution is adequate for an approximately  $25 \times 10^4$  mesh elements for one runner blade passage from Figure 39 in turbine mode.

#### ***5.2.6. Roughness Effect for the Runner in Turbine Mode***

The roughness effect is investigated to see the effect on the designed components. The walls have been chosen as smooth wall in the simulations. The roughness of the walls should be chosen with considering the manufacturing process of each component. The welding, molding and machining operations determine the surface roughness. Therefore, the roughness effect of the runner surface is investigated due to the crucial importance of the design of the Pump-Turbine. In turbine mode, the hydraulic efficiency of the smooth wall assumed Pump-Turbine runner decreases 0.23 % when the roughness of hub, shroud and blades are chosen as 3.2 micron.

#### ***5.2.7. Runner Blade in Turbine Mode***

In the simulations, the calculated angles and dimensions of the runner are used, also these parameters are given in Table 4. After some simulations, the runner blade shape chosen as NACA 0010 – 05 to obtain uniform exit conditions for each mode with adjusted leading edge profile and angles. A runner efficiency is reached enough to obtain 500 kW energy from the head of 28.15 meters and discharge of 2 m<sup>3</sup>/s. The velocity vectors in meridional view show that the flow does not separate and follows the meridional paths of the runner passage as shown in Fig. 40.

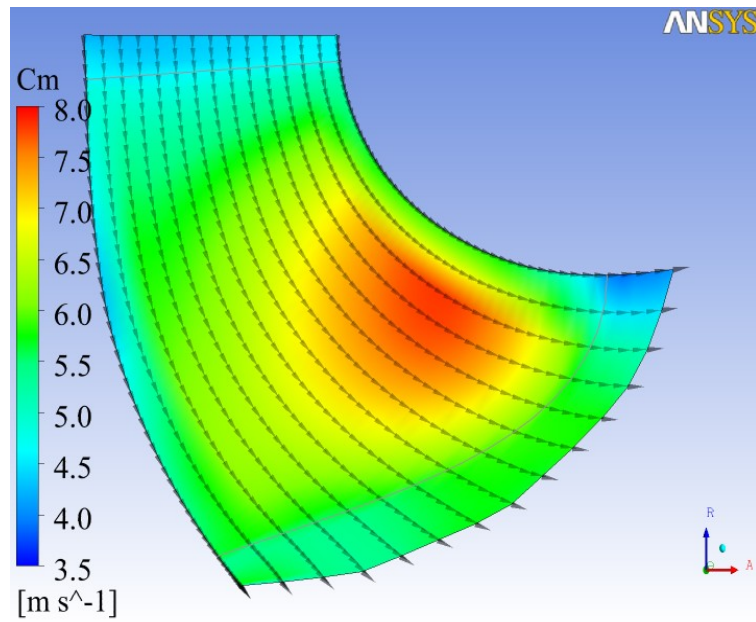


Figure 40. The velocity vectors on meridional section in turbine mode

The pressure distribution in meridional view show that the flow pressure decreases smoothly in meridional section of the runner as shown in Fig. 41.

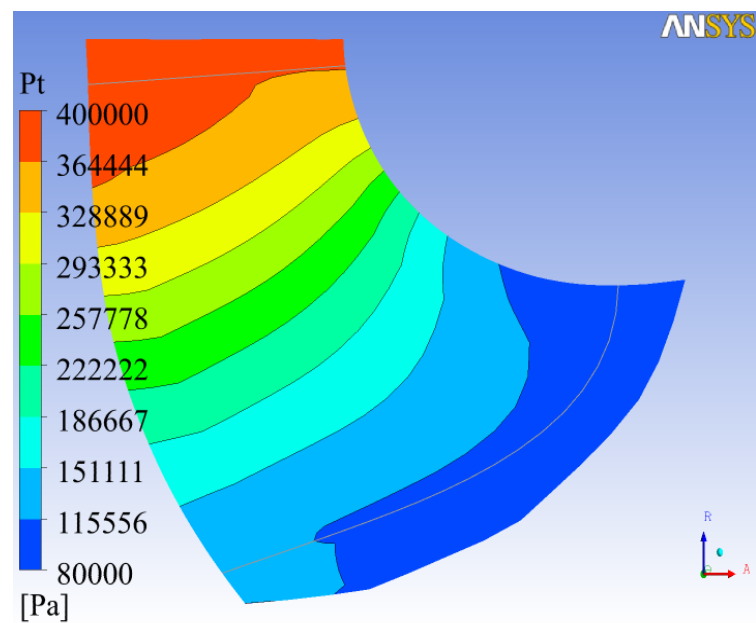


Figure 41. Total pressure distribution on meridional section in turbine mode

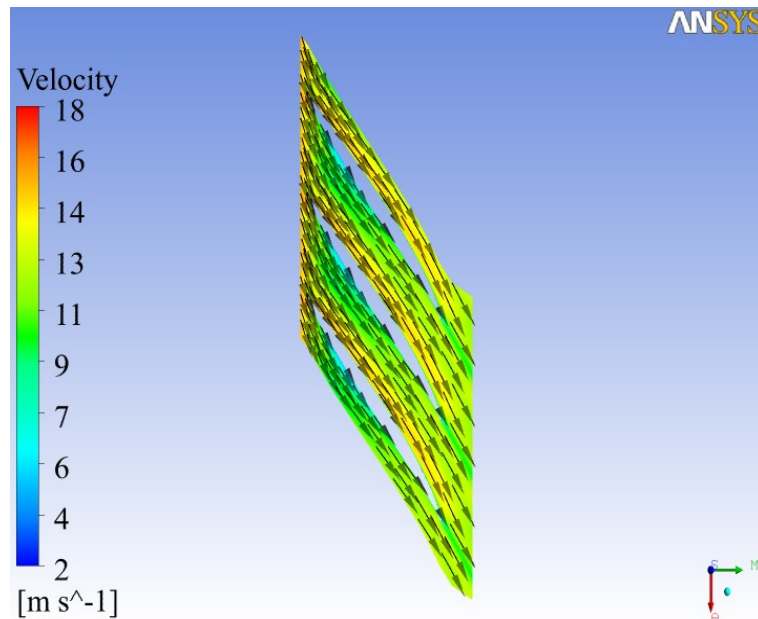


Figure 42. Velocity vectors at meridional mid-section in turbine mode

The velocity vector are plotted to detect the flow separations. After adjusting the blade angles, it is obtained that the flow inside the runner follows the blade profile. The mid-section meridional velocity vectors are plotted and no separation is detected as shown in Fig. 42. Also, closer to the hub and shroud velocity vectors are plotted to see the flow behavior in Fig. 43 and Fig. 44 respectively.

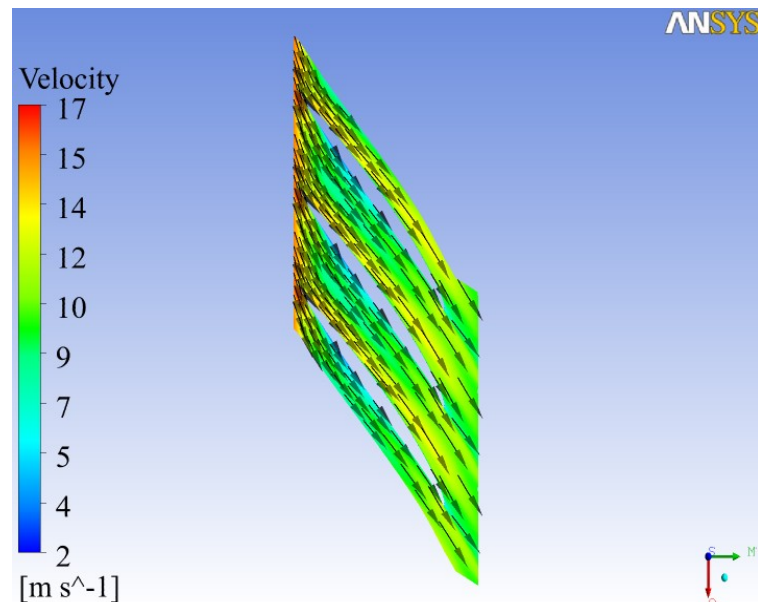


Figure 43. Velocity vectors at closer to the hub meridional section in turbine mode

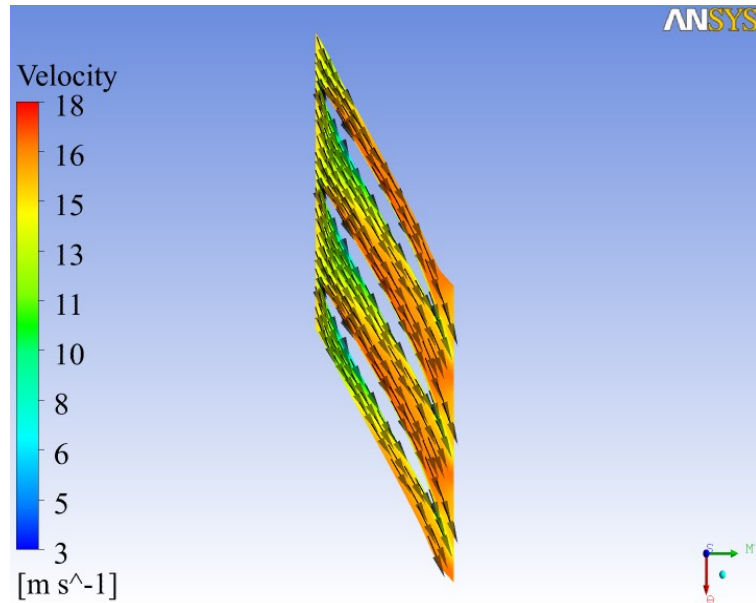


Figure 44: Velocity vectors at closer to the shroud meridional section in turbine mode

The velocity vector show that the flow inside the runner follows the blade profile as illustrated in Fig. 45. So, the 3-D streamlines are also plotted for checking inter blade vortex formation and no visible formation occurs.

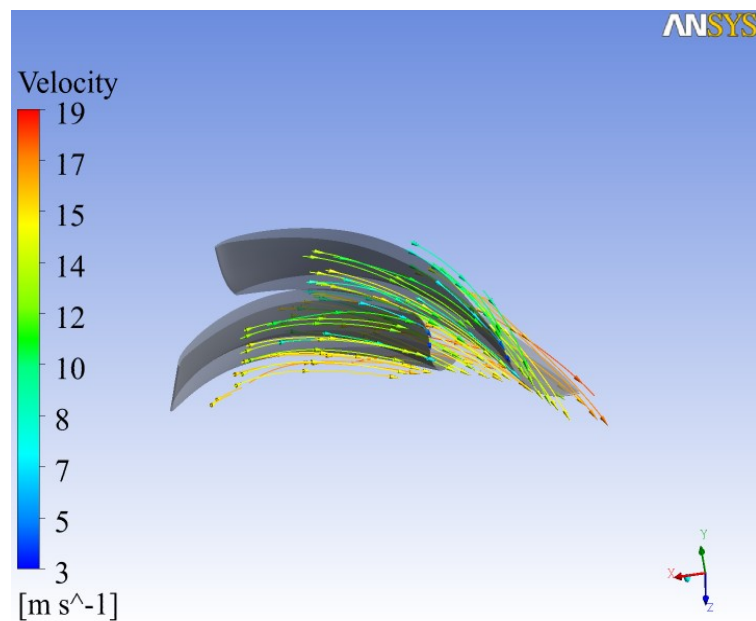


Figure 45: Velocity streamlines in runner blade passage in turbine mode

### 5.3. Spiral Case Results in Turbine Mode

The spiral case is used to distribute flow uniformly around turbine runner in turbine mode. Therefore the spiral case is designed to distribute flow uniformly around the guide vanes. After designing the spiral case in turbine mode, the flow behavior inside is investigated in pump mode.

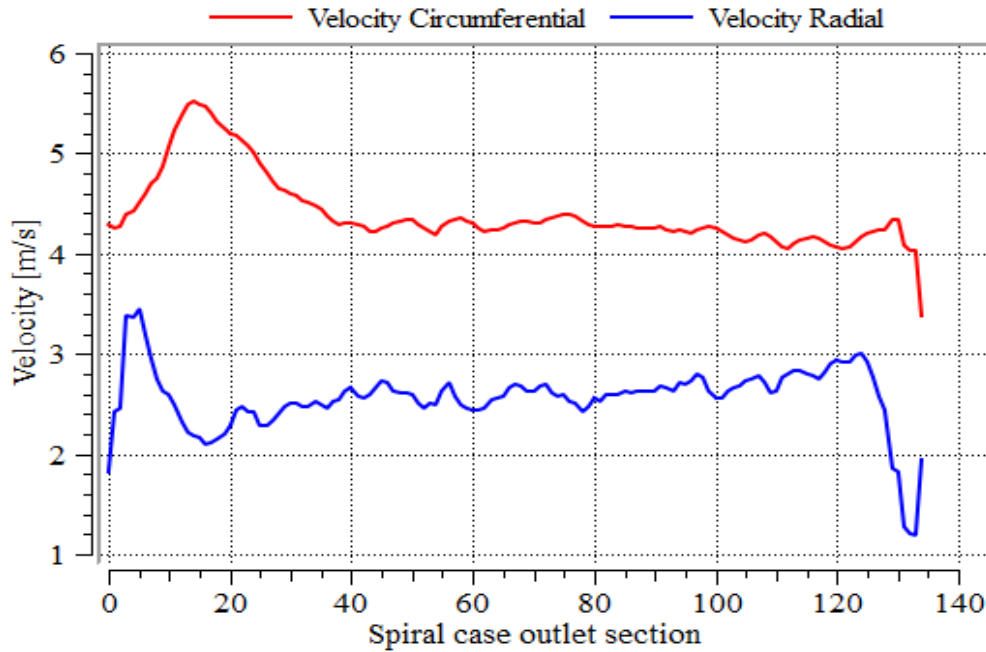


Figure 46. Radial and peripheral velocity distributions at the spiral case outlet

The spiral case is designed to obtain radially uniform exit condition. To understand the results of the simulations, the radial flow velocity at the exit location of the spiral is plotted Fig. 46 in turbine mode. The exit radial velocity distribution is almost smooth except small section. This flow condition is enough for a balanced operation of the turbine from the experiences [11, 20, 21, 22]. The total pressure distribution on the spiral case mid-plane is plotted in Fig. 47.

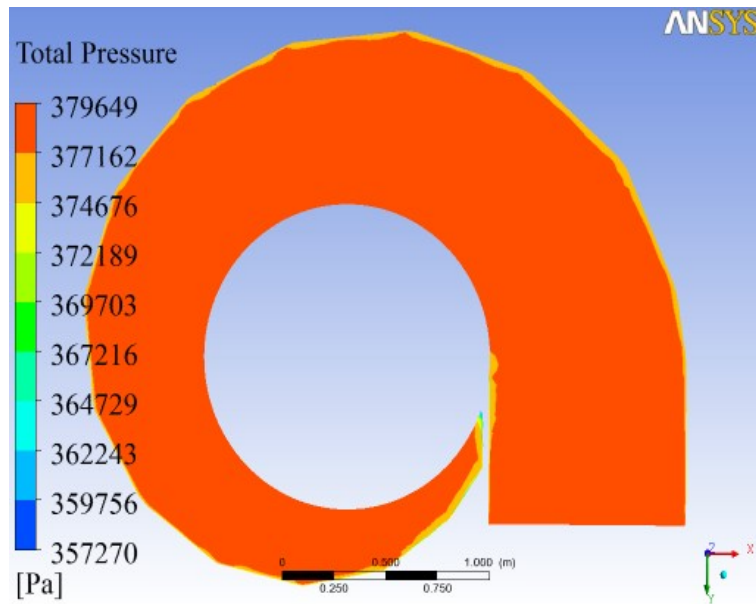


Figure 47. Total pressure distribution on the spiral case mid-plane in turbine mode

The pressure distribution and velocity vectors are plotted to illustrate the flow inside the spiral case. The turbine mode pressure and velocity distributions are plotted in Fig.48 and Fig.49 respectively.

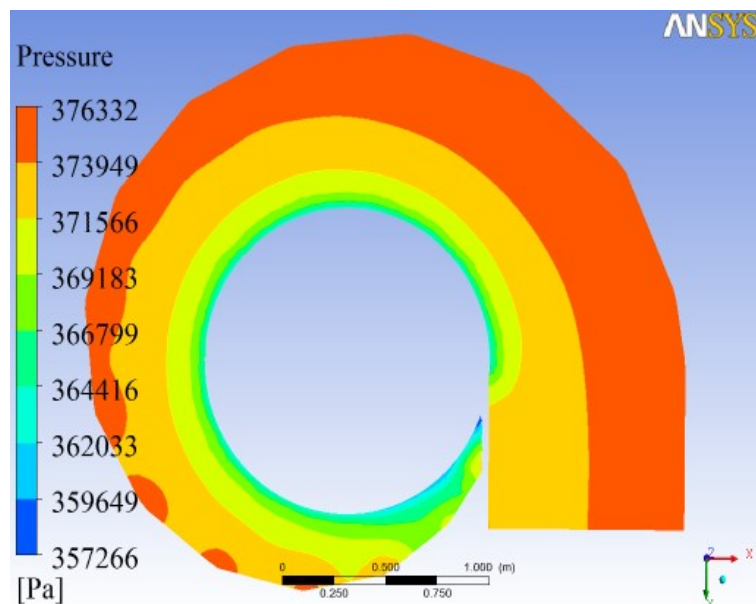


Figure 48. Velocity vectors on the spiral case mid-plane in turbine mode

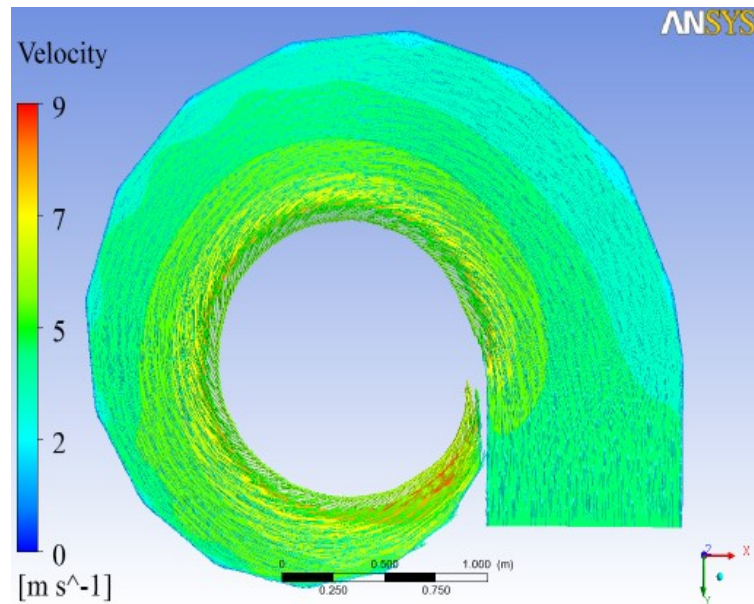


Figure 49. Velocity vectors on the spiral case mid-plane in turbine mode

#### 5.4. Stay Vane Results in Turbine Mode

When defining the stay vane profile, NACA profiles are chosen from Bladegen. These profiles are chosen with considering not only the better flow behavior but also structural reasons. Because the main function of the stay vanes is to carry the hydraulic load of the turbine upper and lower parts. A symmetrical NACA 0030-05 profile is chosen for the stay vanes from the results of the simulations.

In the turbine mode, the stay vane optimum angle is adjusted with respect to the inlet condition of the guide vanes. The inlet angle of the fluid is also determined from the design of the spiral case. Then, blade loadings of the stay vanes are investigated at mid-section, closer to the shroud and closer to the hub regions. The mid-span loading distribution of the stay vane is plotted in Fig. 50 .



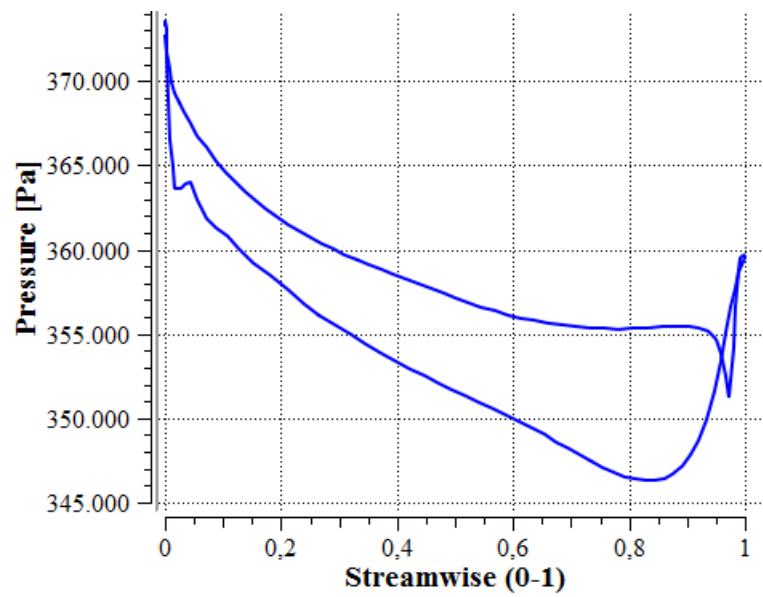


Figure 50. Blade loading on stay vane at mid-meridional section in turbine mode

The average stream wise total pressure is investigated for the hydraulic losses of the stay vanes. The average total pressure and static pressure versus stream wise location is plotted in Fig. 51 in stay vane passage. The average total pressure decreases 373318 Pa to 373046 Pa from leading edge to trailing edge of the stay vanes.

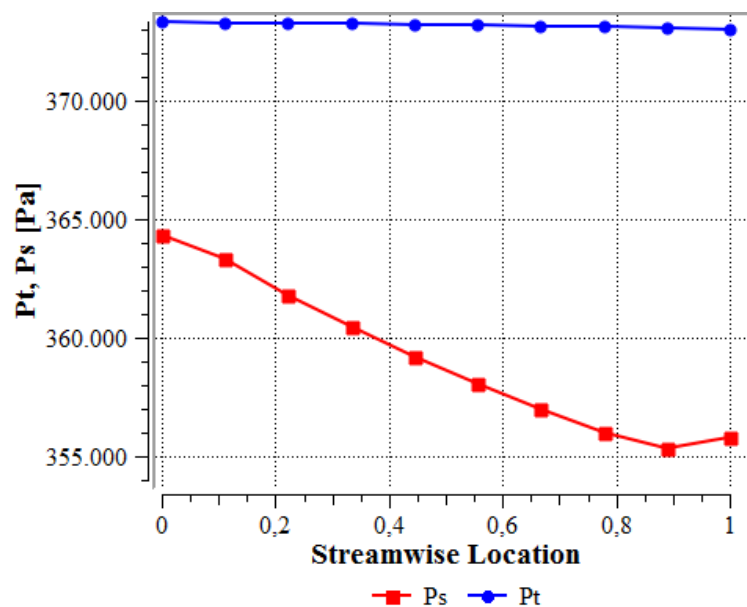


Figure 51. Streamwise Plot of Total pressure and Pressure through the stay vane passage in turbine mode

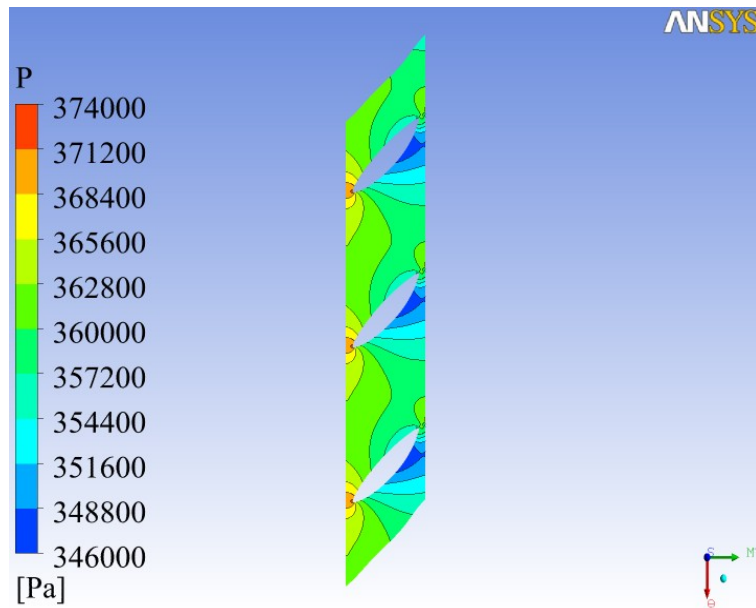


Figure 52. The Static Pressure Distributions in stay vane passage in turbine mode

The distribution of the static pressure contour in stay vane passage, that is given in Fig. 52, illustrates the gradual pressure decrease in the passage. This shows that the inlet and outlet angles of the stay vane for the passage are convenient from the literature and experiences [11, 20, 21, 22].

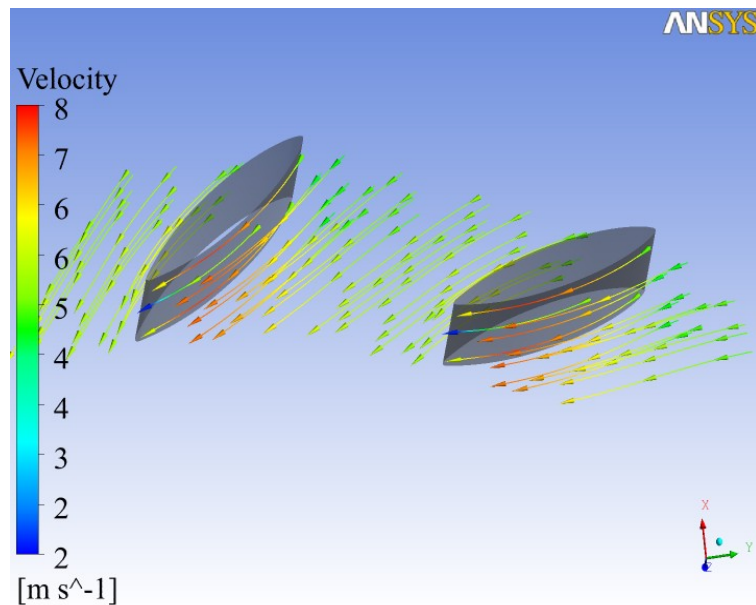


Figure 53. Velocity streamlines in stay vane passage in turbine mode

The velocity streamlines in stay vane passage are also illustrated to check inter blade vortex formation and no visible formation occurs between the stay vanes in Fig. 53. The velocity vector show that the flow inside the stay vane passage follows the blade profile. The stay vanes are also simulated with the spiral case to see the effect of the adjacent parts. The velocity vectors and total pressure distribution on the mid-plane of the spiral case are plotted in Fig. 54. The distribution of the total pressure is almost uniform except the last section. This pressure distribution is convenient for the Pump-Turbine working conditions from the literature and experience.

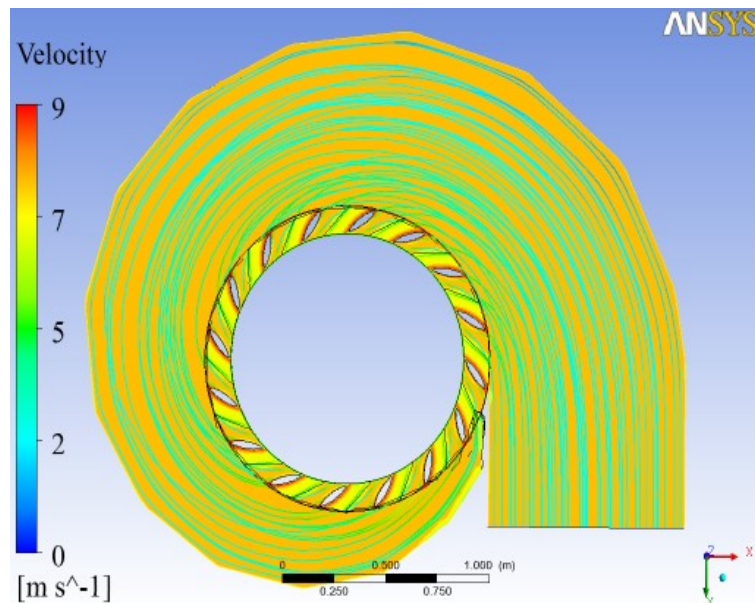


Figure 54. Total pressure distribution and velocity streamlines on the mid-plane of spiral case and stay vanes in turbine mode

### 5.5. Guide Vane Results in Turbine Mode

When defining the guide vane profile, NACA profiles are chosen from BladeGen. These profiles are chosen with considering not only the better flow behavior but also structural reasons. When increasing the thickness of the guide vanes, the hydraulic efficiency is decreases. A symmetrical NACA 0020-05 profile is chosen for the guide vanes from the results of the simulations.

In the design point of the guide vane, the important things are profile, location and length. At the working condition of the turbine design point, the chosen guide vane is located enough distance from the runner to obtain as far as possible uniform runner inlet with minimizing the effect of the guide vane trailing edge wakes. Also, there should be enough clearance between the trailing edge of the guide vane and leading edge of the runner blade at the guide vane maximum opening. From this point of view, the guide vane trailing edge radius and runner leading edge radius are adjusted with the theoretical methods. The ratio of the trailing edge of the guide vane to the leading edge of the runner blade is chosen 1.04 as a minimum value according to the literature. This ratio is selected as 1.06 for the final design of the guide vane and runner.

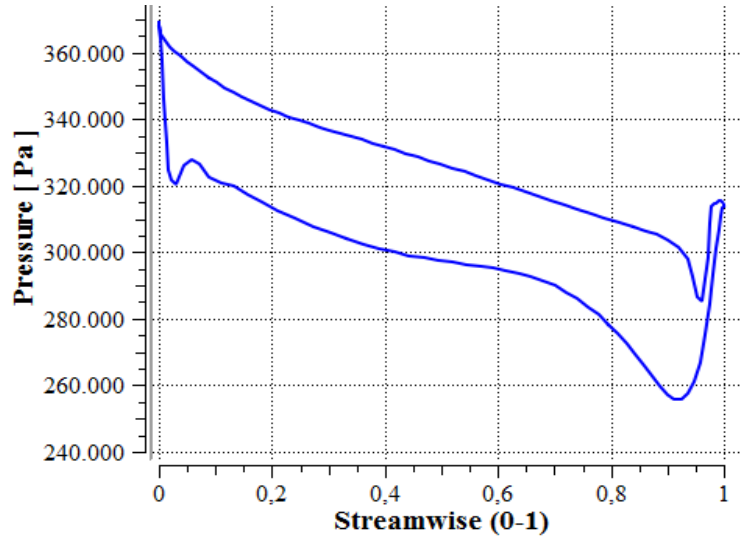


Figure 55. Blade loading on guide vane at mid-section in turbine mode

In the turbine mode, the guide vane optimum angle is adjusted with respect to the inlet condition of the Pump-Turbine runner. The inlet angle of the fluid is also determined. Then, blade loadings of the guide vanes are investigated at mid-section, closer to the shroud and closer to the hub regions. The mid-section loading distribution of the guide vane is plotted in Fig. 55.

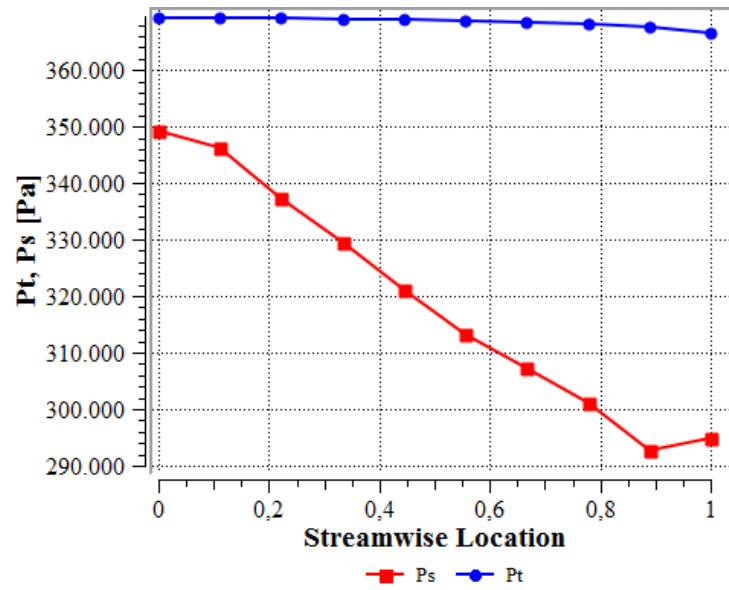


Figure 56. Streamwise Plot of Total pressure and Pressure through the guide vane passage in turbine mode

The average stream wise total pressure is investigated for the hydraulic losses of the guide vanes. The average total pressure and static pressure versus stream wise location is plotted in Fig. 56. The average total pressure decreases 369195 Pa to 367618 Pa from leading edge to trailing edge of the guide vanes.

The distribution of the static pressure contour in guide vane passage that is given in Fig. 57 illustrates the gradual pressure decrease in the passage. This shows that the inlet and outlet angles of the guide vane for the passage are convenient from the literature and experiences [11, 20, 21, 22].

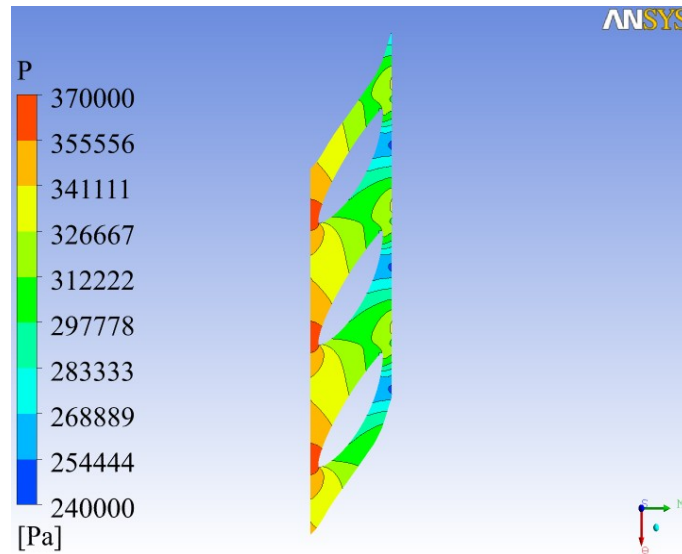


Figure 57. The Static Pressure Distributions in guide vane passage

The velocity streamlines in guide vane passage are also illustrated to check inter blade vortex formation and no visible formation occurs. The flow inside the guide vane passage follows the blade profile as given in Fig. 58.

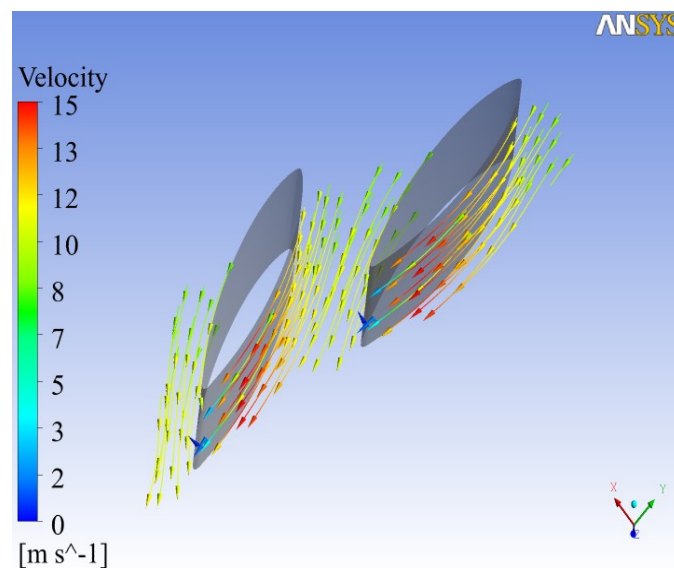


Figure 58. Velocity streamlines in guide vane passage in turbine mode

After finishing the design of the guide vanes, the interaction between the guide vane and runner is also investigated. In this respect, the simulations of the adjacent

parts (guide vane and runner) are held in together to see their effects each other. The velocity streamlines are also illustrated to visualize the flow in guide vane and runner passage in Fig. 59.

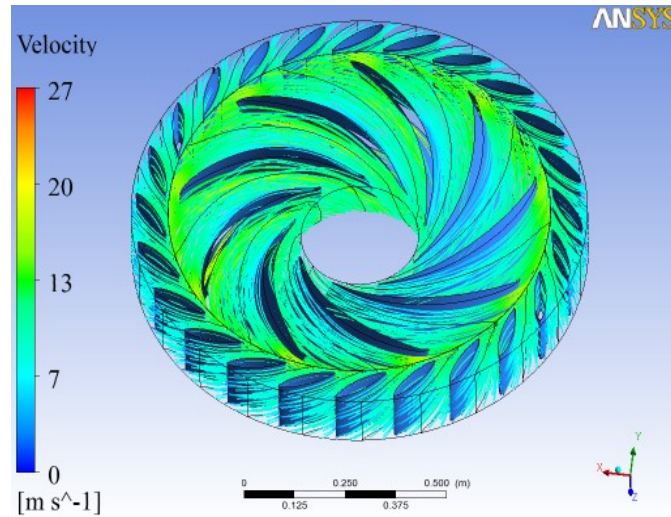


Figure 59. Velocity streamlines in guide vane and runner passage in turbine mode

## 5.6. Draft Tube Results in Turbine Mode

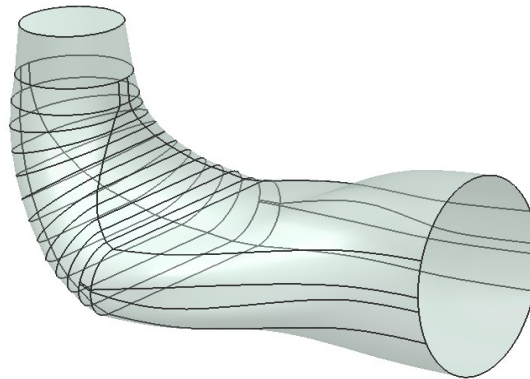


Figure 60: Parametric Draft Tube flow geometry

The design of the draft tube mainly focused on the pressure recovery factor. The design of the draft tube is required to increase the static pressure when the total pressure decreases due to hydraulic losses in turbine mode. After designing the Pump-Turbine runner, inlet and outlet dimensions of the draft tube is calculated for the runner outlet condition of the Pump-Turbine. Then, the sections of the draft

tube between the inlet and outlet are adjusted to make smooth passage for the flow in turbine mode. The flow geometry of the draft tube is created parametrically according to the experiences [11, 20, 21, 22]. The velocity vectors, pressure and total pressure distributions are plotted on the cross-sections inside the draft tube to understand the flow inside it in turbine mode. Then, the angles, length and middle sections are changed to reach the design requirements. For quick iterations and easy design change the draft tube geometry is generated parametrically in Fig.60. The pressure recovery factor reaches 0.80-0.85 for good draft tubes [6]. Finally, the pressure recovery is calculated as 0.86 according to the equation (71) from the CFD results given is Table 8.

Table 8. Draft Tube Simulation Results in Turbine Mode

$P_{out}$	110585 [ Pa ]
$P_{in}$	97260 [ Pa ]
$Q_t$	2.0 [ m <sup>3</sup> /s ]
$A_{in}$	0.36 [ m <sup>2</sup> ]

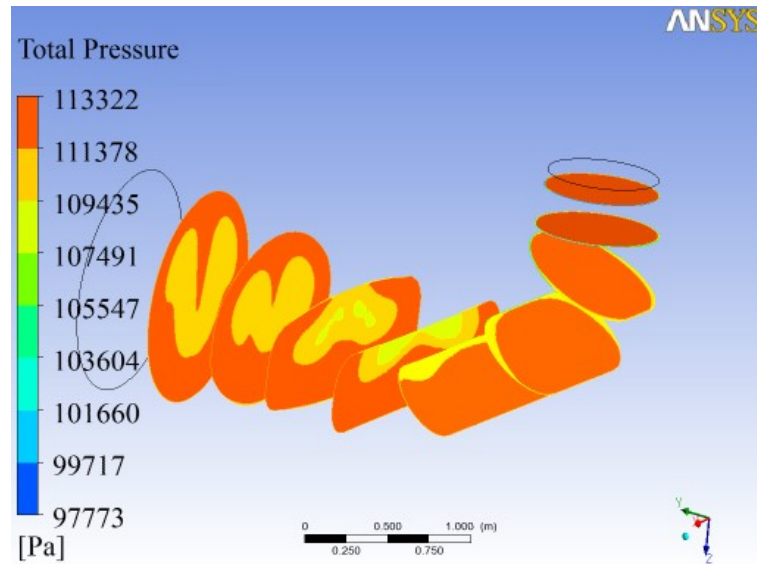


Figure 61. Total pressure change through the draft tube in turbine mode



In the Pump-Turbine there are two modes. In this section, the total and static pressure distributions are plotted in Fig.61 and Fig.62 respectively in turbine mode. In turbine mode, the total pressure decreases due to hydraulic losses, and the static pressure increases in the flow direction in Fig.61.

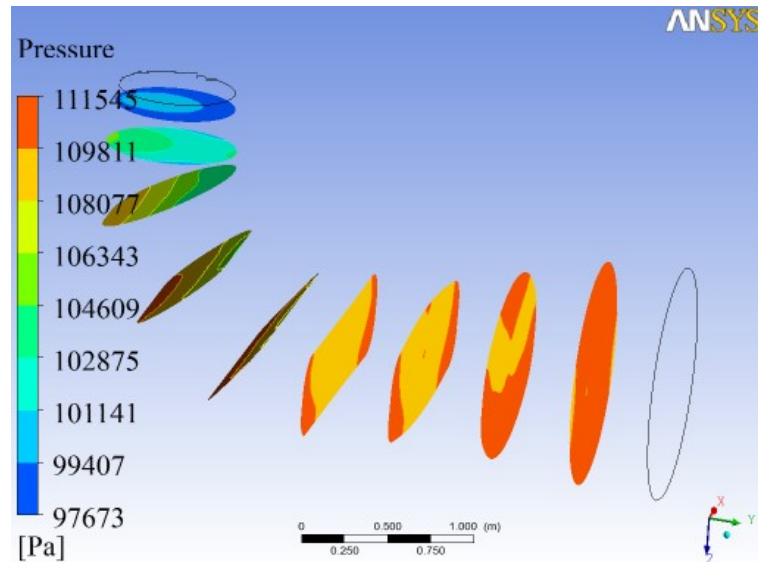


Figure 62. Pressure change through the draft tube in turbine mode

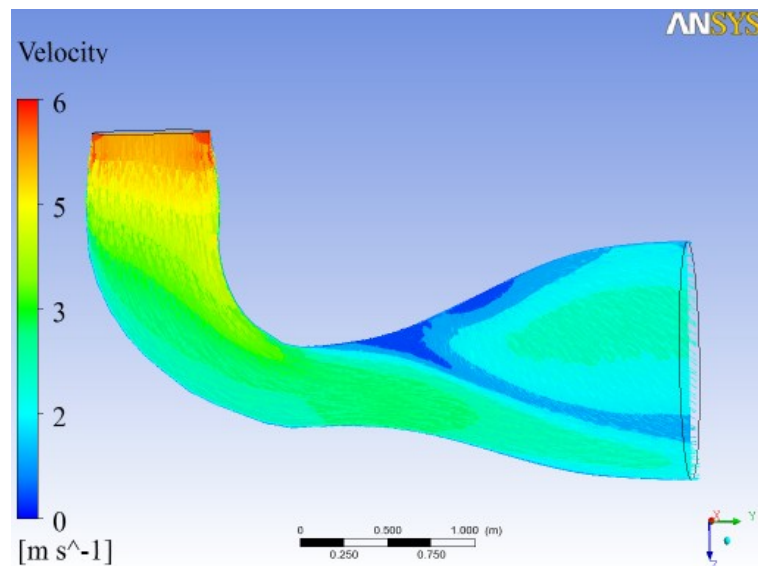


Figure 63. Velocity vectors and contours on the draft tube mid-section in turbine mode

The flow separations are eliminated by changing the geometry of the draft tube and the velocity vectors on the mid cross-section are obtained without any separations as shown in Fig. 63. Also in the turbine mode to visualize the behavior of the flow inside the draft tube, the streamlines are plotted in Fig. 64.

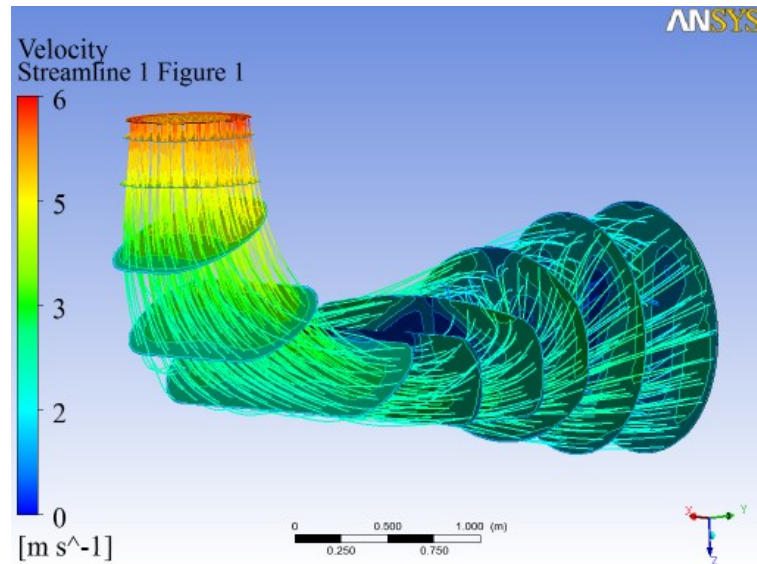


Figure 64. Draft tube velocity contours and streamlines in turbine mode

### 5.7. Final Model CFD Results and Hydraulic Losses in Turbine Mode

The efficiency of the each part of the turbine is given in the Table 9. The overall hydraulic efficiency of the components also can be calculated as below:

Table 9. Efficiencies of the Pump-Turbine parts and hydraulic losses

	Spiral Case	Stay vanes	Guide Vanes	Runner	Draft Tube
Efficiency [%]	99.35	99.41	99.57	96.96	99.22
$\Delta H$ [m]	0.25	0.22	0.16	26.42	0.09
Hydraulic Efficiency of the Pump-Turbine in turbine mode					94.6

## 5.8. Discussion of Turbine Mode Results

2 m<sup>3</sup>/s discharge and 28.15 m head are chosen to design 500 kW Pump-Turbine. The design procedure is used for the Pump-Turbine parts: spiral case, stay vanes, guide vanes, runner and draft tube. The Pump-Turbine is a reversible hydraulic machine that can work not only in turbine mode but also in pump mode. Turbine mode results are only discussed in this section.

In the turbine mode, the water flows the spiral case, stay vanes, guide vanes, runner and draft tube in stream wise direction. So, the water enters the spiral case firstly. The flow is distributed uniformly around the runner. The radial and circumferential velocity at spiral case outlet section is plotted in Fig. 46 to understand the flow distribution. Also, the pressure distribution on the mid-plane is plotted in Fig. 48 and it is seen that pressure distribution around the vanes is almost uniform. This spiral case design is convenient according to these results for a balanced turbine mode operation. The head loss value and 99.35 % hydraulic efficiency of the spiral case given in Table 9 are convenient for the predicted preliminary spiral case design requirements.

After passing the spiral case, the flow enters the stay vane passage. The stay vane profile and position are adjusted according to the guide vane inlet condition with the simulation results. The inlet flow angle of stay vanes are adjusted to obtain required inlet condition of the guide vanes. Therefore, the stay vanes are simulated with the spiral case as given in Fig. 54 and they are improved together. Then, it is obtained that the stay vane outlet flow angle is convenient for the guide vane inlet condition. The length, number and thickness are designed not only hydraulic reasons but also structural reasons. The head loss value and 99.41 % hydraulic efficiency of the stay vanes given in Table 9 are convenient for the predicted preliminary stay vane design requirements.

After passing the stay vanes, the flow enters the guide vane passage. The guide vane outlet flow angle is determined in the preliminary design calculations as in

equation (38). The outlet diameter of the guide vane is also determined in the preliminary design. The length of the guide vane is determined for the number of guide vanes as in equation (23). The guide vane operating angle is calculated for an optimum turbine design. Then, the guide vane profile and position are adjusted according to the runner inlet condition with the simulation results. The head loss value and 99.57 % hydraulic efficiency of the guide vanes given in Table 9 are convenient for the predicted preliminary guide vane design requirements.

After passing the guide vanes, the flow enters the runner blade passage. The circulation value are calculated theoretically at runner inlet and outlet location as in equation (58). The flow angles are calculated at inlet and outlet sections with including the blade profile given in Fig. 29. The angles of the runner blade are calculated with respect to the area distribution, rotational speed of the runner and flow behavior at these locations. Then turbine mode theoretical inlet and outlet blade angles are illustrated as  $\delta_1$  and  $\delta_2$  in Fig. 20 respectively. The final runner blade has been obtained after more than two hundred simulations. In the simulations, the blade angles and meridional profile are designed together. Then, the final runner blade is obtained without leading edge shock as illustrated in Fig. 33 and without cavitation as illustrated in Fig. 37. 96.96 % hydraulic efficiency value of the runner given in Table 9 is convenient for the predicted preliminary runner design requirements.

After passing the runner, the flow enters the draft tube. The draft tube inlet diameter is calculated according to the outlet section of the runner. The draft tube is designed with considering the hydropower plant and turbine orientation. There are some types of the draft tube [11]. The convenient type of the draft tube is chosen in the draft tube design. The flow separations at walls are eliminated by adjusting the draft tube dimensions as illustrated in Fig. 63. The pressure recovery factor, that is main design parameter of the draft tube, is calculated as 0.86 for the final draft tube geometry with an equation (71). The pressure recovery factor value and 99.22 % hydraulic efficiency of the draft tube given in Table 9 are convenient for the predicted preliminary draft tube design requirements according to the

literature and experiences [11, 20, 21, 22]. Also, the pressure distributions inside the draft tube is investigated and plotted in Fig. 61 and Fig. 62.

The turbine mode performance results of the Pump-Turbine parts are tabulated in Table 9. These values are found for the parts with smooth wall assumptions. The roughness effect is also investigated in section 5.2.6. So, each part of the Pump-Turbine should be designed with considering the manufacturing conditions. 94.6 % hydraulic efficiency value of the Pump-Turbine given in Table 9 is convenient for the predicted preliminary turbine design requirements.

## ***CHAPTER 6***

### ***PUMP MODE RESULTS***

#### **6.1. Final Design Mesh Characteristics**

The same mesh data is used for each mode. The mesh data of the final designed Pump-Turbine part is given in Table 7.

#### **6.2. Runner Simulation in Pump Mode**

The designed runner is simulated in pump mode to investigate the pump mode behavior. It is discussed that the Pump-Turbine runner is designed in each mode simultaneously. In this section, the results of the Pump-Turbine runner simulations in pump mode are illustrated and commented on the results.

The calculated preliminary runner dimensions are used in these simulations. The head of the Pump-Turbine in pump mode with considerable efficiency value is the main target at design condition. In the simulations, the wide range is investigated with the coarser mesh ( approximately  $3 \times 10^4$  elements per 1 blade passage ) and upwind scheme to decrease the computational requirements. Then, the fine mesh ( approximately  $25 \times 10^4$  elements per 1 blade passage ) and other turbulence models are used to obtain results closer to the real flow behaviors.

##### ***6.2.1. Meridional Profile Design in Pump Mode***

The results of the simulations gives the importance for the meridional profile of the

Pump-Turbine runner. In the pump mode design, the pump mode leading edge angles of the runner blade are adjusted with the meridional profile determined in turbine mode. After adjusting the runner blade pump mode leading edge angles, the inlet edge cavitation zones are eliminated. The final meridional profile and one of the preliminary designs are illustrated before in Fig. 31.

### 6.2.2. Leading Edge Design in Pump Mode

The calculated outlet angles in turbine mode is modified to obtain shock free entrance in pump mode. The angle misalignment is eliminated by adjusting the blade angles and meridional profile together. For each angle change of the leading edge in pump mode, the runner blade is again designed in turbine mode. After obtaining the required turbine mode flow behaviors, the runner is simulated in pump mode. This procedure is terminated after obtaining the design requirements in each mode.

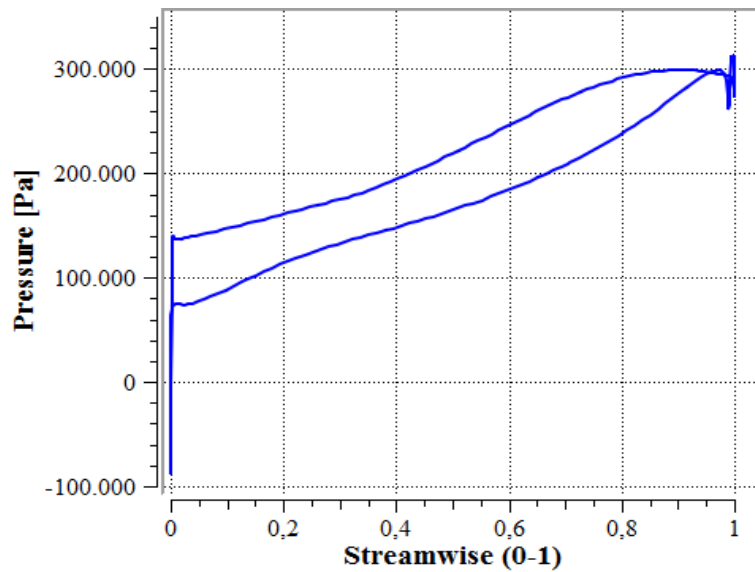


Figure 65. Blade Loading at closer to the shroud meridional section on non-final blade design in pump mode

In pump mode previous simulations, the results show the wrong blade leading edge angle due to the peak pressure at the blade leading edge. As an example, one of the previous blade loading of the pump mode simulation is given in Fig. 65.

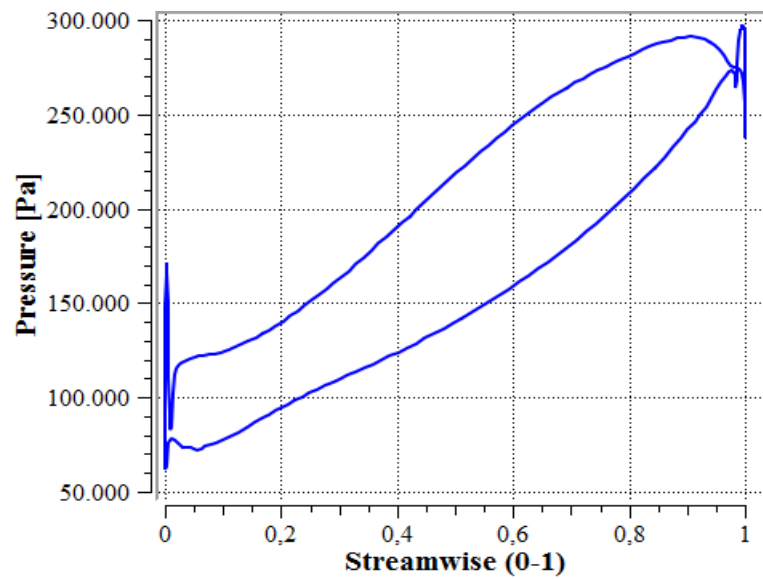


Figure 66. Blade Loading at closer to the shroud meridional section on final blade design

The peak pressure at leading edge of the runner blade is eliminated with adjusting the blade leading edge angle of the pump mode. After adjusting the angles, the blade loading of the runner blade is obtained smoothly. The blade loading of the final design is given in Fig. 66 in pump mode.

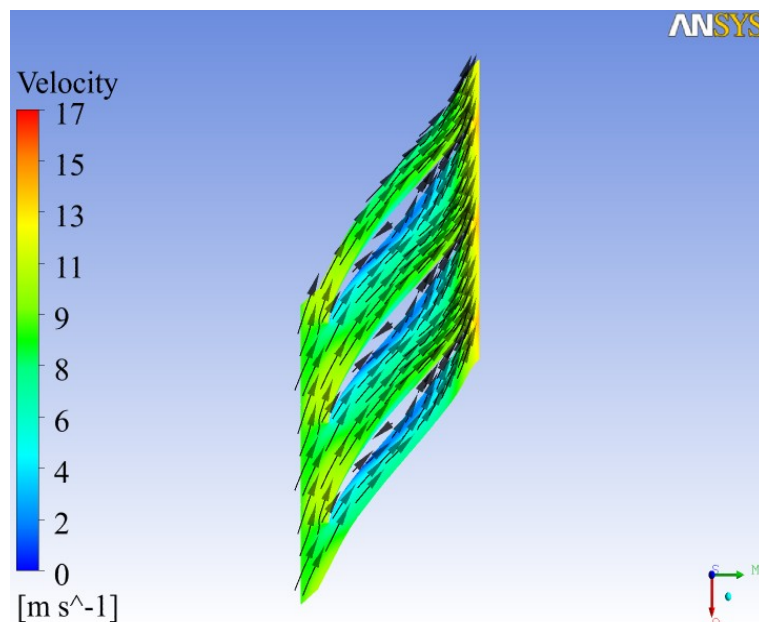


Figure 67. Velocity vectors at mid-meridional section for preliminary runner blade in pump mode



The inlet angles of the runner blade are adjusted for axially inlet flow in pump mode. Before adjusting the blade angles leading edge to trailing edge, the velocity vectors are plotted to see the preliminary blade profile and flow angle inside the runner passage in Fig. 67.

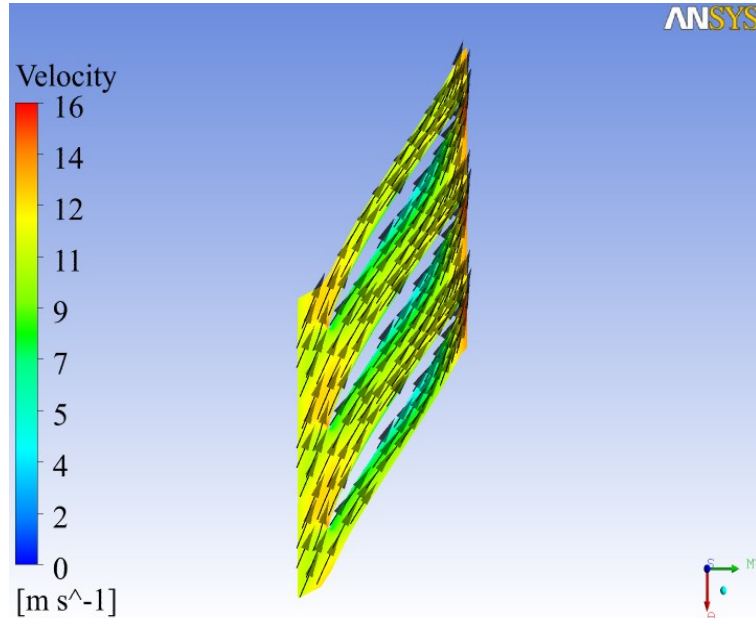


Figure 68. Velocity vectors at mid-meridional section for final runner blade in pump mode

After adjusting the blade inlet and outlet angles, the smooth angle change is made from leading edge to trailing edge of the blade. It is obtained that the profile of the final runner blade is followed by the liquid flow inside the passage in pump mode. This can be seen from the velocity vector plot of the final runner design in pump mode as in Fig. 68.

### ***6.2.3. No Swirl Inlet Condition in Pump Mode***

The Pump-Turbine runner is designed for no swirl outlet condition in turbine mode. The blade angles are adjusted to obtain no swirl at outlet in turbine mode. In design procedure, the pump mode design are also performed with turbine mode design. So, the design of the runner is completed in each mode together. The

normal boundary condition is applied at inflow region in pump mode given in Fig. 13. The final blade simulation results are obtained in pump mode. The streamwise plot of alpha and beta in pump mode are plotted in Fig. 69. It is obvious that zero alpha degree is obtained at pump mode leading edge of runner blade. Also, the inlet condition of the runner blade is assumed as no swirl in the design procedure. This results shows the design procedure and results are appropriate each other.

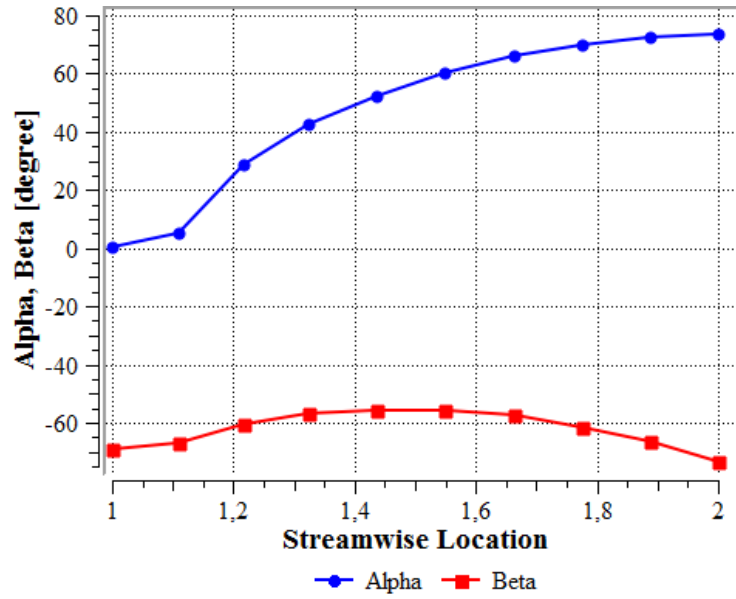


Figure 69. Streamwise Plot of Alpha and Beta in pump mode

#### 6.2.4. Design without Cavitation in Pump Mode

To detect the cavitation zones on the blade, the pressure distribution is plotted on blade surfaces in each mode. The pressure on the blade less than water vapor pressure is determined in previous simulations with plotting the pressure contour on the blade surface. This problematic regions are eliminated by adjusting the blade angles. The minimum pressure on the blade is obtained greater than water vapor pressure. In pump mode, the minimum pressure zone is obtained on the leading edge. It is closer to the hub region.

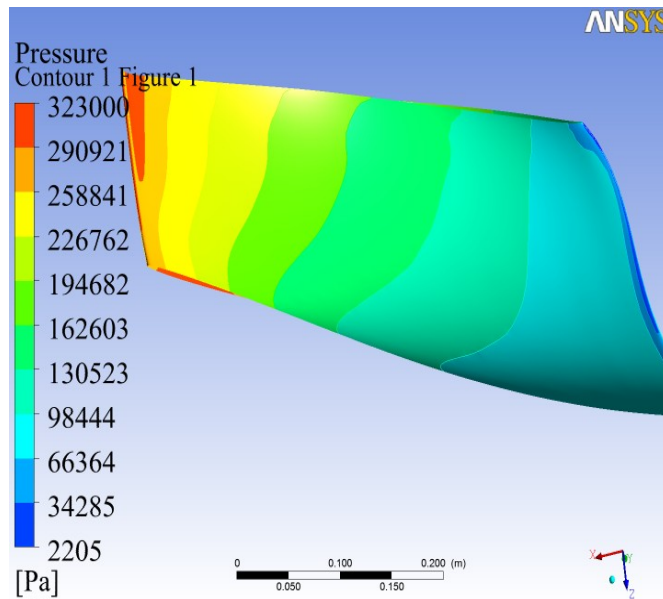


Figure 70. Pressure distribution on the runner blade in pump mode

The pressure contour on the final runner blade for pump mode is obtained with minimum pressure greater than the water vapor pressure as in Fig. 70. Therefore, cavitation on the runner blade is eliminated. In the pump mode simulations, the streamwise blade loadings of the final runner blade at mid-section is plotted in Fig. 71.

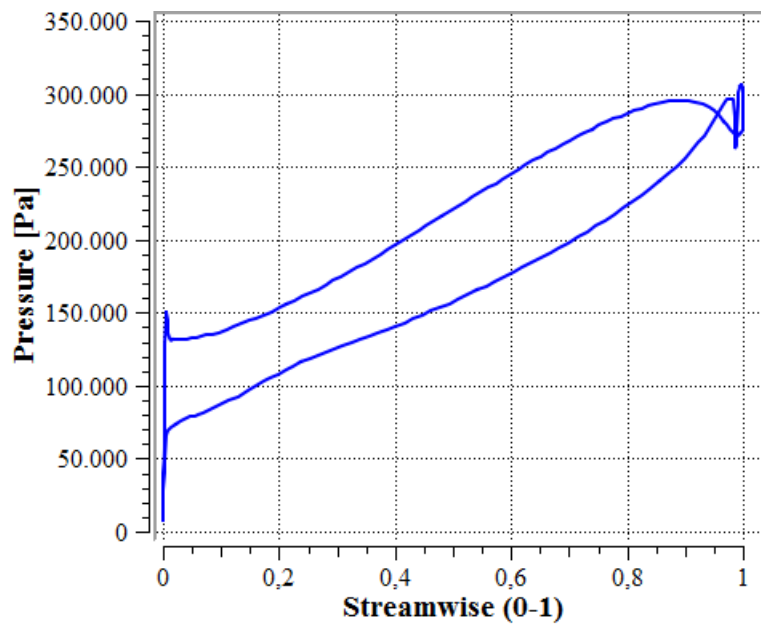


Figure 71. Pressure on the blade meridional section with minimum pressure zone

### 6.2.5. Mesh Independency in Pump Mode

The aim of the mesh independency is to find the results without change with increasing mesh fineness. The simulation results should converged and they should be independent from mesh fineness.

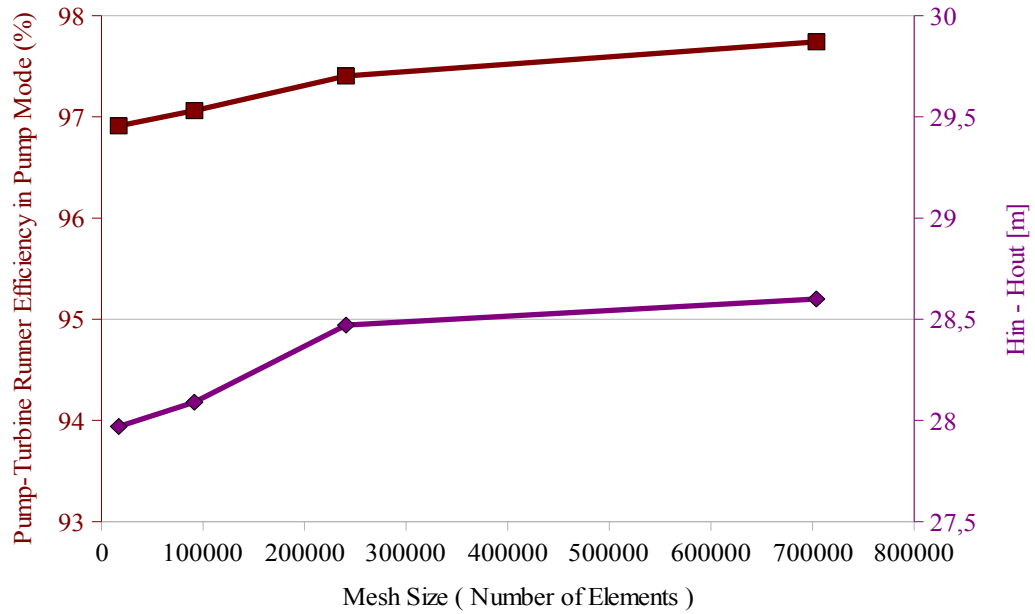


Figure 72. Runner efficiency and head difference versus mesh size in pump mode

Due to the crucial importance of the design of the Pump-Turbine runner, the results of its simulations are investigated for mesh independency. Consequently, head difference between inlet and outlet of the Pump-Turbine runner and its hydraulic efficiency are plotted in Fig. 72 in pump mode.

When the number of the mesh element increases, the time and performance needs of the simulation increases. Mesh independency criteria is chosen for nearly constant results to obtain closer results to accurate results. Therefore, the mesh independent solution is adequate for an approximately  $25 \times 10^4$  mesh elements for one runner blade passage from Fig. 72 in pump mode.

### 6.2.6. Roughness Effect for the Runner in Pump Mode

The roughness effect is investigated to see the effect on the designed components in pump mode. The simulations of the design period the walls have been chosen as smooth wall. The roughness of the walls is described in the turbine mode section. In pump mode, the hydraulic efficiency of the smooth wall assumed Pump-Turbine runner decreases 0.17 % when the roughness of hub, shroud and blades are chosen as 3.2 micron.

### 6.2.7. Runner Blade Final Version in Pump Mode

In the simulations, the calculated angles and dimensions of the runner are used also these parameters are given in Table 4. After some simulations, the runner blade shape chosen as NACA 0010 – 05 to obtain uniform exit conditions for each mode with adjusted leading edge profile and angles. An acceptable runner efficiency is reached enough to obtain 28.15 meters head with discharge of  $1.6 \text{ m}^3/\text{s}$  in pump mode. The velocity vectors in meridional view show that the flow does not separate and follows the meridional paths of the runner passage in pump mode simulations as shown in Fig. 73.

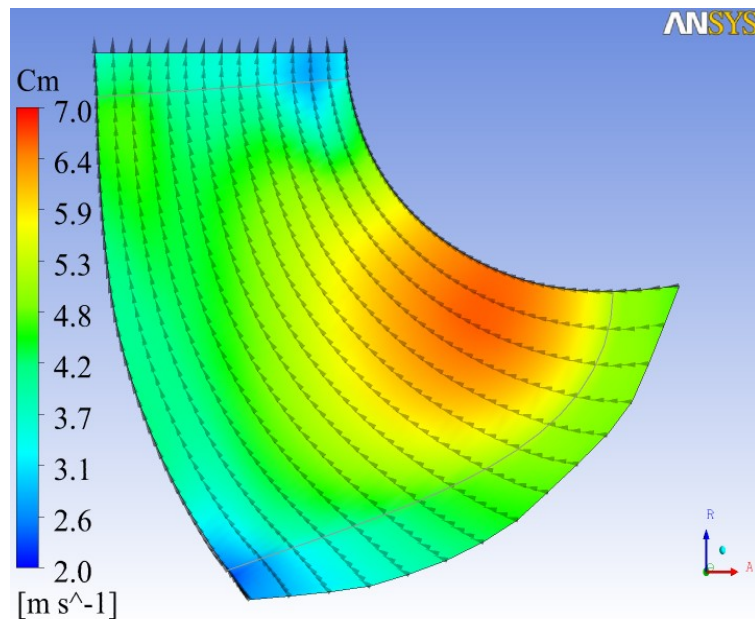


Figure 73. The velocity vectors on meridional section in pump mode

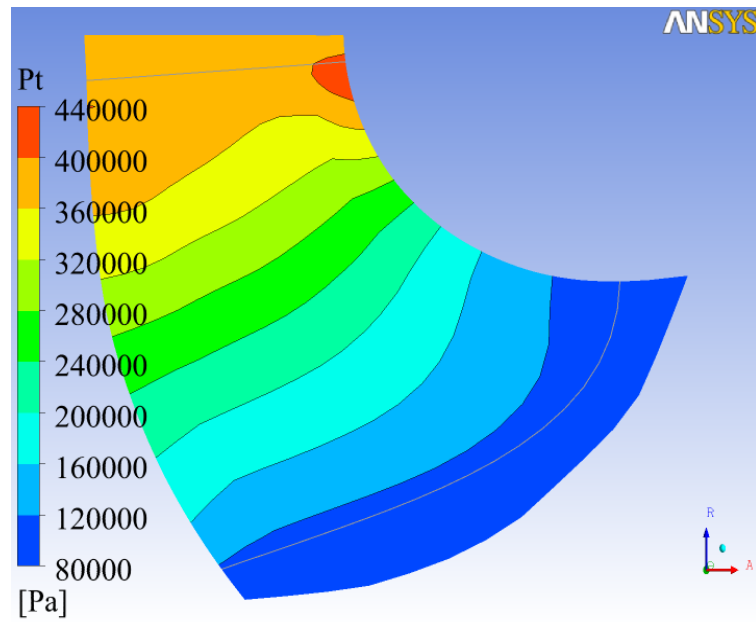


Figure 74. Total pressure distribution on meridional section in pump mode

The pressure distribution in meridional view show that the flow pressure increases smoothly in meridional section of the runner in pump mode as shown in Fig. 74.

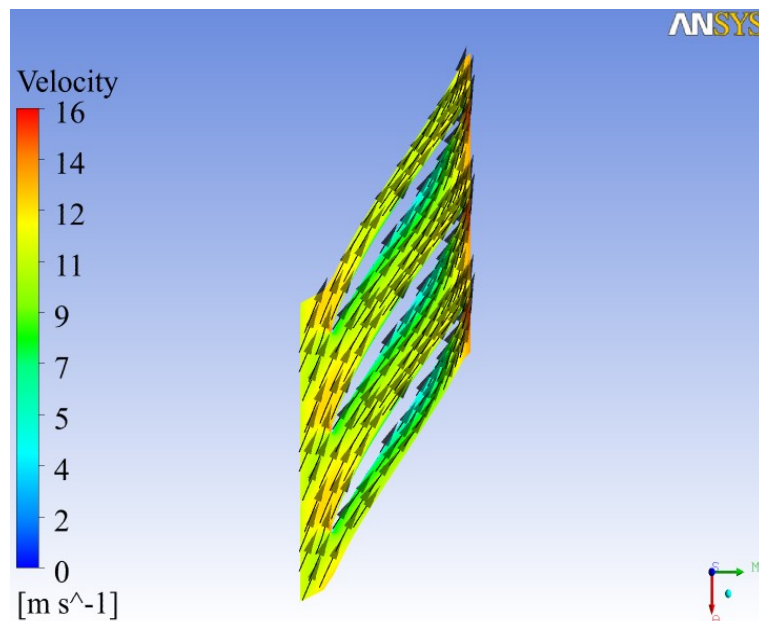


Figure 75. Velocity vectors at meridional mid-section in pump mode

The velocity vector are plotted to detect the flow separations. After the adjusting the blade angles, it is obtained that the flow inside the runner follow the blade

profile.

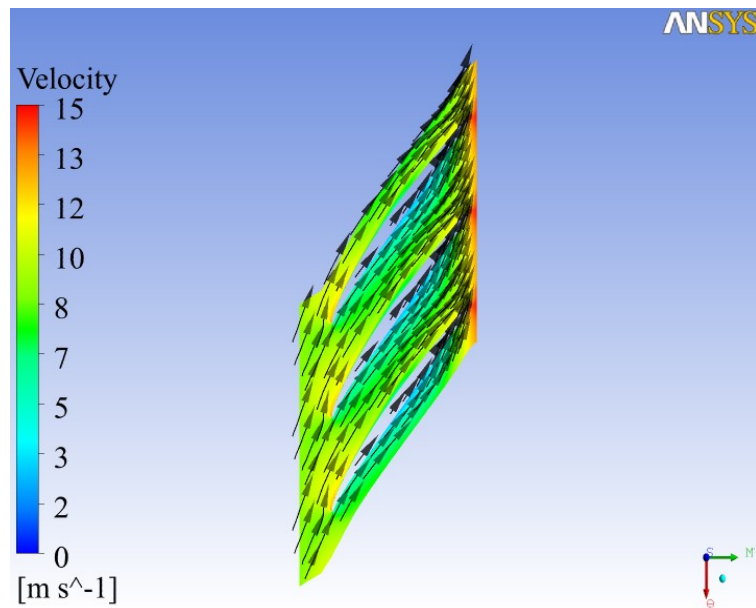


Figure 76. Velocity vectors at closer to the hub meridional section in pump mode

The mid-section meridional velocity vectors in pump mode are plotted and no separation is detected as shown in Fig. 75. Also in pump mode simulation, closer to the hub and shroud velocity vectors are plotted to see the flow behavior in runner as in Fig. 76 and Fig. 77 respectively.

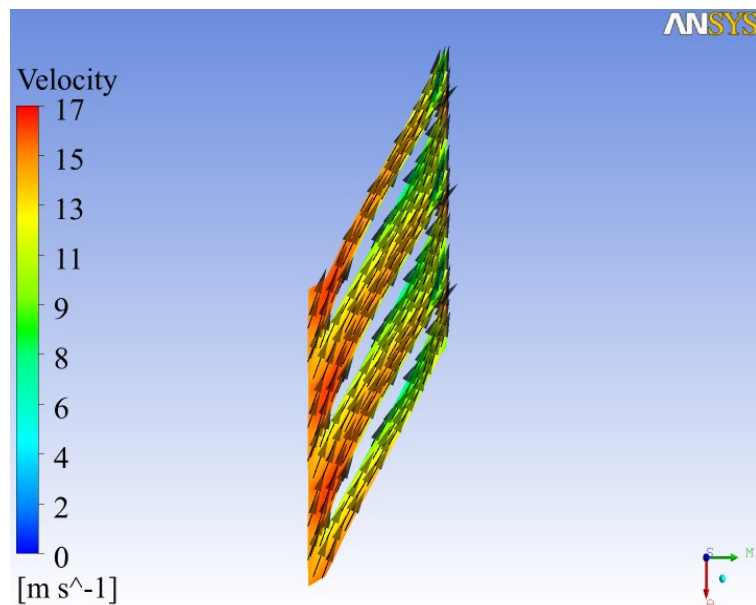


Figure 77: Velocity vectors at closer to the shroud meridional section in pump mode

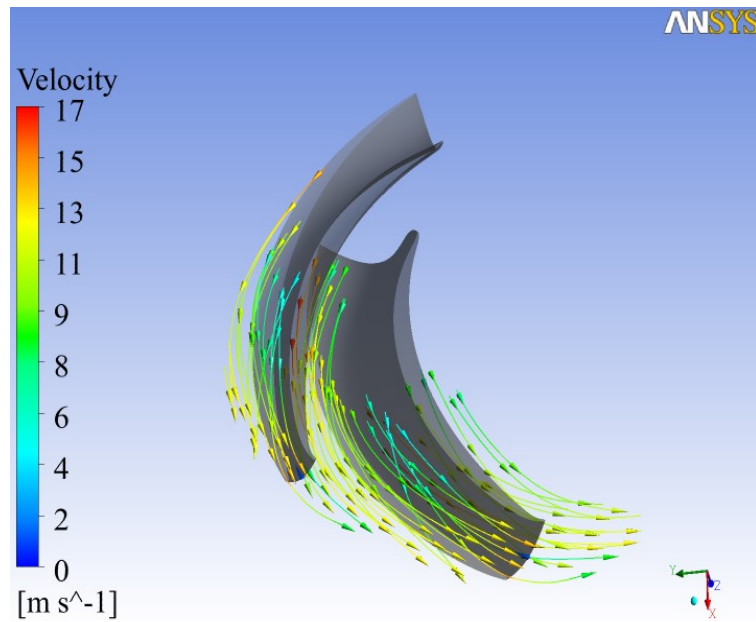


Figure 78. Velocity streamlines in pump mode

The velocity vector show that the flow inside the runner follows the blade profile. So, the 3-D streamlines are also plotted to visualize the flow inside the runner in Fig. 78.

### 6.3. Spiral Case Results in Pump Mode

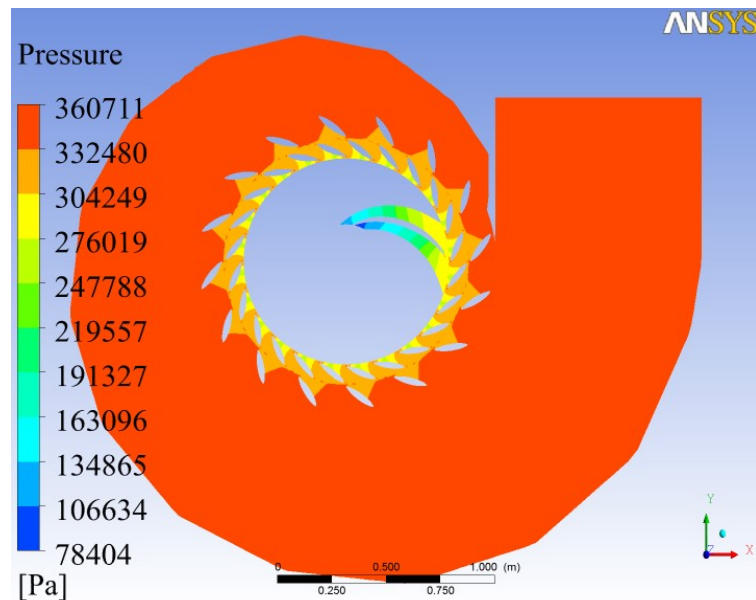


Figure 79. Pressure distribution on the spiral case mid-plane with stay vanes in pump mode



The spiral case is used to distribute flow uniformly around turbine runner in turbine mode. After designing spiral case in turbine mode, it is simulated with pump mode properties. The flow behavior inside is investigated with plotting the pressure and velocity distributions in pump mode. The pressure distribution and velocity vectors are plotted to visualize the flow inside the spiral case in pump mode. The pressure and velocity distributions, in Fig.79 and Fig.80 respectively, show that the spiral case works in the pump mode.

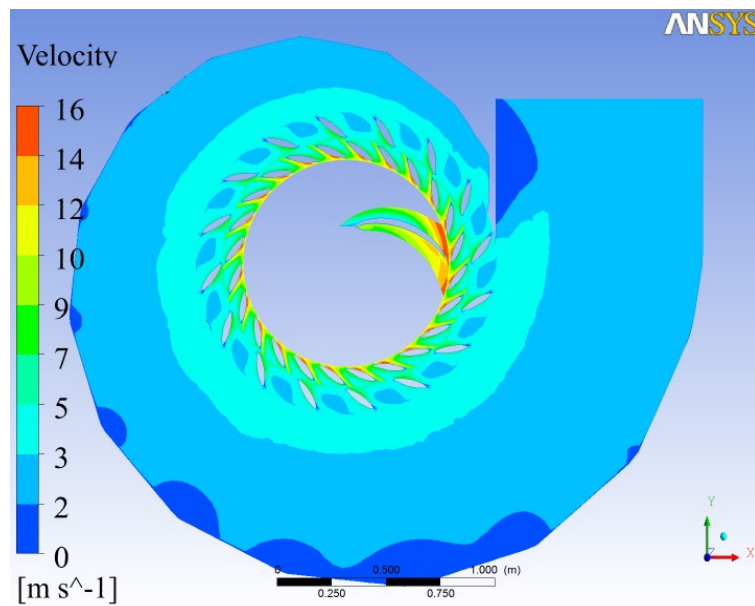


Figure 80. Velocity distribution on the spiral case mid-plane with stay vanes in pump mode

#### 6.4. Stay Vane Results in Pump Mode

The profile and location of the stay vanes are discussed and detailed in previous sections. The profile of the stay vanes chosen as a symmetrical NACA 0030-05 profile with considering both turbine mode and pump mode. The flow between the stay vanes is investigated by plotting the velocity and pressure distributions in pump mode. In this respect, blade loadings of the stay vanes are investigated. The mid-section blade loading distribution of the stay vane is plotted in Fig. 81. The main reason for the stay vanes is to carry the load between the upper and lower head covers. The hydraulic effect is important for the turbine mode. In pump mode,

the total pressure decrease for this blade loading is acceptable as given in Table 10.

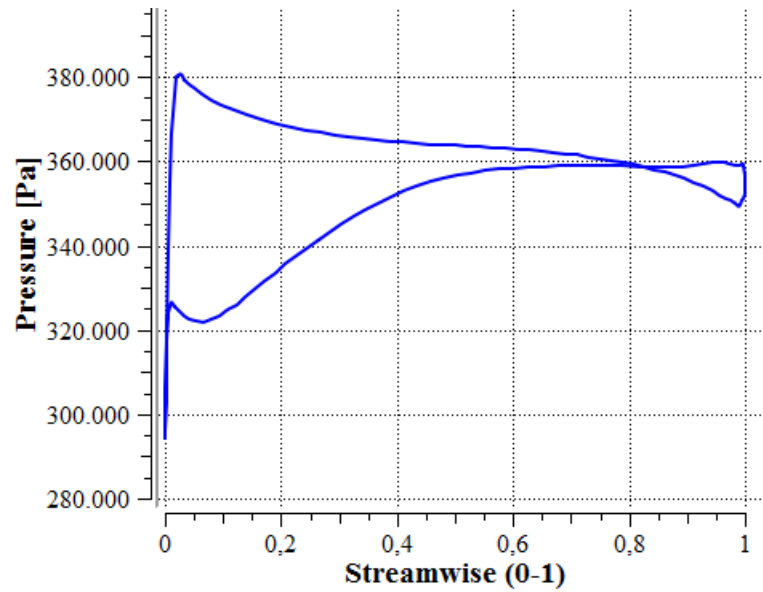


Figure 81. Blade loading on stay vane at mid-span

The average stream wise total pressure is investigated for the hydraulic losses of the stay vanes. The average total pressure and static pressure versus stream wise location is plotted in Fig. 82 in stay vane passage. The average total pressure decreases 380342 Pa to 378756 Pa.

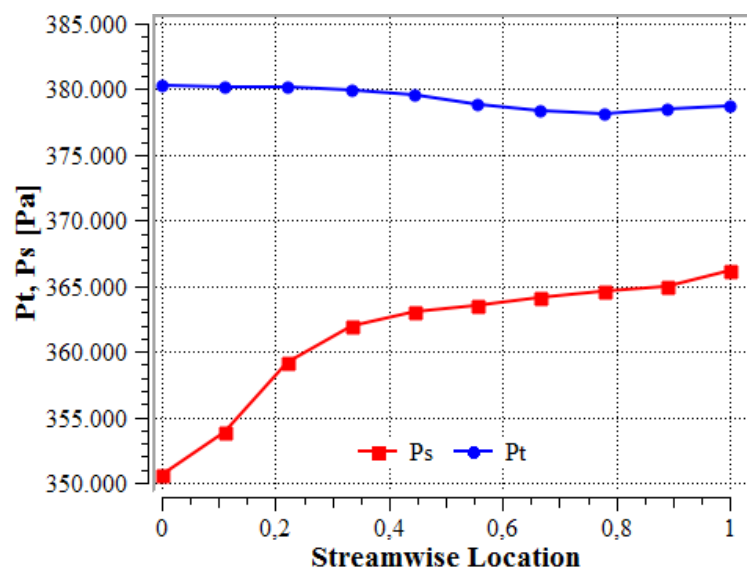


Figure 82. Stream wise Plot of Total pressure and Pressure through the stay vane passage in pump mode

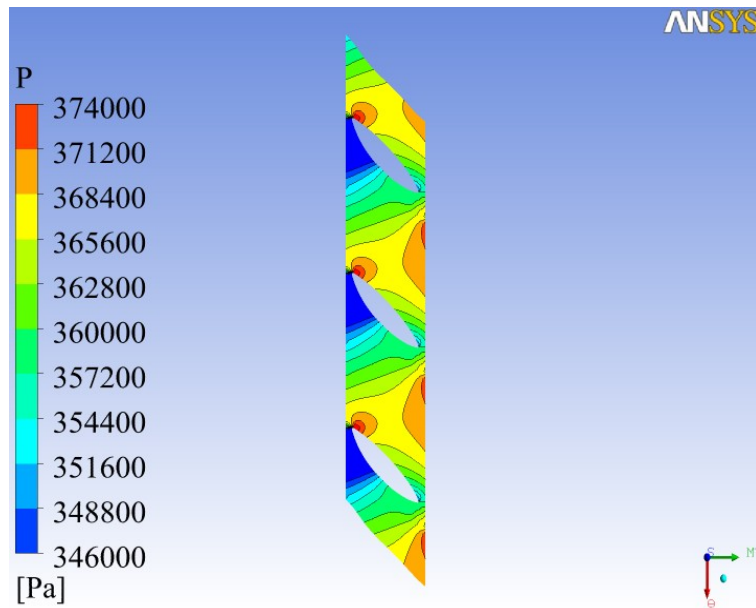


Figure 83. The Static Pressure Distributions in stay vane passage in pump mode

The distribution of the static pressure contour in stay vane passage, that is given in Fig. 83, illustrates the gradual pressure decrease in the passage in pump mode. This shows that the inlet and outlet angles of the stay vane for the passage are convenient from the literature and experiences [11, 20, 21, 22].

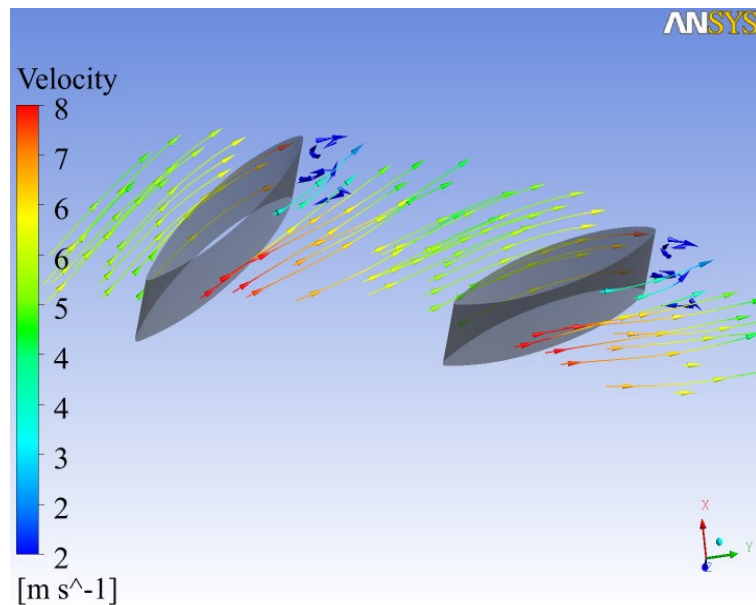


Figure 84. Velocity streamlines in stay vane passage

The velocity streamlines in stay vane passage are also illustrated to check inter blade vortex formation and no visible formation occurs. The flow inside the stay vane passage follows the blade profile as given in Fig. 84. The flow is separated at closer to the spiral case, but this separation disappears inside the spiral case in Fig. 85. The velocity vectors and total pressure distribution on the mid-plane of the spiral case are plotted in Fig. 85. The distribution of the total pressure is almost uniform. This pressure distribution is convenient for the pump mode working conditions from the literature.

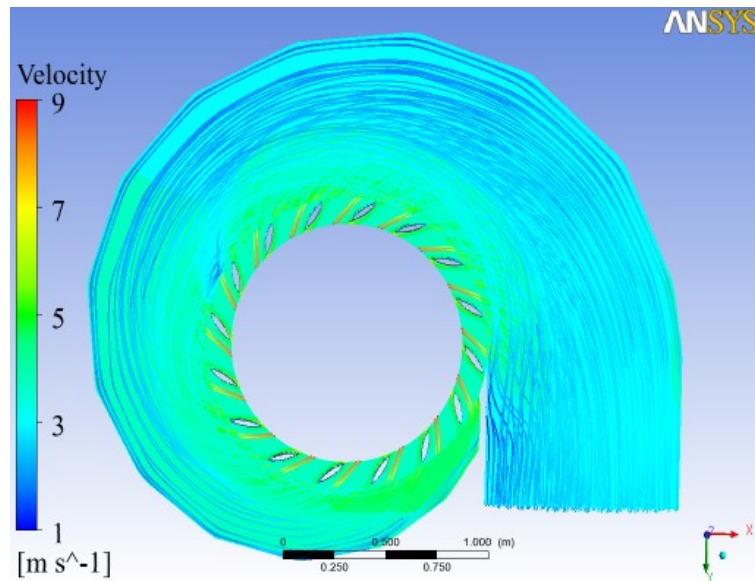


Figure 85. Pressure distribution and velocity streamlines on the mid-plane of spiral case and stay vanes

## 6.5. Guide Vane Results in Pump Mode

The profile and location of the guide vanes are discussed and detailed in previous sections. The profile of the guide vanes chosen as a symmetrical NACA 0020-05 profile with considering both turbine mode and pump mode. The guide vanes can rotate about regulation centers. Therefore, the guide vane position angle can be changed by rotating about regulation centers to determine the throat area. The throat area of the guide vanes determine the discharge in pump mode. In the pump mode, the guide vane optimum angle is adjusted with respect to the outlet condition of the Pump-Turbine runner. The flow between the stay vanes is

investigated by plotting the velocity and pressure distributions in pump mode. In this respect, blade loadings of the guide vanes are investigated. The mid-section blade loading distribution of the guide vane is plotted in Fig. 86. This blade loading distribution does not effect the total pressure decrease too much in the guide vane passage and decrease in total pressure is acceptable as given in Table 10.

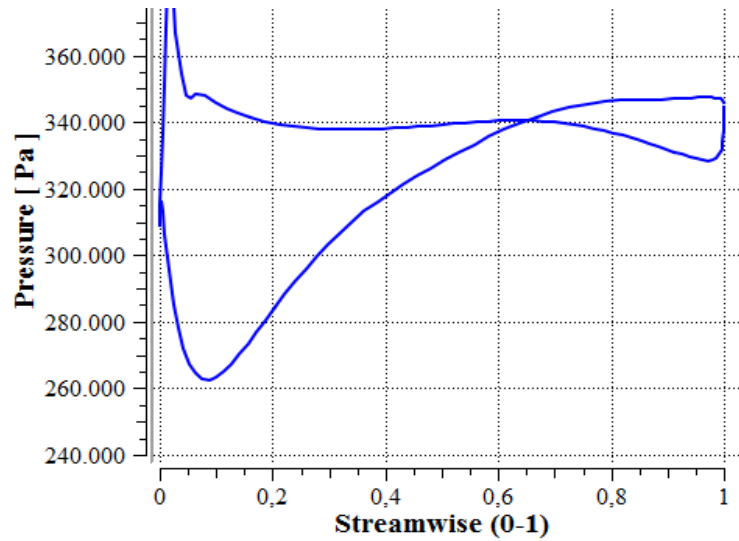


Figure 86. Blade loading on guide vane at mid-span

The average stream wise total pressure is investigated for the hydraulic losses of the guide vanes. The average total pressure and static pressure versus stream wise location is plotted in Fig. 87. The average total pressure decreases 383887 Pa to 380661 Pa.

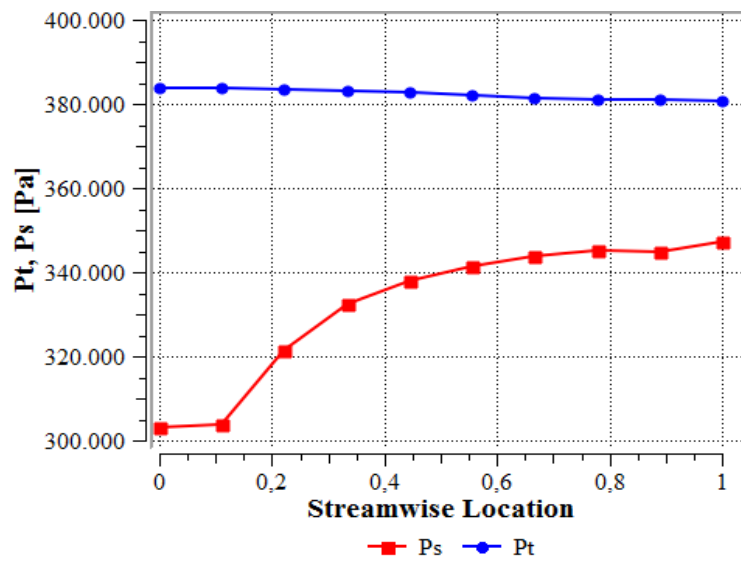


Figure 87. Stream wise Plot of Total pressure and Pressure through the guide vane passage

The distribution of the static pressure contour in guide vane passage that is given in Fig. 88 illustrates the gradual pressure decrease in the passage. This shows that the inlet and outlet angles of the guide vane for the passage are convenient from the literature.

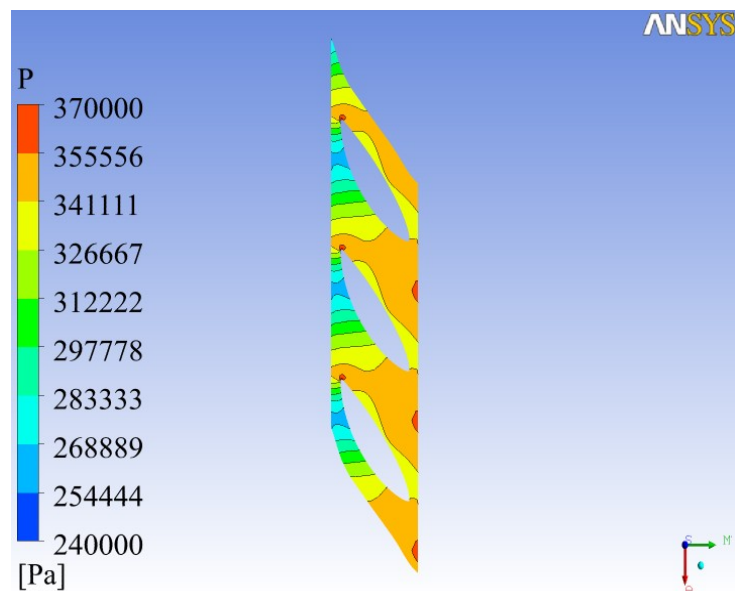


Figure 88. The Static Pressure Distributions in guide vane passage

The velocity streamlines in guide vane passage are also illustrated to check inter blade vortex formation and no visible formation occurs. The flow inside the guide vane passage follows the blade profile as given in Fig. 89.

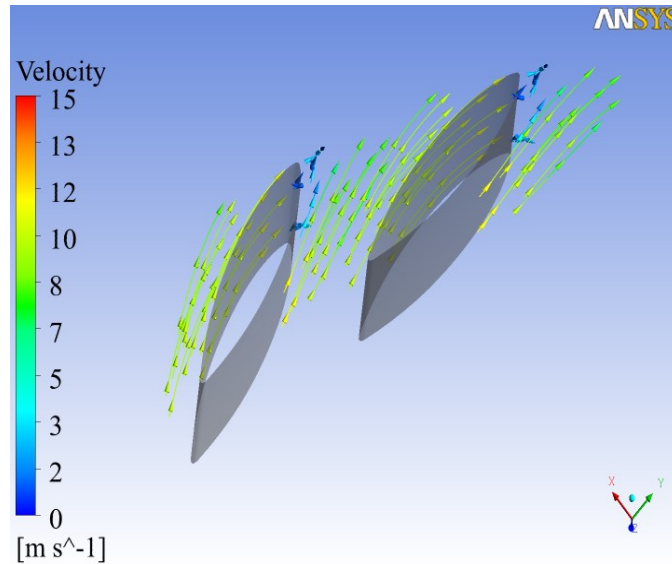


Figure 89. Velocity streamlines in guide vane passage in pump mode

The guide vanes are simulated with the runner in pump mode. The velocity streamlines are illustrated to visualize the flow in guide vane and runner passage in Fig. 90 in pump mode.

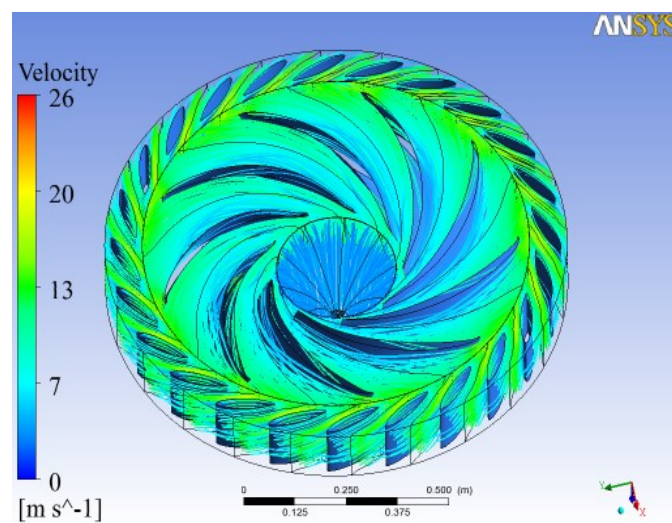


Figure 90. Velocity streamlines in guide vane and runner passage in pump mode

## 6.6. Draft Tube Results in Pump Mode

The design of the draft tube mainly focused on the pressure recovery factor in turbine mode. Designed geometry of the draft tube in turbine mode is simulated with the pump mode conditions to visualize the flow behavior inside the draft tube. The velocity vectors, pressure and total pressure distributions are plotted on the cross-sections inside the draft tube to understand the flow inside it in pump mode. In the previous section, the draft tube is generated parametrically. Then, parametrically generated the draft tube geometry is modified. Then, it is checked for each working conditions.

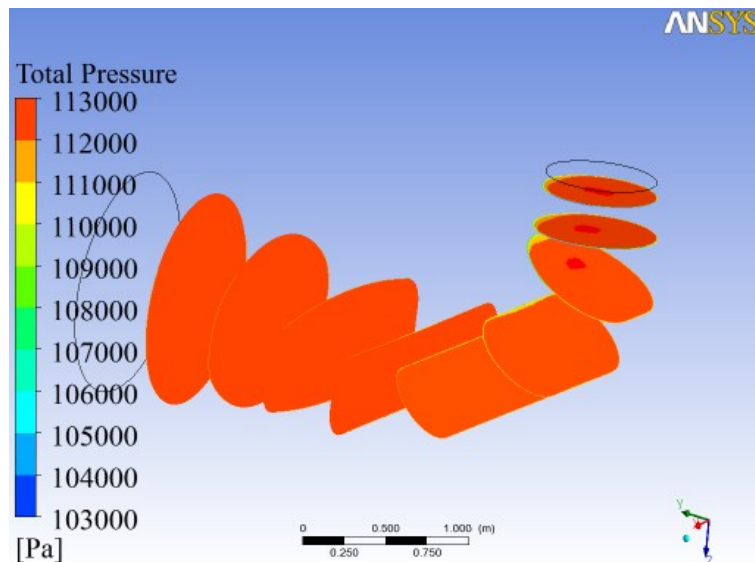


Figure 91. Total pressure change through the draft tube in pump mode

The total and static pressure distributions are plotted in Fig.91 and Fig.92 respectively in pump mode.



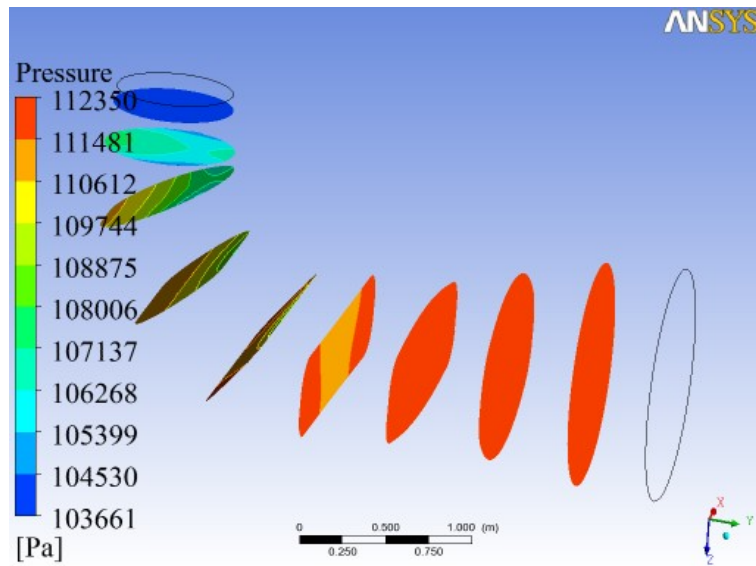


Figure 92. Pressure change through the draft tube in pump mode

The flow separations are eliminated by changing the geometry of the draft tube in each mode and the velocity vectors on the mid cross-section are obtained without any separations as shown in Fig.93.

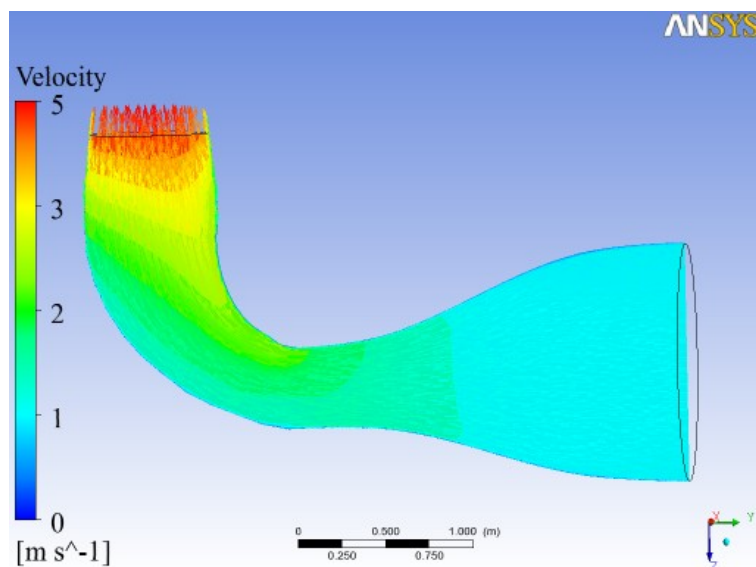


Figure 93. Velocity vectors and contours on the draft tube mid-section in pump mode

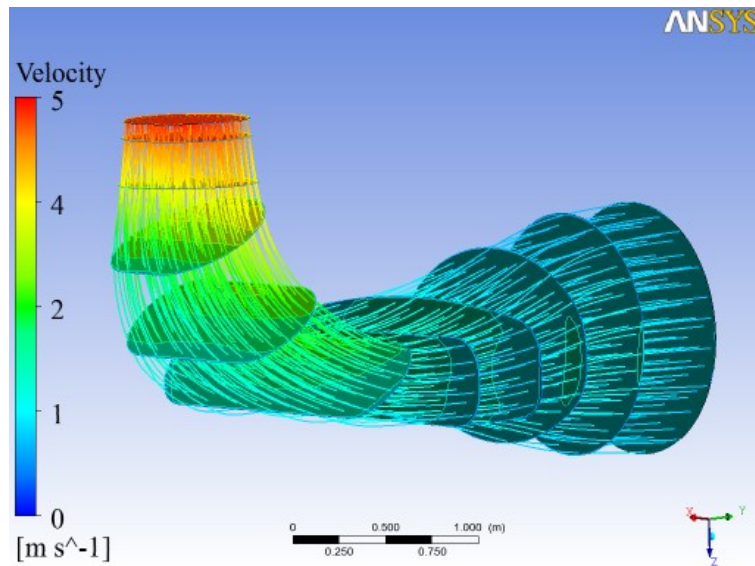


Figure 94. Draft tube velocity contours and streamlines in pump mode

In the pump mode to visualize the behavior of the flow inside the draft tube, the streamlines are plotted in Fig.94. It is seen that the geometry of the draft tube is convenient for the pump mode condition.

## 6.7. Final Model CFD Results and Hydraulic Losses in Pump Mode

The efficiency of the each part of the turbine after modification considering the pump mode is given in the Table 10. The overall hydraulic efficiency of the components also can be calculated as below:

Table 10. Efficiencies of the Pump-Turbine parts and hydraulic losses

	Spiral Case	Stay vanes	Guide Vanes	Runner	Draft Tube
Efficiency [%]	98.16	99.58	99.16	97.46	99.76
$\Delta H$ [m]	0.63	0.16	0.33	28.92	0.03
Hydraulic Efficiency of the Pump-Turbine in turbine mode					94.24

## 6.8. Discussion of Pump Mode Results

The Pump-Turbine is designed as a pump for  $1.6 \text{ m}^3/\text{s}$  discharge and 28.5 m head. The design procedure of the Pump-Turbine parts is same as in turbine mode. the flow and runner rotation directions are chosen as reverse. The same parts in the previous section are simulated in pump mode and redesigned if required any change. Pump mode results are only discussed in this section.

In th pump mode, the water flows the draft tube, runner, guide vanes, stay vanes and spiral case in streamwise direction. So, the water enters the draft tube firstly. The water is transferred lower reservoir to runner with draft tube. The draft tube is simulated with the pump mode properties. The design of the draft tube is discussed in previous sections. The flow inside the draft tube is obtained without separations as illustrated in Fig. 93. In turbine mode, the pressure recovery factor is important. However, how efficiently water is transferred to the runner is important in pump mode. In the turbine mode, 99.76 % hydraulic efficiency value of the draft tube given in Table 10 is convenient for the predicted preliminary draft tube design requirements according to the literature and experiences [11, 20, 21, 22]. Also, in pump mode the pressure distributions inside the draft tube is investigated and plotted in Fig. 91 and Fig. 92.

After passing the draft tube, the flow enters the runner blade passage. No circulation inlet boundary condition is used for the pump mode design calculations. The normal boundary inlet condition is also applied for the runner inlet in pump mode. The angles and profiles are adjusted for the pump mode as in turbine mode. The final runner blade has been obtained after more than two hundred simulations. In the simulations, the blade angles and meridional profile are designed together. Then, in the pump mode the final runner blade is obtained without leading edge shock as illustrated in Fig. 66 and without cavitation as illustrated in Fig. 70. 97.46 % efficiency value of the runner given in Table 10 is convenient for the predicted preliminary runner design requirements.

After passing the runner, the flow enters the guide vane passage. The guide vane inlet flow angle is adjusted for the outlet condition of the runner in pump mode. The guide vanes are rotated about guide vane regulation centers given in Fig. 15 to adjust the guide vane angle for outlet condition of the runner. So, the guide vane operating angle is determined for an optimum pump design condition. The head loss value and 99.16 % hydraulic efficiency of the guide vanes given in Table 10 are convenient for the predicted preliminary guide vane design requirements.

After passing the guide vanes, the flow enters the stay vane passage. The stay vane profile and position are adjusted according to the guide vane inlet condition with the simulation results in turbine mode. The stay vanes are simulated in pump mode conditions. The pressure and velocity distributions are also plotted in Fig.83 and Fig. 85 to illustrate the flow inside stay vane passage. The head loss value and 99.58 % hydraulic efficiency of the stay vanes given in Table 10 are convenient for the predicted preliminary stay vane design requirements.

After passing the stay vanes, the flow enters the spiral case. The spiral case is simulated for pump mode conditions. The simulations of the spiral case is performed with stay vanes to see their interactions. Also, the pressure and velocity distributions on the mid-plane are plotted in Fig. 79 and Fig. 80 respectively to understand the flow distribution in pump mode. The designed spiral case is convenient according to these results for the pump mode operation. The head loss value and 98.16 % hydraulic efficiency of the spiral case given in Table 10 is convenient for the predicted preliminary spiral case design requirements.

The pump mode performance results of the Pump-Turbine parts are tabulated in Table 10. These values are found for the parts with smooth wall assumptions. The roughness effect is also investigated in section 6.2.6. So, each part of the Pump-Turbine should be designed with considering the manufacturing conditions. 94.24 % hydraulic efficiency of the Pump-Turbine given in Table 10 is convenient for the predicted preliminary pump design requirements.

## ***CHAPTER 7***

### ***CHARACTERISTICS OF THE PUMP-TURBINE***

#### **7.1. Pump-Turbine Working Conditions**

A combination of turbine and pump design is used for design of a Pump-Turbine. In the design procedure, Pump-Turbine is designed as a pump with pump mode properties at optimum pump point. Also, Pump-Turbine is designed as a turbine with turbine mode properties at optimum turbine point. However, the design range of the Pump-Turbine design requires other conditions except optimum points. In this design range the simulation are held for the steady-state conditions. But data obtained from the outside conditions of the design range was needed to plot the four-quadrant makes difficult to simulations due to the flow stability.

Hydraulic performance characteristic of the Pump-Turbine determines the relation between the optimum pump head and optimum turbine head as in equation (2). So the optimum turbine mode head is higher than the optimum pump mode head. So the low head turbine working conditions and high head pump mode working conditions have a tendency of unstable internal flow in a pump turbine.

The internal flow through a hydraulic machines can be simulated with the computer codes and CFD tools. These programs helps to understand the flow patterns, pressure and velocity distributions inside the turbine parts. After making the simulations the data of the simulated domain is illustrated and plotted by the post process section. These visualizations and graphs make easier to realize the flow behavior. Design with CFD methods makes easier rapidly to simulate various

models. Also, it is cheaper than the other design methods. Because of these reasons, design with CFD methods is popular in hydraulic machinery. The next step after the CFD design should be the model test data comparison with the CFD results.

The design of the Pump-Turbine starts with the theoretical design methods and experience curves. The preliminary dimensions of the Pump-Turbine are determined from the theoretical design methods and experience curves. The preliminary dimensions of the Pump-Turbine are synchronous speed, wicket gate height, blade angles, runner inlet and outlet diameters, etc. After obtaining the preliminary dimensions, simulations are held for the pump mode or the turbine mode.

In the past, the design of the Pump-Turbine has been focused on the pump mode conditions. So, the design has started from the pump mode than it was controlled for the turbine mode. However, the turbine mode characteristics are also investigated now. Therefore, the Pump-Turbine is the designed for each mode both design conditions and off-design conditions with the help of CFD tools [2].

## 7.2. Four Quadrant Characteristics of the Pump-Turbine

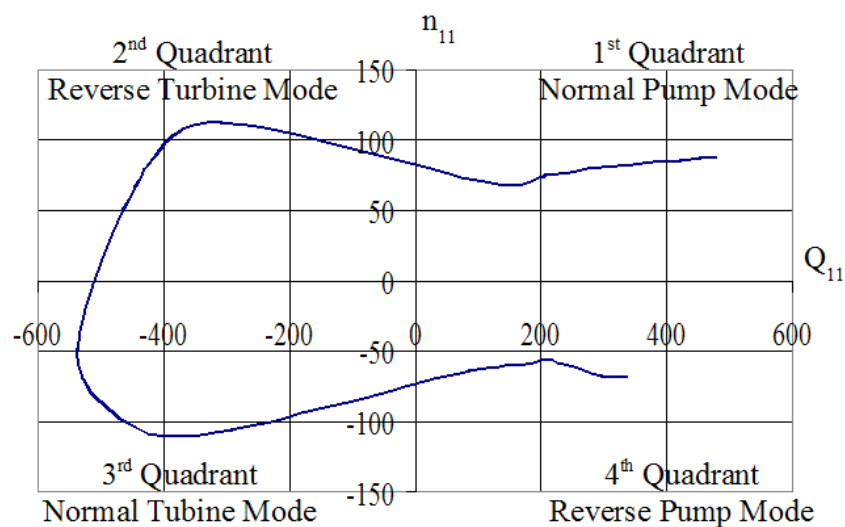


Figure 95. Four-quadrant Characteristics of the Pump-Turbine

All working conditions are represented by the four-quadrant characteristics of the Pump-Turbine. The points obtained from the simulations and performance curves for turbine and pump give the data of the four-quadrant diagram. The four-quadrant diagram is plotted with respect to the unit discharge  $Q_{11}$  on the abscissa and unit speed  $n_{11}$  on the ordinate as determined in the equations (72) and (73). When plotting the four-quadrant diagram, the runner of the Pump-Turbine is simulated each condition and the efficiencies of the other components are used from the optimum point conditions.

$$Q_{11} = \frac{Q\sqrt{H}}{D_1^2} \quad (72)$$

$$n_{11} = \frac{nD_1}{\sqrt{H}} \quad (73)$$

Where:

- $Q$  : the discharge of the Pump-Turbine in each mode [ m<sup>3</sup>/s ]
- $H$  : the head of the Pump-Turbine in each mode [ m ]
- $D_1$  : the diameter of the Pump-Turbine runner [ m ]
- $n$  : the rotational speed of the Pump-Turbine runner [ rpm ]

The Pump-Turbine runner is simulated for all working conditions. The four-quadrant simulation conditions of the Pump-Turbine are tabulated in Table 11.

Table 11. The Simulation Conditions of the Pump-Turbine

	1 <sup>st</sup>	2 <sup>nd</sup>	3 <sup>rd</sup>	4 <sup>th</sup>
$n$ [ rpm ]	500	500	500	500
$Q$ [ m <sup>3</sup> /s ]	0.75 – 3.0	1.0 – 2.0	1.0 – 4.0	0.5 – 1.8
$H$ [ m ]	10 – 45	10 – 30	15 – 85	30 – 50

In the analysis of the pump mode direction (1<sup>st</sup> and 4<sup>th</sup> quadrant), the rotational speed of the Pump-Turbine runner is chosen as constant (500 rpm). Then, the

head variation is investigated with the discharge. On the other hand, in the analysis of the turbine mode direction (2<sup>nd</sup> and 3<sup>rd</sup> quadrant), the rotational speed of the Pump-Turbine runner is chosen as constant (500 rpm) in the reverse direction. Then, the discharge of each head value is found with the guidance of the CFD results.

### ***7.2.1. 1<sup>st</sup> Quadrant Normal Pump Mode***

In this quadrant, pump characteristics of the Pump-Turbine are investigated. Hence, the normal pump characteristics diagram is plotted to understand the normal pump mode behavior.

The mass flow inlet in normal direction of the draft tube inlet section and total pressure outlet are used as inputs in the pump mode simulation. In the design, inlet cavitation and reverse flow in the low discharge regions are dissipated by adjusting the angles and dimensions for the optimum pump mode conditions with considering the CFD results. After adjusting the angles of the Pump-Turbine runner for the pump design point, the runner is simulated for discharge other than the design point. The normal pump (1<sup>st</sup> quadrant) characteristic diagram is plotted with data obtained from the results of the normal pump-mode simulations.

In the normal pump mode simulations with higher discharge than the discharge at the pump design point, the relative angle of the flow is smaller than the inlet angles of the runner blade. The flow can separate from the high pressure surface (H.P.S.) of the pump mode leading edge due to this negative incidence. As a result of this separation, the shock loss increases and unstable flow patterns occur at these locations. The cavitation occurs on the H.P.S. with increasing discharge due to the separation [6].

In the normal pump mode simulations with lower discharge than the discharge at the pump design point, the relative angle of the flow is larger than the inlet angles of the runner blade. The flow can separate from the low pressure surface (L.P.S.) of the pump mode leading edge due to this positive incidence. As a result of this



separation, the shock loss increases and unstable flow patterns occur at these locations. After one point, the cavitation occurs on the L.P.S. with decreasing discharge due to the separation [6].

The settling of the upper and lower reservoirs should be designed with considering the data obtained from the normal pump mode analysis. And the design head should be chosen between upper points to minimize the loss due to the inflow shock. The guide vane angles are obtained for only optimum design points. So, the rotating stall is not investigated in this research. But there are many researches about rotating stall in the Pump-Turbines.

### ***7.2.2. 2<sup>nd</sup> Quadrant Reverse Turbine Mode***

In this quadrant the simulation are held in turbine mode with reverse rotation of the Pump-Turbine runner. The understanding of the Pump-Turbine behavior is important in this quadrant. Since, it identifies the Pump-Turbine working conditions after the failure of the power for rotating generator-motor [32]. However, in the analysis only constant speed of rotation simulations are held. Also, in this quadrant all speed of rotation should be used with related head to understand the complete characteristics of the Pump-Turbine.

These simulations are difficult simulations. Since, the flow through the runner of the Pump-Turbine has the flow separations and unsteady tendency. So, the convergence criteria of these analyses are kept larger than the design conditions. In this quadrant, the simulations appear like the rotating stall case in pumping operation.

In the reverse turbine mode simulations, the results of the simulations are not converged at some points. Also from the test results in literature, the water does not enter uniformly over the entire circumference of the Pump-Turbine runner [32].

### **7.2.3. 3<sup>rd</sup> Quadrant Normal Turbine Mode**

In this quadrant, turbine characteristics of the Pump-Turbine are investigated.

Total pressure inlet condition is given with an angle calculated with respect to the head, discharge and inlet dimensions for turbine mode. Moreover, the mass flow outlet is used in the turbine mode simulation.

In the design, misalignment of the flow angle and the runner blade angles at the inlet section is adjusted and cavitation regions are eliminated. Nearly no swirl outflow is obtained with adjusting the runner blade angles. After adjusting the angles of the Pump-Turbine runner for the turbine design point, the runner is simulated for other discharge values.

In the normal turbine mode simulations with higher discharge than the discharge at the turbine design point, the relative angle of the flow is smaller than the inlet angles of the runner blade. The flow can separate from the L.P.S. of the turbine mode leading edge due to this incidence. As a result of this separation, the shock loss increases and unstable flow patterns occur at these locations. The cavitation occurs on the L.P.S. with increasing discharge due to the separation [6].

In the normal turbine mode simulations with lower discharge than the discharge at the turbine design point, the relative angle of the flow is larger than the inlet angles of the runner blade in turbine mode. The flow can separate from the H.P.S. of the turbine mode leading edge due to this incidence. As a result of this separation, the shock loss increases and unstable flow patterns occur at these locations. After one point, the cavitation occurs on the H.P.S. with decreasing discharge due to the separation.

The settling of the upper and lower reservoirs should be designed with considering the data obtained from the normal turbine mode analysis. And the design head should be chosen between upper points to minimize the loss. The guide vane angles are obtained for only the turbine design point. So, the guide vane angles are

adjusted to give the related angle to flow. For the other simulations the guide vane are not used. Only the efficiency at the design point is used to plot the turbine performance curve.

#### **7.2.4. 4<sup>th</sup> Quadrant Reverse Pump Mode**

In this quadrant the simulation are held in pump mode with reverse rotation of the Pump-Turbine runner. The understanding of the Pump-Turbine behavior is important in this quadrant. Since, it identifies the Pump-Turbine working conditions after the load rejection like the power failure [32]. However, in the analysis only constant speed of rotation simulations are held for only the runner of the Pump-Turbine. However, in this mode the flow should change the direction when passing from the runner to guide vane passages. So, this also increases the hydraulic loss. Also, in this quadrant all speed of rotation should be used with related discharge to understand the complete characteristics of the Pump-Turbine.

These simulations are also difficult simulations. Since, the flow through the runner of the Pump-Turbine has the flow separations and unsteady tendency. So, the convergence criteria of these analyses are kept larger than the design conditions.

In the reverse pump mode simulations with high discharge, the relative flow angle is different from the inlet angles of the runner blade. So, the flow can separate from the H.P.S. of the pump mode leading edge due to this incidence. As a result of this separation, a wide dead water zone is developed at these locations on H.P.S. .

In the reverse pump mode simulations with low discharge, the water enters the crown side. So, the dead water zone developed at this locations.

## ***CHAPTER 8***

### ***CONCLUSION***

#### **8.1. Summary of the Developed Work**

The design of Pump-Turbine is investigated and a design methodology of Pump-Turbine hydraulic equipments with CFD tools is developed. The design methodology uses head and power as main inputs. Then, the hydraulic parts of the Pump-Turbine are designed according to the main design parameters which are efficiency, discharge, rotational speed, specific speed, meridional profile, guide vane properties, blade angles etc.

The design methodology of the Pump-Turbine with CFD methods is developed according to the values of the head and power determined for each unit. After taking the main input parameters, design parameters of each part are changed to see their effects on the design with the help of the CFD tools. The design of the hydraulic machine at different operating regions are investigated with ANSYS CFX v.12.

In the preliminary design stage, the type of the turbine, power, head and some parameters are determined. After the determination of the preliminary dimensions, the design of the Pump-Turbine improved for turbine and pump mode together to reach the design requirements.

The design of the Pump-Turbine starts with the runner of the Pump-Turbine. After the runner design, the guide vane properties are determined to obtain required

runner inflow conditions. Then, the stay vanes and spiral case are designed according to the constant velocity moment principle. Finally, draft tube geometry is determined for runner outlet section properties with considering the pressure recovery factor. Then, hydraulic efficiency terms of the Pump-Turbine for turbine and pump mode are improved using CFD to 94.60 % and 94.24 % respectively. The problematic regions on the runner blade are also investigated. The blade and flow angles are adjusted with changing the parameters according to the CFD results. Also, the problematic regions in spiral case and draft tube are investigated with plotting the velocity vectors and pressure distribution on the sections of the flow domains. Then, the geometries are improved to decrease the hydraulic loss.

A Pump-Turbine runner preliminary design calculation steps are also given in section 3.3. Then, spiral case, stay vanes, guide vanes and draft tube design methodologies are described with the CFD results in Chapters 5 and 6. Finally, 500 kW power Pump-Turbine for 28.15 m head is designed with 89.15 % hydraulic cycle efficiency.

## **8.2. Contributions of the Developed Work**

The parts of a Pump-Turbine are designed with the developed design methodology. This methodology includes the theoretical methods, computer codes and the CFD tools.

With the help of this work a Pump-Turbine can be designed and manufactured completely with the developed design methodology in Turkey. This design methodology can be completed by the mechanical design to manufacture the parts. A know-how of this design will be available to local manufacturers in Turkey and may have a big impact on the economy.

During this work, the manufacturing capability of the hydropower equipment is also developed and the workers are qualified in this area. Some work has been

already published about the parametric modeling [11] and design of a Francis Turbine [20] and design of a Pump-Turbine [21].

This unique technology can be used to balance the difference in energy supply and demand. Therefore, the energy in the network can be used efficiently. This research can be continued by the model tests by future researchers in the area of a model test setup will be made available to the university. Furthermore this technique can be used to design several pump-turbines for the available locations given in Table 2 in Turkey.

### **8.3. Conclusion**

The general dimensions of the Pump-Turbine are determined according to the hydraulic machinery theory. Then, the preliminary design geometries are generated with the theoretical design methods and experience curves and they are improved with the help of the CFD tools until reaching the design requirements. The design methodology makes it possible to increase the hydraulic efficiency of the Pump-Turbine about 30 % in each mode.

Steady state simulations are held in this thesis. Mesh independency for each part is investigated with different number of elements and the results are detailed for the Pump-Turbine runner in sections 5.2.5. and 6.2.5. in each mode. The simulations at design point are converged and results are obtained as mesh independently. However while simulating the off-design conditions in Chapter 7, the simulations were difficult and convergence results are obtained by increasing the number of elements at some points for the stability.

The general dimensions of the Pump-Turbine parts are obtained with theoretical design methods and experience curves according to head and discharge values. The design methodology of a Pump-Turbine is developed by integrating CFD tool. So, this methodology can be used any head and discharge value for further designs from the design point of view. Each mode performance by means of hydraulic

efficiency can be improved according to Chapter 3. This methodology can be used to shorten the design periods. So, this methodology can be applied for the under consideration HSPS projects in Table 2.

#### **8.4. Future Works**

The work covered in the thesis is made for the steady state simulations with the CFD tools. In the future this analysis can be extended with unsteady simulations to understand the behavior of the Pump-Turbine characteristics in four-quadrant deeply. Also, model test of the Pump-Turbine can be useful to construction of the pump-turbines in Turkey.

## **REFERENCES**

- [1] Saraç, M. "*Pompaj Depolamalı Hidroelektrik Santraller*", Proceeding of Nuclear & Renewable Energy Resources Conference, Ankara, Turkey, pp.372-377, 2009.
- [2] Nowicki, P., Sallaberger, M. and Bachmann,P. "*Modern Design of Pump-turbines*", Proceeding of IEEE Electrical Power & Energy Conference (EPEC), 2009.
- [3] Sallaberger M., Bachmann P., Michaud Ch., Sick M. and Doerfler P. "*Modern Hydraulic Design of Large Pump-turbines*", The Int. J. on Hydropower and Dams, Issue 5, 2003.
- [4] Raabe, J. "*Hydropower: The Design, Use, and Function of Hydromechanical, Hydraulic, and Electrical Equipment*" VDI-Verlag, Verlag des Vereins Deutscher Ingenieure, Dusseldorf, 1985.
- [5] "*Large Hydro*", Hydro Media, Va-tech Hydro.  
<http://ebookbrowse.com/hydro-media-media-center-large-hydro-large-hydro-en-1-pdf-d160471975>  
(accessed 05/08/11)
- [6] Krivchenko, G.I. "*Hydraulic Machines: Turbines and Pumps*". Mir Publishers, Moscow, 1986.
- [7] Sallaberger, M. and Thoma, W. "*Upgrading Potential of Pump-Turbines shown on the Projects Dalesice and Zarnowiec*" , Proceedings of Uprating and Refurbishing Hydropower Plants Conference, Prague, Czech Republic, 2001.
- [8] Sallaberger M., Bachmann P., Michaud Ch., Sick M.,Doerfler P. "*Modern*



*Hydraulic Design of Large Pump-turbines*", The Int. J. on Hydropower and Dams, Issue 5, 2003.

- [9] Nowicki, P., Sallaberger, M., Bachmann, P. "*Modern Design of Pump-turbines Design Features and Operation Behavior*", Proceedings of Waterpower XV, Chattanooga, Tennessee, USA, 2007.
- [10] Nowicki P., Sallaberger M., Bachmann P. "*Modern Design of Pump-Turbines*", Proceedings of IEEE Electrical Power and Energy Conferences, Montreal, Canada, 2009.
- [11] Yildiz, M. and Celebioglu, K. "*Parametric Modeling of a Francis Turbine*", Proceedings of Nuclear & Renewable Energy Resources Conference, Ankara, Turkey, pp. 402-407, 2009.
- [12] Fayolle, D. and Lafon, S. "*Variable Speed Applied to Hydraulic Schemes History of a Technology and Today's State of Art*", 2008.  
<http://www.power-consulting-associates.com/OUR-PUBLICATIONS.aspx>  
(accessed 04/07/11)
- [13] Orchard, B., Klos, S. "*Pumps as Turbines for Water Industry*", World Pumps, pp. 22-23, August 2009.
- [14] Rawal, S., Kshirsagar, J.T., "*Numerical Simulation on A Pump Operating in A Turbine Mode*", Proceedings of the Twenty-Third International Pump Users Symposium, pp. 21-27, Houston, Texas USA, 2007.
- [15] Scherer, K. "Andritz Vatech Hydro Giga-Watt Generation Panel Session", Hydro Generators , 2008.
- [16] Suul, J., Uhlen, K. "*Wind Power Integration in Isolated Grids Enabled by Variable Speed Pumped Storage Hydropower Plant*", Proceeding of IEEE International Conference on Sustainable Energy Technologies (ICSET 2008), pp.399-404, Singapore, 2008.

- [17] Paul, K. "*Design Features of the Helms Pumped Storage Project*", IEEE Transactions on Energy Conversion, Vol. 4, No. 1, 1989.
- [18] Fujihara, T., Imano, H., Oshima, K., "*Development of Pump Turbine for Seawater Pumped-Storage Power Plant*", Hitachi Review Vol. 47, No.5, 1998.
- [19] "*Pumped Storage Plant*"  
<https://mediawiki.middlebury.edu/wiki/OpenSourceLearning/Hydropower>  
 (accessed 25/07/11)
- [20] Yildiz, M., Okay, G. and Celebioglu, K. "*Design of a Francis Turbine for a Small Hydropower Project in Turkey*" Proceedings of ASME 10<sup>th</sup> Biennial Conference on Engineering Systems Design and Analysis (ESDA 2010), Istanbul, Turkey, 2010.
- [21] Yildiz, M., Celebioglu, K. and Albayrak, K. "*Hesaplamalı Akışkanlar Dinamiği Metotları ile Pompa-Türbin Tasarımı*", 7. Pompa-Vana Kongresi, İstanbul, Türkiye, 2011.
- [22] Okay, G., "Utilization of CFD Tools in The Design Process of A Francis Turbine", Middle East Technical University, MS Thesis, Ankara, Turkey, 2010.
- [23] "*Suter Curve for Turbo Pump*", PIPENET Training Manual, 2005.
- [24] "*Estimating Reversible Pump-Turbine Characteristics*", A Water Resources Technical Publication, Engineering Monograph No.39, United States Department of the Interior Bureau of Reclamation, 1977.
- [25] Petermann, H. "Akım Makinaları". Matbaa Teknisyenleri Basımevi, İstanbul, Türkiye, 1978.
- [26] Franke, G., Fisher, R., Powell, C., Seidel, U. and Koutnik, J. "*On Pressure Mode Shapes Arising from Rotor/Stator Interactions*", Sound and Vibration, pp.14-18, 2005.

- [27] Yan, J., Koutnik, J., Seidel, U., Hübner, B. and Scherer, T. "*Compressible Simulation of Rotor-Stator Interaction in a Pump-Turbine*", 3<sup>rd</sup> IAHR International Meeting of the Workgroup on Cavitation and Dynamic Problems in Hydraulic Machinery and Systems, Brno, Czech Republic, pp. 261-270, 2009.
- [28] Pulpitel, L., Vesely, J. and Mikulasek, J. "*Comments to Vibrations and Pressure Oscillations Induced by the Rotor Stator Interaction in a Hydraulic Turbine*", 3<sup>rd</sup> IAHR International Meeting of the Workgroup on Cavitation and Dynamic Problems in Hydraulic Machinery and Systems, Brno, Czech Republic, pp. 305-314, 2009.
- [29] Berten, S., Dupont, P., Farhat, M. and Avellan, F. "*Rotor-Stator Interaction Induced Pressure Fluctuations: CFD and Hydroacoustic Simulations in the Stationary Components of a Multistage Centrifugal Pump* ", Proceedings of FEDSM2007, 5<sup>th</sup> Joint ASME/JSME Fluids Engineering Conference, San Diego, California USA, 2007.
- [30] Ansys CFX, Release 12.0, User Manual.
- [31] Drtina, P., Sallaberger, M. "*Hydraulic Turbines-Basic Principles and State-of-the Art Computational Fluid Dynamics Applications*". Proceedings of the Institution of Mechanical Engineers, Vol 213 Part C, pp.85-102, 1999.
- [32] Kubota, T., Kushimoto, S. "*Visual Observation of Internal Flow Through High-Head Pump-Turbine*", Proceedings of IAHR-ASME-ASCE Joint symposium on Design and Operation of Fluid Machinery, pp. 609-620, 1978.